Biofilm formation of the quorum sensing model organism *Vibrio harveyi*

Dissertation der Fakultät für Biologie der

Ludwig-Maximilians-Universität München

Department I, Microbiology

by **Elaine Marie Rabener**

Munich, December 2014

The research described in this thesis was performed from October 2010 to November 2013 under the supervision of Prof. Dr. Kirsten Jung at the Ludwig-Maximillians-University of Munich.

1. Evaluator: Prof. Dr. Kirsten Jung
2. Evaluator: Prof. Dr. Marc Bramkamp

Date of Submission: 18th December, 2014

Date of Defense: 4th May, 2015

“In the middle of difficulty lies opportunity.” Albert Einstein

Dedicated to my father

Statutory Declaration

Hereby, I declare that I have authored this thesis independently, that I have not used other than declared sources and resources. Also, I declare that I have not submitted a dissertation without success and not passed the defense. The present dissertation neither the entire dissertation nor parts of it has been presented to another examination board.

Munich, 18th December, 2014

Elaine Marie Rabener

Summary

The marine bacterium *Vibrio harveyi* is a model organism with a complex quorum sensing system. This molecular system includes three autoinducers, each having its own synthase and sensor hybrid kinase. The information sensed by the kinases is channeled via phosphorylation of two proteins (LuxU and LuxO) to reach the master regulators (AphA and LuxR) which induce or repress genes for bioluminescence, type III secretion, and, among others biofilm formation.

Biofilms are found in every niche of every environment, and are often considered as a source of disease. Biofilms can be comprised of single or multiple bacterial species. The formation of biofilms is a complex process that involves many genes and also involves signaling in concert with the environment and with neighbouring cells.

In this study, interest centered on the formation of biofilms of *V. harveyi* and how biofilm formation is affected by quorum sensing. Therefore, a flow system for biofilm formation was established in order to perform a time scale biofilm experiment of *Vibrio harveyi* wildtype.

As is the case for other bacteria, it was shown that autoinducers influence biofilm formation by *V. harveyi*. Therefore, first the wild type was compared to a quorum sensing ON mutant and a quorum sensing OFF mutant. It was found that the quorum sensing system must be intact for complete biofilm formation, because both mutants showed severe defects in their biofilm structures and biomass volumes compared to the wildtype. Further, a comparision of macrocolonies among these three strains was performed.

As a quorum sensing OFF mutant formed no biofilm, it was of interest to determine which autoinducer has the greatest effect on biofilm formation. In this thesis, it is shown that AI-2 is essential for the initial attachment of the cells to the surface, and also it is inferred that microcolonies start to build when all three autoinducers are produced. The AI-2 synthase deletion mutant was complemented using *in trans* and chromosomal integrated copies. These complemented strains were able to fully restore bioluminescence to wildtype levels and partially restore biofilm formation to wildtype levels.

An additional line of research in this thesis involves the importance of exopolysaccharides for biofilm formation and structure. Various phenotypes were characterized generating novel deletion mutants of genes coding for putative proteins involved in polysaccharide production. Exopolysaccharide levels were determined by glucose quantification and the mutants showed decreased glucose levels compared to the wildtype. Also, the biofilms formed by the mutant strains showed only monolayers. Chromosomal integration of the missing gene(s) in the respective deletion mutants showed increased biofilm volume and structure as well as increased glucose levels compared to deletion mutant copies only.

Furthermore, colony morphology using biofilm macrocolony formation of specific strains was analysed. Additionally, the wildtype, quorum sensing ON and Off mutant strains were analysed on single cell level using Scanning Electron Microscopy. Interestingly, the wild type cells are filamentous on the edge of each macrocolony while this was not the case for the other mutants. This implies that the elongation of the wild type cells on the macrocolony edge is triggered via quorum sensing.

In conclusion, all deletions resulted in severe defects in biofilm formation compared to the wildtype biofilm. Most notably, lack of AI-2 had the greatest effect on biofilm formation by *V. harveyi*.

Table of contents

Statutory Declaration **4**

Summary **5**

Table of contents **6**

Table of abbreviations, acronyms and symbols **9**

List of tables **11**

List of figures **12**

1 Introduction **14**

1.1 Bacterial communities *14*

1.2 Cell-cell communication by QS *14*

1.3 Vibrio harveyi, its quorum sensing system and bioluminescence *15*

1.4 The global autoinducer AI-2 ..... *22*

1.5 Biofilms *24*

1.6 QS-regulated phenotypes *26*

1.6.1 Exopolysaccharides 26

1.6.2 Colony morphology 28

1.7 Aims of this thesis *29*

2 Materials and methods **30**

2.1 Materials *30*

2.1.1 Chemicals 30

2.1.2 Enzymes 31

2.1.3 Kits 31

2.1.4 Bacterial growth media 32

2.1.5 Antibiotics 32

2.1.6 Strains 32

2.1.7 Plasmids 34

2.1.8 Oligonucleotides 35

2.2 Methods *36*

2.2.1 Cultivation techniques 36

2.2.1.1 Cultivation of Escherichia coli and Vibrio harveyi 36

2.2.1.2 Stock cultures 37

2.2.2 Molecular biology and genetics 37

2.2.2.1 Modification of DNA 37

2.2.2.2 Isolation of plasmids 37

2.2.2.3 Isolation of genomic DNA 37

2.2.2.4 Polymerase chain reaction 37

2.2.2.5 Colony polymerase-chain reaction ... 38
2.2.2.6 Electrophoretic separation of DNA-fragments ... 39
2.2.2.7 Determination of DNA or plasmid concentration ... 39
2.2.2.8 DNA-sequence analysis ... 39
2.2.2.9 qRT-PCR ... 39
2.2.2.10 Competent cells and transformation ... 40
2.2.2.11 Generation of deletion mutants ... 41
2.2.2.12 Complementation in trans ... 42
2.2.2.13 Chromosomal complementation ... 42
2.2.2.14 Constitutive green fluorescent protein tagging of strains ... 43
2.2.2.15 GFP-promoter fusions and GFP-Hybrid proteins ... 43
2.2.3 Bioluminescence assays ... 44
2.2.4 Measurements of exopolysaccharide production ... 45
2.2.5 Biofilm formation ... 45
2.2.5.1 Flow systems using confocal laser scanning microscopy ... 45
2.2.5.2 Macrocolonies and Scanning Electron Microscopy ... 46

3 Results ... 48

3.1 Effect of quorum sensing on bioluminescence and biofilm formation ... 48
3.1.1 Time-dependent biofilm formation of *V.harveyi* ... 48
3.1.2 Bioluminescence production and biofilm formation are influenced by QS ... 50
3.1.3 Influence of single autoinducers on biofilm formation ... 53

3.2 Identification of genes involved in the production of biofilms ... 57
3.2.1 Bioinformatics: analysis of homology ... 57
3.2.2 Phenotypic characterization of the deletion mutants ... 59
3.2.2.1 Bioluminescence and exopolysaccharide production ... 59
3.2.2.2 Impact of putative EPS genes on biofilm formation ... 60
3.2.2.3 Phenotypic characterization of the knock-in mutant strains ... 62
3.2.2.4 Transcriptional and translational expression of putative exopolysaccharide genes ... 65
3.2.3 Putative LuxR binding sites ... 67

3.3 Colony morphology of macrocolonies ... 67
3.3.1 Bioluminescence and structure of macrocolonies ... 68
3.3.2 Analysing of the macrocolonies via Scanning Electron Micrsocopy ... 72

4 Discussion ... 78

4.1 The influence of QS on bioluminescence and biofilm formation in V. harveyi ... 78
4.1.1 QS affects bioluminescence and biofilm formation ... 78
4.1.2 AI-2 influences the adhesion of *Vibrio harveyi* on surfaces ... 78

4.2 Identification of EPS genes involved in the production of biofilms ... 79

4.3 Colony morphology is affected by QS and EPS production ... 82

4.4 Outlook ... 83

5 References ... 85

6 Appendix ... 93

6.1 pBLAST results of all proteins analysed in this thesis ... 93

6.2 Mean values of bioluminescence production, biofilm formation as well as glucose production of all strains used as well as the qRT-PCR data 99

Acknowledgements 101

Curriculum Vitae ..... Fehler! Textmarke nicht definiert.

Table of abbreviations, acronyms and symbols

Tab. 1: Abbreviations, acronyms and symbols

Symbol	Description
Δ	Deletion of a gene
AB-medium	Autoinducer bioassay medium
AI	Autoinducer
AI-2	Autoinducer 2
AHL	Acyl-homoserine lactone
Amp^R	Ampicillin resistance
as	Antisense
BLAST	Basic Local Alignment Search Tool
bp	Base pairs
CAI-1	*V. cholerae* autoinducer 1
Cam^R	Chloramphenicol resistance
CLSM	Confocal scanning electron micrsocope
DAP	Diaminopimelic acid
DNA	Deoxyribonucleic acid
DNase	Deoxyribonuclease
dNTP	Deoxyribonucleotidtriphosphate
DPD	4,5-dihydroxy-2,3-pentanedione
DTU	Technical University of Denmark, Copenhagen, Denmark
EDTA	Ethylenediaminetetraacetic acid
EtOH	Ethanol
EPS	Exopolysacharide
GC-TOF-MS	Gas Chromatography with Time-of-Flight Mass Spectrometer
GST	Glutathione S transferase
HAI-1	*V. harveyi* autoinducer 1
HCY	Homocysteine
Kan^R	Kanamycin resistance
Kb	Kilo bases
LB-medium	Luria-Bertani medium
MTA	Methyladenosine
NCBI	National Center for Biotechnology Information
NEB	New England Biolabs
No.	Number
OD(x)	Optical density, measured by absorption at a wavelength of x nm
OL	Overlap
o/n	Overnight
PGA	Penicillin G acylase
PIPES	Piperazine-N,N'-bis(2-ethanesulfonic acid)
PCR	Polymerase chain reaction

Symbol	Description
qRT-PCR	Quantitative real-time polymerase chain reaction
QS	Quorum sensing
RE	Restriction enzyme
RLU	Relative light units
RLU/OD(600)	Relative light units per cell density at 600 nm wavelength
RNA	Ribonucleic acid
rpm	Revolutions per minute
RT	Room temperature
R-THMF	*R*-2-methyl-2,3,3,4-tetrahydroxytetrahydrofuran
S	Sense
SAH	S-adenosyl-homocysteine
SAM	S-adenosylmethionine
SDS	Sodium dodecyl sulfate
SN	Supernatant
SRH	S-ribosyl-homocysteine
S-THMF-borate	*S*-2-methyl-2,3,3,4-tetrahydroxytetrahydrofuran-borate
T	Time
THF	N-methyltetrahydrofolate
THPG	5-methyltetrahydropteroyl glutamate
Tris	Tris[hydroxymethyl]aminomethane
UPLC-MS	Ultra performance liquid chromatography Mass Spectrometer
Vps	Vibrio polysaccharide
v/v	Volume per volume
w/o	Without
WT	Wildtype
w/v	Mass per volume

List of tables

Tab. 1: Abbreviations, acronyms and symbols 9
Tab. 2: Effects of *luxS* deletion 24
Tab. 3: Chemicals 30
Tab. 4: Enzymes 31
Tab. 5: Kits 31
Tab. 6: Bacterial growth media 32
Tab. 7: Antibiotics 32
Tab. 8: Strains 32
Tab. 9: Plasmids 34
Tab. 10: Oligonucleotides 35
Tab. 11: Mastermix of PCR reactions 38
Tab. 12: Mastermix for colony-PCR 39
Tab. 13: Homology studies of putative exopolysaccharide producing proteins found in *V. harveyi* WT 58
Tab. 14: Bioluminescence data [RLU/OD (600)] of all strains at 5 h of cultivation in AB media used in this thesis 99
Tab. 15: Mean value of biofilm volumes [µm³] of all strains used in this thesis 99
Tab. 16: Mean value of glucose [µg/ml] detected in all strains used in this thesis 100
Tab. 17: qRT-PCR data of putative exopolsaccharide genes 100

List of figures

Fig. 1: Chemical structures of autoinducers 15
Fig. 2: Scanning electron microscopy of *V. harveyi* WT 16
Fig. 3: Overnight cultivation of *V. harveyi* WT in shaking flasks grown in AB media 17
Fig. 4: Chemical and enzymatic reactions of bioluminescence (Miyashiro and Ruby, 2012) 17
Fig. 5: Chemical structures of AIs produced and recognized by *V. harveyi* WT (modified from NG *et al.*, 2011) 18
Fig. 6: SAM pathway 19
Fig. 7: The QS circuit of *V. harveyi* WT 21
Fig. 8: Growth, bioluminescence and AI levels of *V. harveyi* WT 22
Fig. 9: Scheme of both forms of AI-2 23
Fig. 10: Biofilm formation showing the involvement of QS 26
Fig. 11: Repeating units of levan which is produced by bacteria such as *B. subtilis* (Manandhar *et al.*, 2009) 27
Fig. 12: Experimental set up oft the flow system (Nielsen et al., 2011). 46
Fig. 13: Time-dependent biofilm formation of *V. harveyi* BB120gfp 49
Fig. 14: Volumes of *V. harveyi* BB120gfp biofilms 50
Fig. 15: Bioluminescence assay of WT, Δ*luxO* and MR15 51
Fig. 16: Biofilm formation of *V. harveyi* strains WTgfp, Δ*luxO*gfp and MR15gfp 52
Fig. 17: Volumes of the biofilms of *V. harveyi* strains WTgfp, Δ*luxO*gfp and MR15gfp 52
Fig. 18: Biofilm formation of different GFP-tagged *V. harveyi* strains 54
Fig. 19: Volumes of the biofilm of different GFP-tagged *V. harveyi strains* 55
Fig. 20: Bioluminescence assay of *V. harveyi* strains WT, MR15, MR3, EMR14 and EMR19 56
Fig. 21: Biofilm formation of *V. harveyi* strains WTgfp, MR3gfp, EMR14gfp and EMR19gfp 56
Fig. 22: Volumes of the biofilms of *V. harveyi* strains WTgfp, MR3gfp, EMR14gfp and EMR19gfp 57
Fig. 23: Bioluminescence assay of different *V. harveyi* strains 59
Fig. 24: EPS determination via glucose hydrolysation of different *V. harveyi* strains 60
Fig. 25: Biofilm formation of different *V. harveyi* strains 61
Fig. 26: Volumes of the biofilms of different *V. harveyi* strains 62
Fig. 27: EPS determination via glucose hydrolysation of *V. harveyi* WT, knock-out and knock-in mutants 63
Fig. 28: Biofilm formation of *V. harveyi* WT, knock-out and knock-in mutant strains 64
Fig. 29: Volumes of the biofilms of *V. harveyi* WT, knock-out and knock-in mutant strains 65
Fig. 30: Transcriptional expression of the putative exopolysaccharide genes comparing WT (blue columns) and JMH634 (red columns) 66
Fig. 31: Microscopy of EMR8 after 18 h of cultivation on an AB-agar plate was performed. Black circles indicated GFP-expression 66
Fig. 32: LuxR binding site consensus (Pompeani *et al.*, 2008) 67
Fig. 33: Timeline of the macrocolonies of *V. harveyi* strains WT (top row), *V. harveyi* Δ*luxO* (middle row) and *V. harveyi* MR15 (bottom row) 68
Fig. 34: Macrocolonies of *V. harveyi* strains WT (top row), *ΔluxO* (middle row) and MR15 (bottom row) after 8 days of cultivation 69

Fig. 35: Macrocolonies of *V. harveyi* strains WT (top row), MR3 (second to top row), MR13 (second to bottom row) and MR18 (bottom row) after 8 days of cultivation 70
Fig. 36: Macrocolonies of *V. harveyi* strains WT (top row), MR3 (second to top row), EMR14 (second to bottom row)and EMR19 (bottom row) after 8 days of cultivation 71
Fig. 37: Macrocolonies of *V. harveyi* strains WT (top row), EMR2 (second to top row), EMR3 (middle row), EMR20 (second to bottom row) and EMR23 (bottom row) after 8 days of cultivation..... 72
Fig. 38: Macrocolony of strain MR15 before (right image) and after (left image) fixation 73
Fig. 39: Overview of a *V. harveyi* WT macrocolony, blue arrows indicate rings and red arrow indicates the center..... 73
Fig. 40: Left side shows the center of the WT macrocolony and right side shows the right edge of the macrocolony 74
Fig. 41: WT macrocolony from the center to the first left ring and right edge (left to right images) .. 74
Fig. 42: Center (left image) and left edge (right image) of a Δ*luxO* strain macroyolony 75
Fig. 43: Macroyolony of a Δ*luxO* strain from the center to the second ring left and the left edge (left to right images)..... 75
Fig. 44: Center (left image) and left edge (right image) of a MR15 strain macrocolony, red arrow indicates agar..... 76
Fig. 45: MR15 strain macrocolony from the center, the second ring right and the left edge (left to right images) 77
Fig. 46: pBLAST of VIBHAR_02222 93
Fig. 47: pBLAST of VIBHAR_02221 94
Fig. 48: pBLAST of VIBHAR_05207 94
Fig. 49: pBLAST of VIBHAR_05206 95
Fig. 50: pBLAST of VIBHAR_05205 95
Fig. 51: pBLAST of VIBHAR_05204 96
Fig. 52: pBLAST of VIBHAR_06667 97
Fig. 53: pBLAST of VIBHAR_01320 98
Fig. 54: Phylogenetic tree 98

1 Introduction

1.1 Bacterial communities

Antoni van Leewenhoek was the first person to describe bacteria using a microscope in 1673 (Leewenhoeck and Graaf, 1673). Bacteria were or are used in many ways for purposes useful for humanity. For instance, some bacteria have been used or are still in use for food and drink fermentation, e.g. alcoholic fermentation dating back to the Egyptian era (Messing and Metz, 2006). However, bacteria can harm us in one way or another. They can also cause corrosion of metals or cause diseases by contaminating food and water (Messing and Metz, 2006).

Robert Koch isolated the species corresponding to outbreaks of tuberculosis and cholera. On the other hand, Max von Pettenkofer found that the environment or personal health status contributes to a pathogen´s outbreak or not (Messing and Metz, 2006). Nearly every niche is populated by bacteria (Young, 2006, Stoodley *et al.*, 2002), the soil (*Bacillus subtilis*, Bassler, 2002), water (*Vibrio cholerae,* Blokesch and Schoolnik, 2007) and even in the air are bacteria (*Actinobacteria*, Bowers *et al.*, 2011). Bacteria may live sessile or free in the environment. Partly this choice is made via signaling with other cells and/or the environment (Karatan and Watnick, 2009).

1.2 Cell-cell communication by QS

There are various cell-cell communication systems, one of them is termed quorum sensing (QS) which is based on sensing of cell density (Bassler and Losick, 2006). It involves the production of chemical molecules termed autoinducers (AIs) by a synthase, their export or diffusion through the cell membrane, binding and import of the AI by other proteins as well as a response by a regulator within the bacterial cell. The regulator switches genes on or off depending on the amount of sensed AIs (proportinonal to the number of bacteria). The AIs can be produced and recognized by the same species or by other species (Kaper and Sperandio, 2005; Surette *et al.*, 1999, Ng *et al.*, 2012, Bassler, 2002, Bassler and Losick, 2006). Bacteria can adapt quickly via QS to a changing environment, e.g. when entering a host, the bacterial mixture needs to be tested by the one entering (Bassler and Losick, 2006, Bassler, 2002, *Geier et al.*, 2008, Gibbs and Greenberg, 2011). QS results in collective behavior of bacteria, e.g. including bioluminescence, biofilm formation, virulent gene expression and sporulation (Ng *et al.*, 2012, Bassler and Losick, 2006). With the QS mechanism bacteria can alter their phenotypic status in a population-sensitive manner (Pérez and Hagen, 2010).

Nealson *et al.* (1970) described the first QS phenomena in *Aliivibrio fischeri*, finding that there is an autoinduction causing bioluminescence during the growth of the bacteria. This is also the simplest form of QS: having one synthase LuxI (inducer of lux) producing an AI (acyl-homoserine lactone, AHL) which diffuses through the cell membrane, it can be taken up by the same cell again and binds to the response regulator LuxR (regulator of lux). At high cell densities, the AI is detected in sufficient amounts, to cause a luciferase enzyme to be produced and so bioluminescence to occur (Kaper and Sperandio, 2005). Greenberg *et al.* (1979) described the production of bioluminescence in *Vibrio harveyi*. Furthermore, they found that bioluminescence in *V. harveyi* but not in *A. fischerii* can be induced by the secretion of AIs of other marine bacteria. They concluded that *A. fischerii*´s

autoinduction system is species-specific while the *V. harveyi´*s autoinduction system is not. This indicated that QS in a bacterium can be a very complex protein-protein interaction system involving more than one synthase and receptor pair (Pérez and Hagen, 2010).

On the whole, there are three systems of QS found to date: the AHL/LuxI-LuxR system in Gram-negative bacteria, the oligopeptide signaling system in Gram-positive bacteria (autoinducer oligopeptides, AIP) and the universal AI-2 signaling system in both. Each signal is detected by sensor hybrid kinases and the signal is transferred via phosphorylation cascades to the master regulator, then transcription of target genes are regulated (Bassler, 2002, Bassler and Losick, 2006, Henke and Bassler, 2004b). There is a great structural diversity when it comes to AIs (Fig.1, Ryan and Dow, 2008).

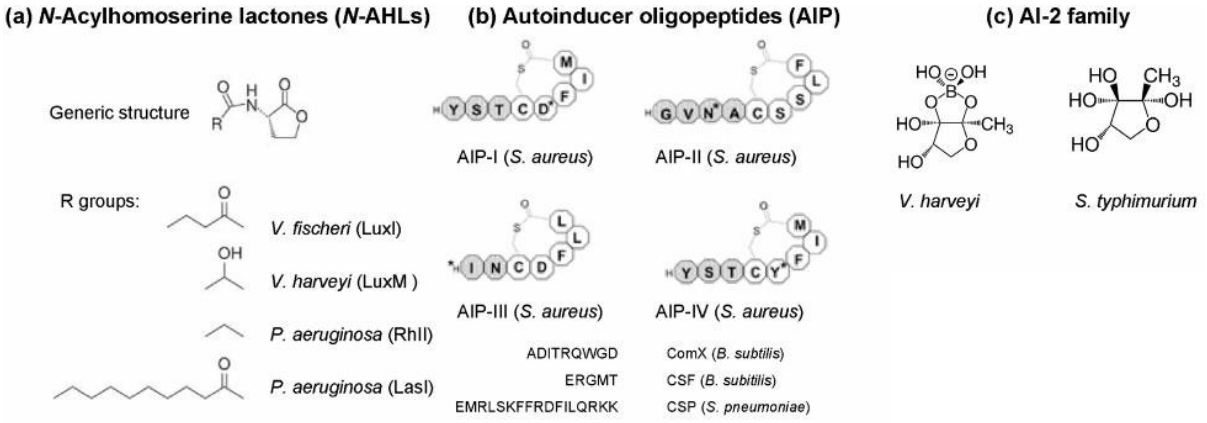

Fig. 1: Chemical structures of autoinducers

(a) *N*-AHLs, (b) AIP, (c) AI-2 (modified from Ryan and Dow, 2008).

Since the 1970s, the mechanism of QS has been found to regulate various processes in different bacteria, to name a few:

- in *Erwinia carotovora* production of antibiotics,
- in *Pseudomonas aeruginosa* formation of biofilms and expression of virulent genes;
- in *Escherichia coli*, *Staphylococcus aureus* and among other *Vibrio cholerae* expression of virulent genes (Kaper and Sperandio, 2005).

It was shown that *Pseudomonas aeruginosa* uses QS to trigger group behaviour of its own kind but that the signals are fatal to others. Furthermore, some groups of *Staphylococcus aureus* produce oligopeptides which inhibit QS in other *S. aureus* groups (Bassler, 2002, Bassler and Losick, 2006).

1.3 Vibrio harveyi, its quorum sensing system and bioluminescence

In 2010, the QS model organism *Vibrio harveyi* ATCC-BAA1116 was reclassified to *Vibrio campbellii* ATCC-BAA1116 by Lin *et al.*, however in this thesis the name *Vibrio harveyi* is still used. In the appendix a family tree is shown (Fig. 54). *Vibrio harveyi* is found in the gut of marine animals and

also free-living in tropical marine waters or adhered to surfaces (Farmer and Janda, 2005, Henares *et al.*, 2012, Henke and Bassler, 2004a, Bassler *et al.*, 1997, Suginata *et al.,* 2013, Lin *et al.*, 2010). It belongs to the ɣ-Proteobacteria to the family of *Vibrionaceae* (Farmer and Janda, 2005, Thompson *et al.*, 2004, Suginata et al., 2013). It is a Gram-negative bacterium and facultatively anaerobic (Fig. 2, Farmer and Janda, 2005, Annous *et al.*, 2009, Henares *et al.*, 2012, Henke and Bassler, 2004a, Bassler *et al.*, 1997, Suginata *et al.,* 2013, Lin *et al.*, 2010). They are straight rods ranging through 0.5-0.8 µm x 1.4-2.6 µm. The bacteria are motile, having one polar flagellum (Farmer and Janda, 2005). The *Vibrionaceae* rods convert to coccoids when starved on nutrients, filaments are formed when starved on nitrogen; and phosphorus starvation leads to swollen large rods (Farmer and Janda, 2005).

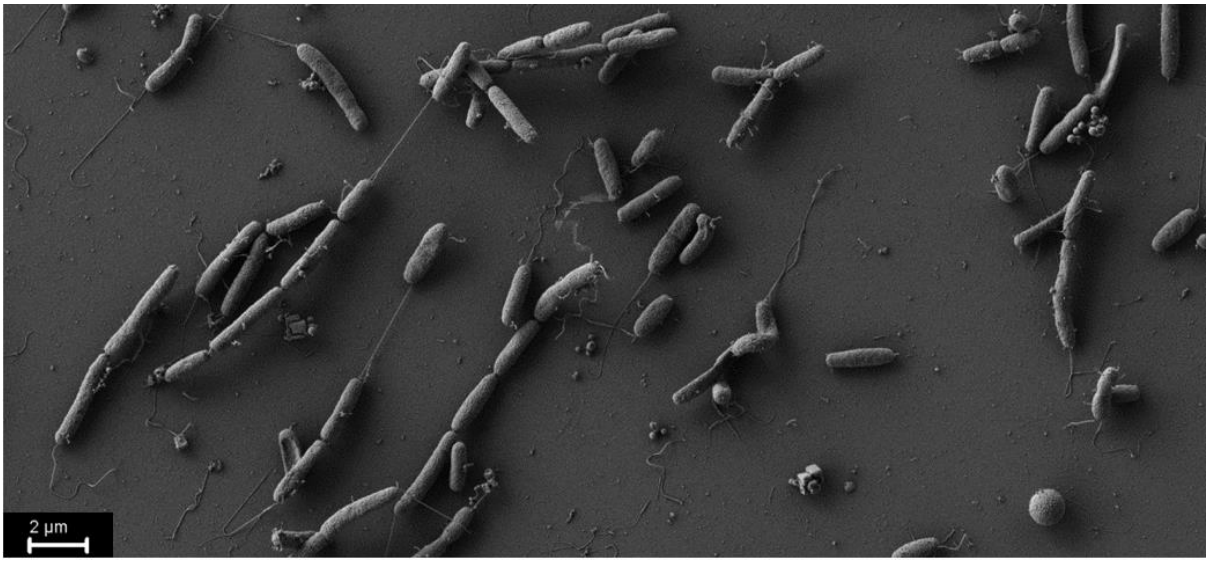

Fig. 2: Scanning electron microscopy of *V. harveyi* WT

The bacteria were grown in AB media to exponential phase, image taken by Axel Müller and Professor Dr. Gerhard Wanner in 2011.

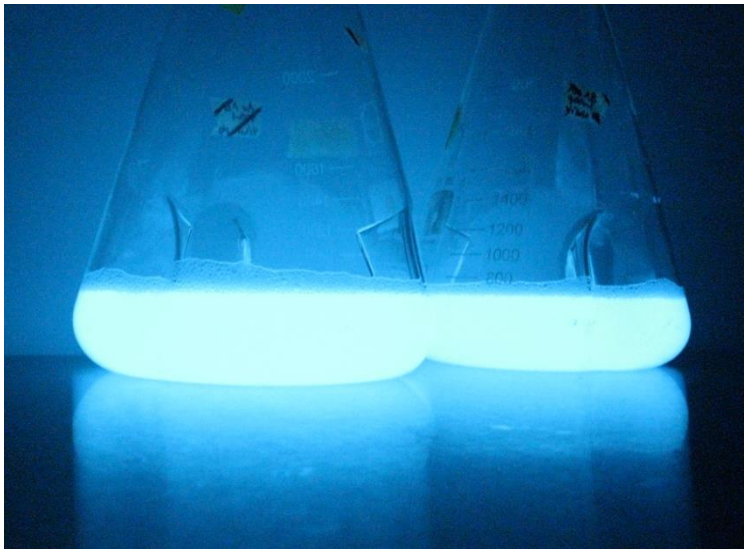

Fig. 3: Overnight cultivation of *V. harveyi* WT in shaking flasks grown in AB media

Image taken with a Canon powerShot A650 IS and an exposure time of 15 s by Matthias Reiger and Axel Müller in 2011.

Many marine bacteria of the class of *Vibrios* share an outstanding characteristic: bioluminescence (Fig. 3, Gode-Potratz and McCarter, 2011, Henke and Bassler, 2004b, Farmer and Janda, 2005). The *luxCDABEGH* operon is responsible for bioluminescence. The enzyme luciferase is a heterodimer, the genes *luxA* and *luxB* encode for the α and β subunits, respectively. Depicted in Fig. 4 is the luciferase catalyzed reaction using the substrates: oxygen, a long chain aldehyde (RCOH) and a flavin mononucleotide ($FMNH_2$). Light of 490 nm wavelength is the energy output from oxidation (Miyashiro and Ruby, 2012; Nijvipakul *et al.*, 2008).

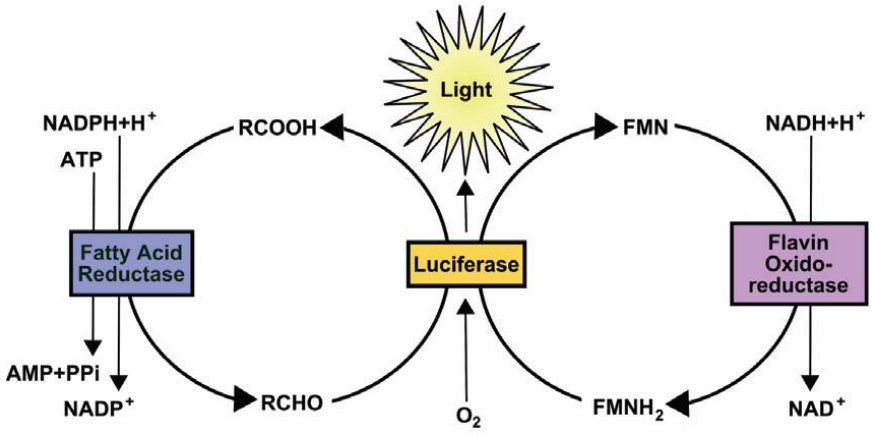

Fig. 4: Chemical and enzymatic reactions of bioluminescence (Miyashiro and Ruby, 2012)

Vibrio harveyi is an opportunistic pathogen of marine animals causing vibriosis, a lethal disease in aquatic and marine fish and shrimp farming (Suginata *et al.*, 2013). Therefore, virulence factors are

important study topics. Recently, QS was found to positively regulate virulence genes coding for caseinase and gelatinase while it negatively regulates phospholipase activity. Hemolysin and lipase were found to be regulated independently from QS (Natrah *et al.*, 2011).

In the model organism *V. harveyi*, the acyl homoserine-lactone (AHL) HAI-1 (harveyi autoinducer 1), a N-(3-hydroxybutyryl)-homoserinelactone, was the first to be discovered in 1970 by Nealson *et al.*. In 1979, AI-2 (autoinducer 2), a (2S,4S)-2-methyl-2,3,4-tetrahydroxytetrahydrofuran-borate, was discovered by Greenberg *et al.*. CAI-1 (cholera autoinducer 1), a (Z)-3-aminoundec-2-en-4-one (Ea-C8-CAI-1), was discovered in 2004 (a) by Henke and Bassler. In 2012, Henares *et al.* discovered the intracellular nitric oxide (NO) dependent H-NOX (heme-nitric oxide/oxygen) sensor which binds the soluble kinase HqsK (H-NOX-associated quorum sensing kinase) in presence of NO. The chemical structures were discovered later: HAI-1 in 1989 by Cao and Meighen, AI-2 in 2002 by Chen *et al.* and CAI-1 in 2011 by Ng *et al.* (Fig. 5).

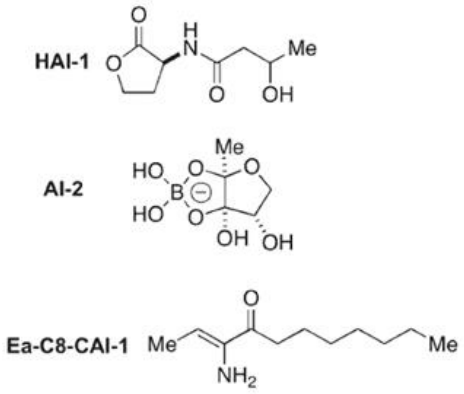

Fig. 5: Chemical structures of AIs produced and recognized by *V. harveyi* WT (modified from NG *et al.*, 2011)

HAI-1 is an intra-species AI while CAI-1 is an intra-genius AI and AI-2 is an inter-species AI (Anetzberger *et al.*, 2012, Henke and Bassler 2004a, Henke and Bassler, 2004b). All three are products of the in the S-adenosyl-methionine (SAM) pathway (Yajima, 2011, Wei *et al.*, 2011, Vendeville *et al.*, 2005, Pereira *et al.*, 2012).

SAM and either acylated acyl carriers or acyl-coA thioesters are substrates for the LuxI (*A. fischerii*) or LuxM (*V. harveyi*) synthases in production of AHLs (Fig. 6, Wei *et al.*, 2011, Pereira *et al.*, 2012).

Fig. 6 shows conversion of SAM to S-adenosyl-homocysteine (SAH) which is detoxified by the enzyme Pfs (5'-methylthioadenosine/S-adenosylhomocysteine nucleosidase) to adenine and S-ribosyl-homocysteine (SRH). LuxS hydrolyses SRH to homocysteine (HCY) and the precursor of AI-2: 4,5-dihydroxy-2,3-pentanedione (DPD). DPD is converted to *R*-THMF or to *S*-THMF-borate. The first is bound by LsrB proteins (*E. coli*, *S. typhimurium* and others) and the latter by LuxP proteins (*Vibrio* spp.). Interconvertion between the two forms of AI-2 with the addition of boric acid is possible (Vendeville *et al.*, 2005, Rui *et al.,* 2012, Pereira *et al.*, 2012).

CAI-1 is also produced by the SAM pathway (Fig. 6). CqsA ligates SAM and in *V. harveyi* otcanoyl Coezyme A by cleaving (S)-methyl-5'-thioadenine (MTA) and the coenzymeA off to forme 3-aminotridec-2-4-one (Ea-CAI-1). This molecule reacts to form CAI-1, catalysed by the enzyme VC1059 in *Vibrio cholerae*. *V. harveyi* uses the intermediate Ea-C8-CAI-1 but not the final product of the above described reaction, CAI-1 (Wei *et al.*, 2011, Pereira *et al.*, 2012). *Vibrio cholerae* can detect all three CAI-1 molecules while *V. harveyi* can only detect Ea-CAI-1 and Ea-C8-CAI-1 (Ng *et al.*, 2011, Pereira *et al.*, 2012).

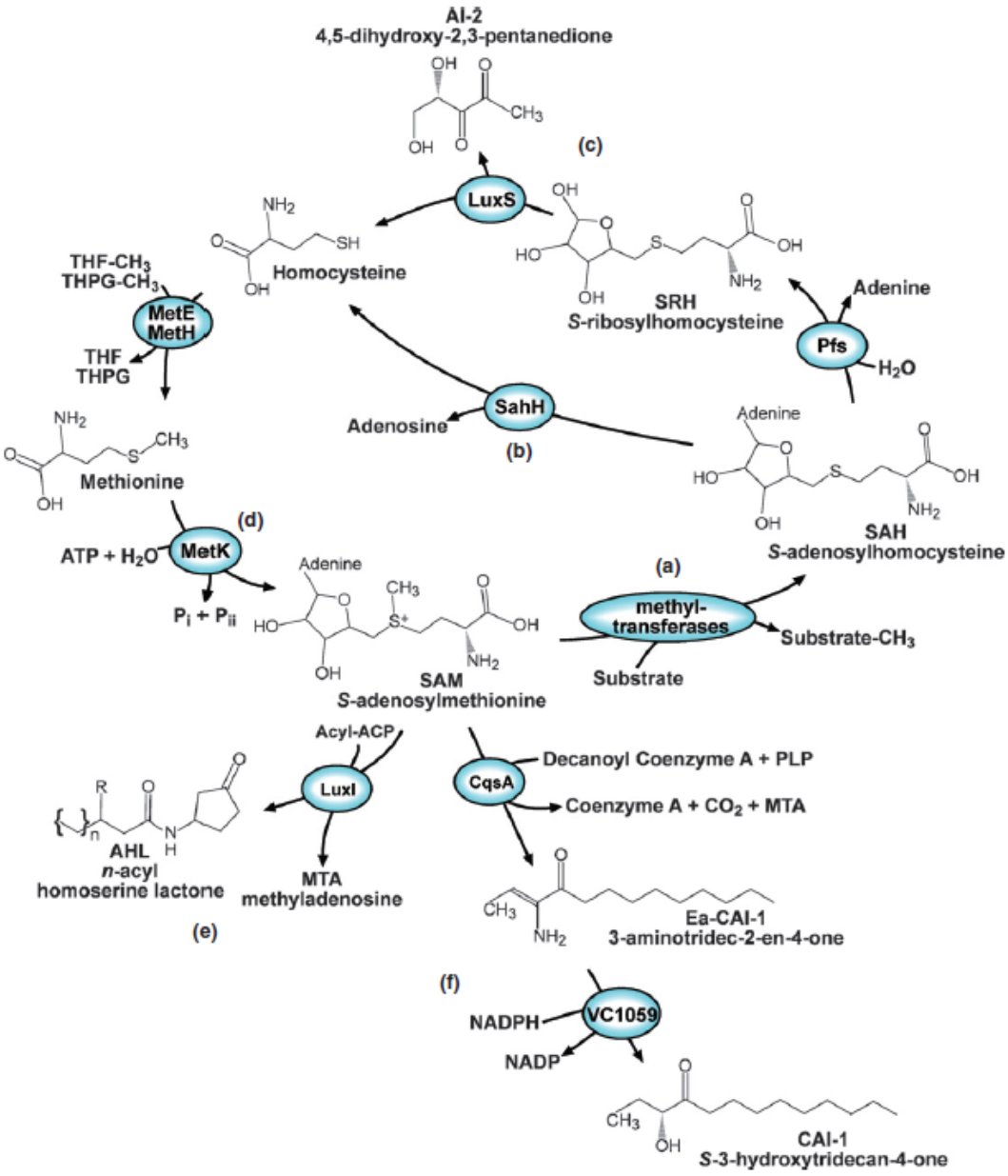

Fig. 6: SAM pathway

Here the synthesis of AIs is shown. a) S-adenosylhomocysteine (SAH) is generated by the transfer of a methyl group from S-adenosylmethionine (SAM) to an acceptor molecule. b) SAH is converted to homocysteine (HCY) via the enzyme SahH. c) Pfs generates SRH and adenine from SAH while LuxS converts SRH to HCY and DPD (AI-2). d) HCY and methionine are regenerated into SAM. e) AHLs are generated using SAM and acyl carrier proteins. f) SAM, CqsA, decanoyl Coenzyme A, a pyridoxal phosphatase aminotransferase like enzyme and in *V. cholerae* VC1059 generate via multiple steps CAI-1, *V. harveyi* has an octanoyl CoA producing Z-3-aminoundec-2-en-4-one (Pereira *et al.*, 2012).

V. harveyi lacks the LuxI/LuxR system common to *A. fischeri* and instead has a more complex system: The AIs HAI-1, AI-2 and CAI-1 are produced by the synthases LuxM, LuxS and CqsA, respectively, and these are secreted through the membrane. The kinase LuxN detects HAI-1. AI-2 is bound to the periplasmic binding protein LuxP which triggers the signal to LuxQ. CqsS detects CAI-1 (Fig. 7, Anetzberger *et al.*, 2012, Henke and Bassler, 2004a, Henares *et al.*, 2012).

At low cell densities, no AIs are detected by the sensor kinases and the phosphate is transferred to the histidine phosphotransferase LuxU which in turn phosphorylates the σ^{54}-dependent response regulator LuxO. Phospho-LuxO activates 4 small RNAs out of 5 (Quorum regulatory small RNAs, Qrr 1-5) and together with the chaperone Hfq, the transcript of the master regulator LuxR is degraded. This results in a basal level of *luxR* transcription, a dark phenotype, type III secretion and among other siderophore production (Henke and Bassler, 2004a, Fenley *et al.*, 2011, Kessel *et al.*, 2013a, Henke and Bassler, 2004b, Anetzberger *et al.*, 2009, Defoirdt *et al.*, 2008, Gode-Potratz and McCarter, 2011, Henares *et al.*, 2012). While *luxR* is only lowly transcribed, *aphA*, another QS master regulator, is transcribed at a maximally high level and is responsible for the fine tuning of the target genes at low cell density (Kessel *et al.*, 2013a). Quorum regulatory RNAs 1-5 act additively in the QS pathway of *V. harveyi* (Fig. 7, Fenley *et al.*, 2011).

At high cell densities, a threshold concentration of AIs is detected by the kinases and thereafter, the kinases act as phosphatases as LuxU and LuxO are dephosphorylated, and *luxR* is transcribed (Anetzberger *et al.*, 2009, Henke and Bassler, 2004a, Fenley *et al.*, 2011, Gode-Potratz and McCarter, 2011, Henares *et al.*, 2012). This means, that with increasing cell density and therefore increasing AI concentration, the small RNAs Qrr1-4 are repressed in a graded manner with the result of the increasing transcription of *luxR*. LuxR regulates nearly 100 genes, e.g. bioluminescence production, biofilm formation and proteolysis occur at high cell density (Pereira *et al.*, 2012, Fenley *et al.*, 2011, Gode-Potratz and McCarter, 2011). Transcription of *AphA* is repressed at high cell density (Fig. 7, Kessel *et al.*, 2013). There are genes regulated by both QS master regulators, as the expression and repression patterns of both overlap (Kessel *et al.*, 2013a).

The content of *luxR* in the cells is regulated by several feedback loops: the autorepression of *luxR* and *luxO*; repression of the LuxR´s antagonist *aphA*; repression of the translation of LuxO and down-regulation of the translation of LuxMN by the Qrr; as well as the activation of the transcription of *qrr 2-4* by LuxR (Fig. 7, Anetzberger *et al.*, 2012).

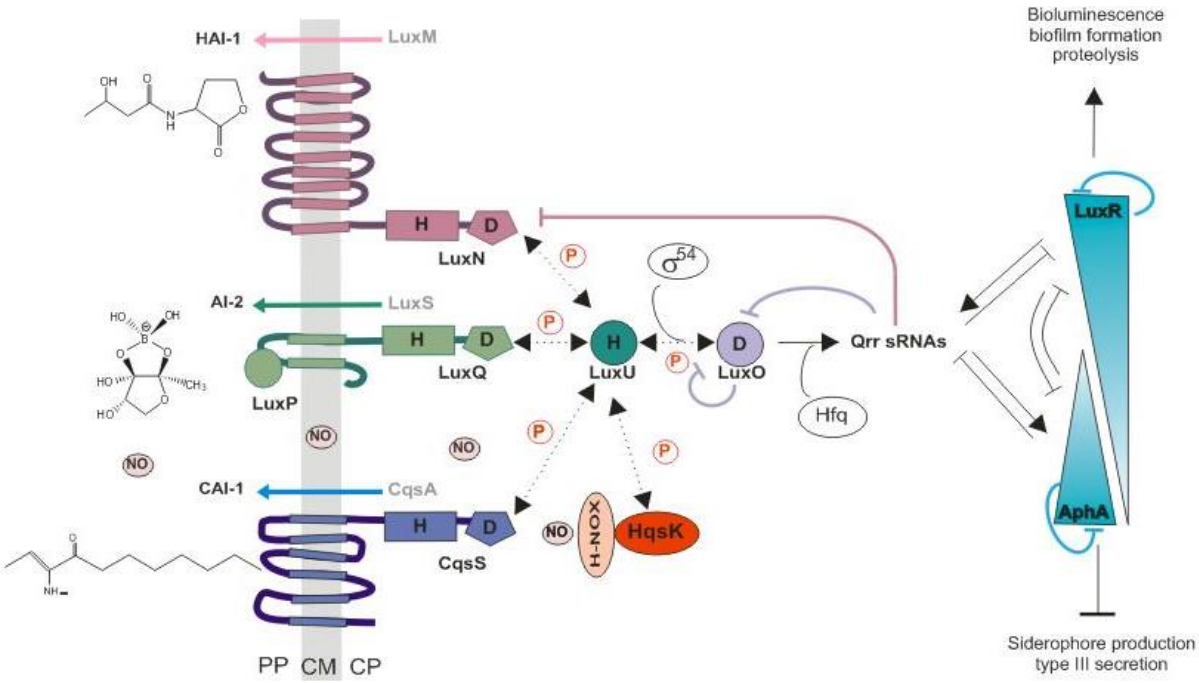

Fig. 7: The QS circuit of *V. harveyi* WT

The AIs HAI-1, AI-2 and CAI-1 are produced by the synthases LuxM, LuxS and CqsA, respectively. At low cell densities, the AIs are hardly available and therefore, can not be recognized by the kinases LuxN, LuxP-LuxQ and CqsS resulting in the phosphorylation of the histidine phosphotransferase LuxU and the σ^{54}-dependent response regulator LuxO. P-LuxO together with the Qrr sRNAs and the chaperone Hfq destabilize the transcript of *luxR* while *aphA* is transcribed resulting in a dark phenotype with type III secretion. At high cell densities, the AIs are detected at a sufficient threshold concentration, dephosphorylation of LuxU and LuxO occurs, the Qrr are repressed, *aphA* is repressed and *luxR* is transcribed resulting in a bright phenotype with biofilm formation and proteolysis. The Qrr repress LuxN and LuxO; LuxO, LuxR and AphA can autorepress themselves. NO binds H-NOX which binds HqsK leading to dephosphorylation of LuxU and therefore, leading to *luxR* expression. In the absence of NO, H-NOX is not bound but HqsK is transfering phosphate to LuxU resulting in *aphA* expression (Anetzberger *et al.*, 2012, Henke and Bassler, 2004a, Henares *et al.*, 2012).

Anetzberger *et al.* (2012) described that the processes in *V. harveyi´*s QS system to work in a time-dependent manner, as AI-2 is the only AI present in the early exponential growth phase, then HAI-1 is detectable and in stationary growth phase CAI-1 reaches its maximal level and remains constant. Meanwhile, AI-2 and HAI-1 arrive at the same molar level (5 µM) and stay constant over the remaining time of the experiment (16 h, Fig. 8). It was shown that AI-2 solely induces the activation of bioluminescence and that HAI-1 increases the level of bioluminescence. It is also shown that with each AI present in the culture, the *luxR* levels increase. All this indicates that *V. harveyi* could use AI-2 synthesised by other bacteria during infections for bioluminescence production as it enhances the metabolisation of oxygen among other beneficial aspects rather than wait for the cell density usually required for bioluminescence production.

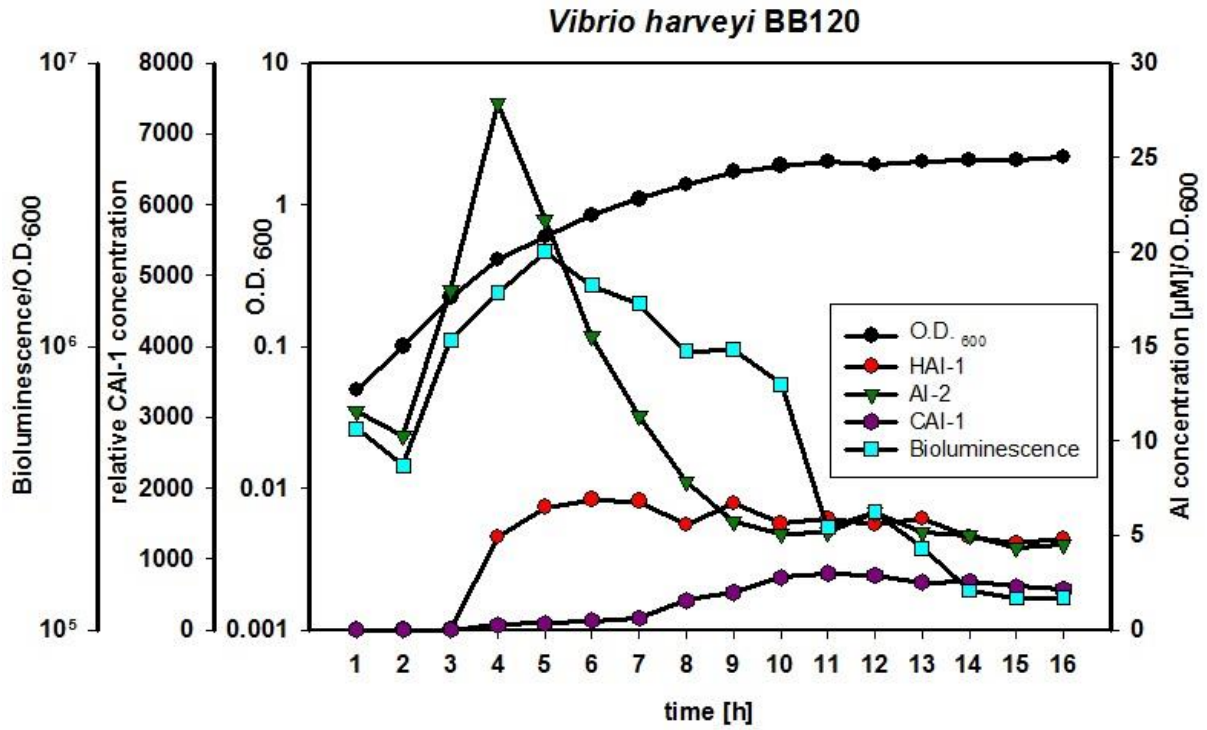

Fig. 8: Growth, bioluminescence and AI levels of *V. harveyi* WT

$OD_{600\,nm}$ (black dots) was measured over 16 h of growth of *V. harveyi* WT in AB medium starting at the $OD_{600\,nm}$ of 0.02 up to an $OD_{600\,nm}$ of 2. AI-2 (green triangles) was measured via a LuxP-GST-binding bioassay, HAI-1 (red dots) was measured using UPLC-MS and CAI-1 (purple dots) was determined from cell-free culture supernatants using a *V. cholerae* MM920 reporter assay and GC-TOF-MS analysis. Bioluminescence (turquoise squares) was performed in microtiter plates using a Centro LB960 from Berthold Technology, modified from Anetzberger *et al.*, 2012.

Defoirdt *et al.* (2008) reported that the combination of CAI-1 and AI-2 causes virulence of *V. harveyi* in brine shrimp, while HAI-1 and AI-2 signaling is necessary to infect rotifers such as *Brachionus plicatilis*. The authors´ hypothesis is that *V. harveyi* uses different AIs and different combinations of AIs for a range of purposes and this hypothesis was confirmed by Anetzberger *et al.* (2012). In *V. fluvialis,* an AHL-type QS system was found as well as AI-2 and CAI-1 systems. The QS system positively controls virulence factors such as an extracellular protease (Wang *et al.*, 2013).

Bassler *et al.* (1997) constructed various *V. harveyi* reporter strains (WT, HAI-1 negative and AI-2 negative) to test cell-free culture supernatants from terrestrial and marine bacteria. They showed that many bacteria produce AI-2 but only a few produce HAI-1. As AI-2 seems to play a significant role in the QS systems of bacteria, it was of interest to investigate further.

1.4 The global autoinducer AI-2

Surette *et al.* (1999) showed that AI-2 is produced by the synthase LuxS in *E. coli*, *V. harveyi* and *S. typhimurium*. They showed via a *luxS* deletion mutant that *V. harveyi* can detect AI-2 from all organisms tested except *E. coli* DH5α as it has a frame shift mutation in the *luxS* gene. However, *E. coli* DH5α can be complemented by $LuxS_{V.h.}$ or $LuxS_{E.c.}$, indicating that LuxS is highly homologous in the tested organisms. The induction of bioluminescence in *V. harveyi* by AI-2 of other bacteria was

also described by Bassler *et al.* (1997). However, as mentioned above, Vendevielle *et al.* (2005) and Rui *et al.* (2012) described that there are two isomeric forms of AI-2: THMF-3-borate and THMF(*R*)-2 (Fig. 9). AI-2 forms are spontaneously rearranged from 4,5-dihydroxy-2,3-pentanedione (DPD), both are interconvertible and are in equilibrium in a given solution (Rickard *et al.*, 2006). The *Vibrio* genus has a different receptor (LuxPQ) for AI-2 binding than the other bacteria (LsrB) (Vendevielle *et al.,* 2005, Rui *et al.*, 2012, Ryan and Dow, 2008). THMF-3-borate is only recognized by *Vibrio* species and the THMF(*R*)-2 is recognized by many bacteria, such as *E. coli*, and *S. typhimurium*.

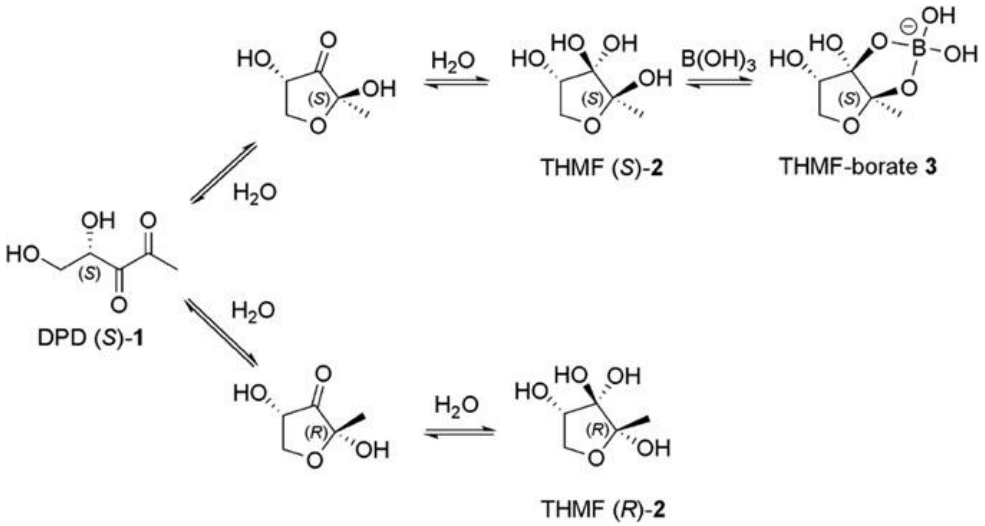

Fig. 9: Scheme of both forms of AI-2

DPD(*S*)-1 converts to either THMF(*R*)-2 or THMF-borate 3 (Rui *et al.*, 2011).

In an AI-2 rich environment, some bacteria like e.g. *E. coli* increase production of AI-2 importer proteins. In doing so, they change the environment´s AI-2 level by taking up their own and other´s AI-2, resulting in an advantage for these *E. coli* cells as the other bacteria might get confused about the actual amount and mixture of bacteria in the current environment (Bassler and Losick, 2006). Further, some bacteria have receptor proteins similar to $LuxR_{A.f.}$ but lack LuxS, meaning they can take up AI-2 but not produce it, e.g. *P. aeruginosa* (Ryan and Dow, 2008).

AI-2 functions in metabolism in some bacteria (e.g. *S.typhimurium*) while it serves as an interspecies signaling molecule in others, e.g. *V. harveyi* (Vendevielle *et al.*, 2005). At the interspecies level, AI-2 controls the production of pathogenicity factors in *Streptococcus pyogenes*, toxin production in *Clostridium perfringens* and mixed biofilm formation of *Streptococcus gordonii* and *Porphyromonas gingivalis* (Auger *et al.*, 2006).

In *Bacillus cereus*, *Vibrio cholerae* and *Eikenella corrodens* AI-2 inhibits biofilm formation while in *Mycobacterium avium*, *E. coli*, *Streptococcus mutans* and *Aggregatibacter actinomycetemcomitans* it enhances biofilm formation (Geier *et al.*, 2008). On the other hand, a *luxS* mutant of *H. pylori* shows stronger initial attachment to surfaces than the wildtype (WT), while *Salmonella enterica* serovar Thyphimurium needs LuxS for initial attachment. Similarly, a *luxS* mutant of *Streptococcus mutans* produces a biofilm with less biomass and a different architecture than the WT (Parsek and

Greenberg, 2005). If genes for the AI-2 import in *E. coli* are deleted, only flat biofilms are formed (Karatan and Watnick, 2009). Additional effects of *luxS* deletion on bacteria are described in Tab. 2.

Tab. 2: Effects of *luxS* deletion

Organims	Defect	Reference
Campylobacter jejuni, C. perfingens, Porphyromonas gingivalis, Streptococcus pneumonia, Streptococcus mutans, Streptococcus pyrogenes, V. vulnificus	Virulence	Doherty *et al.,* 2006
EHEC, EPEC, H. pylori, C. jejuni	Motility	Doherty *et al.,* 2006
Klebsiella pneumonia, P. gingivalis, S. enterica, S. gordonii, S. mutans, H. pylori	biofilm formation	Doherty *et al.,* 2006
EPEC	type III secretion decreased adhesion to epithelial cells	Vendevielle *et al.*, 2005
C. jejuni	biofilm formation	Annous *et al.*, 2009
S. aureus	Growth	Doherty *et al.,* 2006 Lebeer *et al.,* 2007
Lactobacillus rhamnosus GG probiotic	biofilm formation growth	Lebeer *et al.,* 2007
S. pyogenes	Growth	Lebeer *et al.,* 2007

Cuadra-Saenz *et al.* (2012) were able to show that a *S. gondii luxS* mutant forms a distinctly different biofilm than the WT. They also showed that AI-2 influences dual-species biofilms in termes of composition and structure. Bassler and Henke (2004b) described that when *luxS* mutants of both *S. gondii* and *P. gingivalis* are grown together on a glass plate, *P. gingivalis* does not form a biofilm. Furthermore, they showed that *P. aeruginosa* was able to detect AI-2 but not able to produce it, and that AI-2 stimulates virulence factors in *P. aeruginosa.*

Rickard *et al.* (2006) described a similar effect on dual-species biofilms: the *luxS* mutant of *Streptococcus ovalis* 34 together with the *Actinomyces neaslundii* T14V WT produced a thin biofilm with less biomass than their WT dual-species biofilm. Meanwhile, both WTs were able to only form a minimal monospecies biofilm, thus demonstrating the importantance of AI-2 for bacterial biofilm formation in natural environments.

1.5 Biofilms

In natural, medical and engineered systems, the biofilm is the common growth mode of bacteria (Kavita *et al.*, 2013, Stoodley *et al.*, 2002). A biofilm is mostly composed of various bacterial species attached to each other and attached to biotic or abiotic surfaces while being embedded in a matrix consisting of various extracellular substances (Davey and O´Toole, 2000, Bassler and Losick, 2006, Fong *et al.*, 2010, Karatan and Watnick, 2009, Jiang *et al.*, 2011, Rickard *et al.*, 2006, Nakhamchik *et al.*, 2008).

Biofilms are found everywhere in the environment (Davey and O´Toole, 2000, Stoodley *et al.*, 2002). To name a few examples, the opportunistic pathogen *Mycobacterium avium* forms biofilms in drinking water pipes and water distribution systems (Geier *et al.*, 2008), *Proteus mirabilis* is found on catheter walls (Gibbs and Greenberg, 2011), cyanobacterial biofilms that occur in thermal springs are being studied (Davey and O´Toole, 2000), mixed biofilms consisting of *S. gondii* and *P. gingivalis* are found on dental plaque (Bassler and Henke, 2004b), *V. harveyi* exists in mixed biofilms on marine animals (Henares *et al.*, 2012), *V. vulnificus* is found on surfaces of algae, fish, eels and plankton (Nakhamchik *et al.*, 2008), *Lactobacillus lactei* grows as biofilms on food surfaces (Pérez-Núñez *et al.*, 2011), streptococcal and actinomycete biofilms grow on dental plaque (Rickard *et al.*, 2006), and even in agriculture and bioremediation situations biofilms are found (Nilsson *et al.*, 2011).

For *V. cholerae,* as a case point, it was shown that stool samples from patients contain both planktonic and biofilm-aggregates and the aggregates showed higher infectivity (Huq *et al.*, 2008, Fong *et al.*, 2010). It is very common that different species of bacteria live in symbiosis or competition within a biofilm (Davey and O´Toole, 2000, Stoodley *et al.*, 2002, Nadell *et al.*, 2009), e.g. *P. putida* exploits *Acinetobacter sp.* C6 within a mixed biofilm (Nadell *et al.*, 2009).

A biofilm is initially formed by bacterial cells attaching to a surface and beginning to colonize it. Microcolonies start forming and with further growth a mature biofilm emerges. The formation of pillars or mushroom-like structures is characteristic. These pillars or mushrooms are surrounded by fluid-channels. Detachment can occur e.g. due to environmental stresses and the cells enter the planktonic stage again (Fig. 10, Davey and O´Toole, 2000, Stoodley *et al.*, 2002, Fong and Yildiz, 2007, Nadell *et al.*, 2010, Parsek and Greenberg, 2005, Aguilar *et al.*, 2010).

The structural basis or matrix of biofilms includes proteins, nucleic acids, lipids and exopolysaccharides (EPS, Guttenplan and Kearns, 2013, Stoodley *et al.*, 2002, Nilsson *et al.*, 2011, Kavita *et al.*, 2013, Karatan and Watnick, 2009). Biofilms protect bacteria from stresses like cold, heat, antibiotics and also from immune responses by hosts (Davey and O´Toole, 2000, Fong and Yildiz, 2007, Jiang *et al.*, 2011, Nakhamchik *et al.*, 2008, Stoodley *et al.*, 2002, Karatan and Watnick, 2009).

Biofilms are complex multicellular, structured, co-ordinated, common supracellular life form of different communicating bacteria (Davey and O´Toole, 2000, Stoodley et al., 2002). Biofilm formation in many bacteria is associated with QS as this means the neighboring cells can communicate over short distances: the messages are sent and received quickly which can lead to advantages for a monospecies or multispecies population (Guttenplan and Kearns, 2013, Davey and O´Toole, 2000, Henares *et al.*, 2013, Karatan and Watnick, 2009). The involvement of QS in biofilm formation is summarized in Fig. 10. Some bacterial QS systems trigger the expression of motility and adhesion genes which are necessary for adhesion to surfaces and aggregation of microcolonies, while in other bacteria QS controls the expression of extrapolymeric substances like polysaccharides which are necessary for the maturation of the biofilm (Karatan and Watnick, 2009, Aguilar *et al.*, 2010).

QS controls microcolony structures in *P. aeruginosa*, *B. cepacia* and *A. hydrophila*. A QS mutant of *P. putida* forms heterogenous microcolony biofilms while the WT shows a homogenous biofilm. Here, QS affects the architecture (Labbate *et al.*, 2004). Without the 3OC12-AHL gene of *P. aeruginosa,*

only flat biofilms are formed and without pillars, water-channels and polymeric substances (Davey and O´Toole, 2000, Karatan and Watnick, 2009, Stoodley *et al.,* 2002).

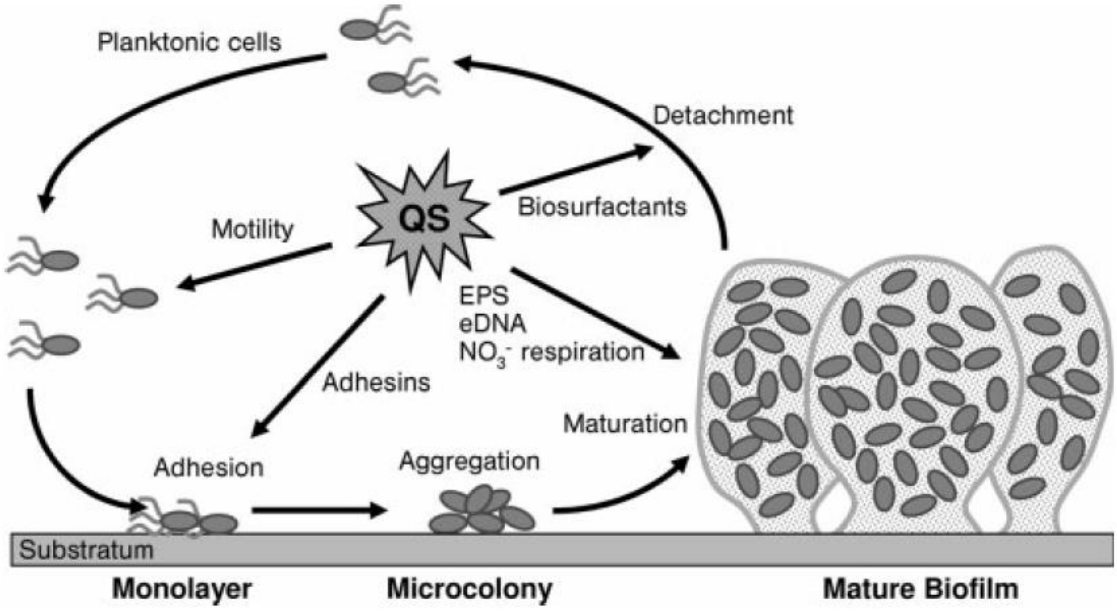

Fig. 10: Biofilm formation showing the involvement of QS

QS triggers the expression of different genes being involved in the different steps of biofilm formation. Motility and adhesins are necessary for the formation of the monolayer and microcolonies while eDNA (extracellular DNA), NO_3^- (nitrate) respiration and EPS (extrapolymeric substances) production are used for the maturation and biosurfactants for the detachment of cells (Aguilar *et al.*, 2010).

The presence of EPS in biofilms has been demonstrated and analysed in experiments using *Vibrios*, *Escherichias*, *Pseudomonas*, *Salmonella*, *Staphylococci* and *Bacilli* (Guttenplan and Kearns, 2013, Stoodley *et al.*, 2002, Nilsson *et al.*, 2011, Kavita *et al.*, 2013, Karatan and Watnick, 2009).

1.6 QS-regulated phenotypes

1.6.1 Exopolysaccharides

As mentioned above biofilm formation is associated with the production of exopolysaccharides (Serra *et al.,* 2013). EPS are carbohydrate polymers consisting of various sugar molecules, e.g. arabinose, galactose, glucose, *N*-acetyl-galactosamine and rhamnose (Hildago-Cantabrana *et al.,* 2014, Dogsa *et al.*, 2013, Kavita *et al.*, 2013, Karata and Watnick, 2009). They are secreted by many bacteria, wether as virulence factors or to protect them from the environment or from host immune systems (Hildago-Cantabrana *et al.,* 2014). Over 30 different polysaccharides have been characterized from biofilm matrices of *P. aeruginosa*, *E. coli*, *S. aureus*, *Burkholderia spp.*, *Bordetella spp.*, *Salmonella spp.*, *S. mutans* and others (Rendueles *et al.*, 2013).

EPS production in some bacteria is necessary for adhesion to surfaces (Karatan and Watnick, 2009, Güvener and McCarter, 2003, Jiang *et al.*, 2011). Stoodley *et al.* (2002) showed that *S. epidermis* uses a polysaccharide for the formation of biofilms. Similarly, it was shown that EPS are responsible for the attachment to surfaces and cell aggregation of *V. cholerae* (Parsek and Greenberg, 2005). Specifically, *V. cholerae* uses chitin polymers for attachment to crustacean shells (Nadell *et al.*, 2009) Also, *P. aeruginosa* binds disaccharides to the mucus of the human lung (Nadell *et al.*, 2009), especially *P. aeruginosa´*s polysaccharide synthesis locus *psl* is reported to be essential for the adhesion to surfaces and other cells (Guttenplan and Kearns, 2013, Ryder *et al.,* 2007, Karatan and Watnick, 2009). In *E. coli,* the polysaccharide Penicillin G acylase (PGA) is responsible for permanent attachment of the cell to a surface (Karatan and Watnick, 2009). Stoodley *et al.* (2002) reported alginate, an exopolysaccharide from *P. aeruginosa,* to be controlled by AIs and furthermore that it is present as soon as attachment of cells to surfaces occurs. On the other hand, Ryder *et al.* (2007) reported alginate was unimportant for the structure but was important for resistance of *P. aeruginosa* biofilms to stress. In contrast, Xiao *et al.* (2012) showed that EPS fills the fluid channels between the microcolonies and also covers and surrounds the bacteria.

Watnick and Kolter (2000), Jiang *et al.* (2011) and Karatan and Watnick (2009) showed that EPS determine the structure and stability of the pillars of biofilms. In *P. putida,* the exopolysaccharide gene clusters *pea* and *peb* cause stability of the biofilm (Nilsson *et al.*, 2011). Fig. 11 depicts the EPS levan from *B. subtilis* which is also found in *P. syringae* and *S. mutans.* In *B.subtilis*, levan is not essential for biofilm formation but it is part of the biofilm matrix in sucrose-rich media contributing to the biofilm´s robustness (Dogsa *et al.*, 2013).

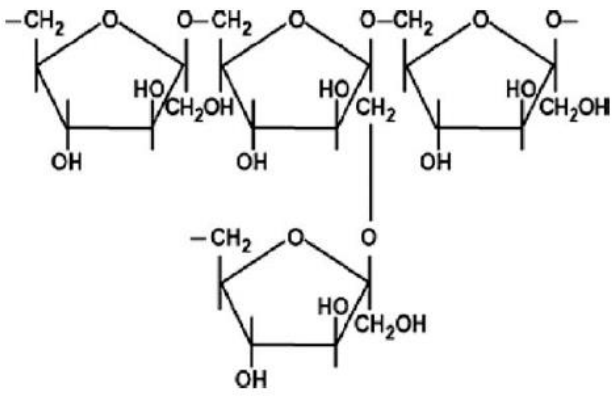

Fig. 11: Repeating units of levan which is produced by bacteria such as *B. subtilis* (Manandhar *et al.*, 2009)

In various bacteria, the results of lacking EPS genes include: decreased adhesion, deformation of the biofilm, and increased sensitivity to biocides and to host defences. On the other hand, some bacteria show increased biofilm formation when lacking EPS, so leading to the conclusion that some bacterial EPS inhibit or destabilize biofilms (*Rendueles et al.*, 2013). One example is described by Jiang *et al.* (2011) who found that an EPS from *Vibrio* sp. QY101 inhibited biofilm formation of Gram-positive and Gram-negative bacteria and disrupted already existing biofilms of *P. aeruginosa*. Also, biofilms of *E. coli* MG1655, *E. faecalis*, *K. pneumoniae*, *S. aureus*, *S. epidermis* and *P. aeruginosa* were

inhibited when cultured in mixed biofilms with uropathogenic *E. coli* strain CFT073. Furthermore, *S. aureus* biofilms were disrupted by *P. aeruginosa´*s polysaccharides Psl and Pel (*Rendueles et al.*, 2013).

It has been reported that biofilm formation is also influenced by QS (Stoodley *et al.*, 2002, Karatan and Watnick, 2009). So called "Stewartan EPS", an acidic polymer of glucose, galactose and glucuronic acid, is regulated by the QS EsaI/EsaR system of the corn pathogen *P. stewartii ssp. stewartii*, and in particular its production is repressed at low cell density because it is required in the structure only of mature biofilms. *esaR* mutants cannot attach to surfaces while *esaI* mutants form only flat biofilms (Aguilar *et al.*, 2010). Also, *Vibrio* polysaccharide gene clusters I and II from *V. cholerae* are necessary for each step of the biofilm formation and are repressed at high cell density in order to disper the biofilm (Guttenplan and Kearns, 2013, Annous *et al.*, 2009, Seper *et al.*, 2014, Huq *et al.*, 2008).

1.6.2 Colony morphology

Some bacterial species like *V. cholerae* show two distinct phenotypic colony morphology states: rugose and smooth (Guttenplan and Kearns, 2013, Huq *et al.*, 2008, Farmer and Janda, 2005). *Vps* (Vibrio polysaccharide) gene expression leads to the rugose phenotype of *V. cholerae* which is associated with biofilm formation (Guttenplan and Kearns, 2013, Karatan and Watnick, 2009). A switch from translucent to opaque colonies has also been described for *N. gonorrhoeae*, *V. vulnificus* and *V. parahaemolyticus* (Farmer and Janda, 2005, McCarter, 1998). Capsular polysaccharide production, virulence and biofilm formation have been associated with opacity (McCarter, 1998). Rugose colony morphology is also seen in *Pseudomonas spp.* which are called wrinkly spreader and also in *E. coli* which colonies become dry and rough (Karatan and Watnick, 2009). Colony morphology in *Pseudomonas spp.* and *E. coli* is associated with high amounts of EPS and robust biofilms (Karatan and Watnick, 2009).

The outgrowth of macrocolonies on agar plates has been described as biofilm formation for *E. coli* in order to investigate the structure and physiology of the colony as well as on single cell level (Serra *et al.,* 2013). Single and multispecies biofilms exhibit different cell morphologies (Davey and O´Toole, 2000). *C. jejuni* e.g. can co-exist in the same population as coccoid cells and filaments (Young, 2006). Furthermore, it was shown that *Serratia liquefaciens* biofilms can consist of cell aggregates, cell chains and filamentous cells unlike *E. coli* or *P. aeruginosa* biofilms (Labbate *et al.*, 2004, Parsek and Greenberg, 2005).

Bacteria need to adapt to changing environments and this can occur by changing their cell morphology, e.g. filamentation, sporulation, extrusion of appendages and also, rod-shaped bacteria turn coccoid or vise-versa. The major determinants of cell shape are the cell wall and the bacterial cytoskeleton. In both *E. coli* and *Bacillus*, model Gram-negative and Gram-positive organisms respectively, two systems exist for cell wall synthesis: one for septation and one for elongation (Pérez-Núñez *et al.*, 2011).

Being able to change shape provides advantages for the attachment of the bacteria to surfaces in the presence of influences from: nutrient flow, neigbouring cells and shear forces. In the stationary phase, it is common for rod-shaped bacteria to turn coccoid due to decreased division. This behavior

is genetically regulated. In the case of nutrient depletion, the population achieves a greater survival rate if the cells are smaller and therefore, the nutrients can be shared by more bacteria (Stoodley *et al.,* 2002, Davey and O´Toole, 2000, Young, 2006). However, cells also enlarge into filaments in the stationary phase or when nutrients are limiting in order to increase their surface area without changing the surface-to-volume ratio or in order to outgrow competitors (Stoodley *et al.,* 2002, Davey and O´Toole, 2000, Young, 2006).

1.7 Aims of this thesis

Vibrio harveyi was used in this thesis as it is an established model organism with a complex QS system. Biofilms are a common way of life for bacteria. Biofilm formation is a serious threat to plant, animal and human life as biofilms have been established regarding every niche.

As there is only little known about biofilm formation of *V. harveyi*, the first aim of this thesis is to establish a flow system in the laboratory and determine the perfect time point for later experiments.

QS has a major effect on bacterial life. The impact of QS on biofilm formation of *V. harveyi* will be determined and therefore, as the second aim, the biofilm structure of the WT will be compared to a QS ON and QS OFF mutant. Also, it will be necessary to determine within the QS system which AI has the most significant effect on biofilm formation. Here, the biofilms of single AI deletion mutants will be analysed in comparision with the WT as aim 3.

In addition, in biofilm formation studies exopolysaccharides have been greatly discussed and as EPS can function either way, promoting or inhibiting biofilms, it is necessary to study bacterial EPS in order to understand biofilms effectively. As the fourth aim of this thesis, a search for genes possibly coding for exoploysaccharides will be undertaken. Knock-out mutants will be generated and characterized for their EPS production and biofilm formation.

Finally, another possibility for biofilm formation is the outgrowth of macrocolonies on agar plates. Here, knock out mutants will be compared to the WT for their colony morphology and structure. Also, Scanning Electron Microscopy will determine differences of the macrocolonies on single cell level of the WT, the QS ON and the QS OFF mutant (aim 5).

2 Materials and methods

2.1 Materials

All chemicals (Tab. 3), enzymes (Tab. 4), kits (Tab. 5), bacterial growth media recipes (Tab. 6), antibiotics (Tab. 7), strains (Tab. 8), plasmids (Tab. 9) and oligonucleotides (Tab. 10) used in this thesis are listed below and referenced.

2.1.1 Chemicals

Tab. 3: Chemicals

Designation	Reference
Agar Agar	Otto Nordwald (Hamburg, Germany)
Agarose	Serva (Heidelberg, Germany)
Acetone	Roth (Karlsruhe, Germany)
Bromophenol blue	Roth (Karlsruhe, Germany)
Caseine	Roth (Karlsruhe, Germany)
$CaCl_2$	Roth (Karlsruhe, Germany)
Cacodylate	Roth (Karlsruhe, Germany)
DAP	Sigma-Aldrich (Munich, Germany)
DNA-Standard (2-Log DNA-Ladder)	New England Biolabs (Frankfurt, Germany)
dNTPs	Fermentas/ Thermo Fisher Scientific (Schwerte, Germany)
EDTA	Roth (Karlsruhe, Germany)
Ethidium bromide	Roth (Karlsruhe, Germany)
EtOH	Roth (Karlsruhe, Germany)
glacial acetic acid	Roth (Karlsruhe, Germany)
Glucose	Roth (Karlsruhe, Germany)
Glutaraldehyde	Electron Microscopy Sciences, Science Services, Munich, Germany
Glycerol	Roth (Karlsruhe, Germany)
HCl	Roth (Karlsruhe, Germany)
H_2SO_4	Roth (Karlsruhe, Germany)
KCl	Roth (Karlsruhe, Germany)
KOH	Merck Millipore (Darmstadt, Germany)
K_2HPO_4	Roth (Karlsruhe, Germany)
KH_2PO_4	Roth (Karlsruhe, Germany)
L-Arginine	Roth (Karlsruhe, Germany)
$MgCl_2$	Roth (Karlsruhe, Germany)
$MgSO_4$	Roth (Karlsruhe, Germany)
NaH_2PO_4	Roth (Karlsruhe, Germany)
Na_2HPO_4	Roth (Karlsruhe, Germany)

Designation	Reference
NaCl	Roth (Karlsruhe, Germany)
NaClO	Roth (Karlsruhe, Germany)
NaOH	Roth (Karlsruhe, Germany)
Nitrogen, liquid	Linde (Munich, Germany)
OsO_4	Electron Microscopy Sciences, Science Services, Munich, Germany
PIPES	Roth (Karlsruhe, Germany)
Phenol	Roth (Karlsruhe, Germany)
Saccharose	Roth (Karlsruhe, Germany)
SDS	Roth (Karlsruhe, Germany)
Tris	Roth (Karlsruhe, Germany)
Tryptone	Roth (Karlsruhe, Germany)
Yeast extract	Otto Nordwald (Hamburg, Germany)

2.1.2 Enzymes

Tab. 4: Enzymes

Designation	Reference
DNaseI	Sigma-Aldrich (Munich, Germany)
RnaseA	Sigma-Aldrich (Munich, Germany)
Proteinase K	Sigma-Aldrich (Munich, Germany)
Taq-DNA-Polymerase	self-made by laboratory technician Sabine Scheu
Phusion-DNA-Polymerase	Finnzymes (Espoo, Finnland)
Phusion-DNA-Polymerase	self-made by Dr. Jürgen Lassak
Q5-DNA-Polymerase	New England Biolabs (NEB, Frankfurt, Germany)
T_4 DNA Ligase	NEB(Frankfurt, Germany)
Restriction enzymes	NEB (Frankfurt, Germany)

2.1.3 Kits

Tab. 5: Kits

Designation	Reference
HiYield Gel Extraktion Kit	SLG (Gauting, Germany)
HiYield Plasmid Mini-Kit	SLG (Gauting, Germany)
Ultra Clean-Microbial DNA Isolation Kit	MO-BIO Laboratories Inc. (California,USA)
Removal of genomic DNA from RNA preparations	Fermentas/ Thermo Fisher Scientific (Schwerte, Germany)
RevertAid H Minus First Strand cDNA Synthesis Kit	Fermentas/ Thermo Fisher Scientific (Schwerte, Germany)

2.1.4 Bacterial growth media

Tab. 6: Bacterial growth media

Designation	Composition	Reference
AB media	1.75% (w/v) NaCl, 1.23% (w/v) $MgSO_4$, 0.2% (w/v) Casein hydrolysate, pH was adjusted to 7.5 using KOH, after autoclaving 1 mM Potassium phosphate-buffer, 10% glycerol and 1 mM Arginine was added	Miller, 1972
LB media	1% (w/v) NaCl, 1% (w/v) Trypton, 0.5% (w/v) yeast extract	Greenberg, *et al.* 1979
Glycerol freezing media	16 mM KCl, 16 mM $NaCl_2$, 0.4 mM $MgSO_4$, 87% glycerol	Modified from Sambrook and Russell (2001)

2.1.5 Antibiotics

Tab. 7: Antibiotics

Designation	final concentration	Reference
Ampicillin	100 µg/ml	Roth (Karlsruhe, Germany)
Carbenicillin	100 µg/ml	Roth (Karlsruhe, Germany)
Chloramphenicol	34 µg/ml	Sigma-Aldrich (Munich, Germany)
Kanamycin	100 µg/ml	Roth (Karlsruhe, Germany)

2.1.6 Strains

Tab. 8: Strains

Strain	Genotype	Reference
Escherichia coli DH5αλpir	Φ80*dlacZ*ΔM15 Δ(*lacZYA-argF*) U196 *recA1 hsdR17 deoR thi-l supE44 gyrA96 relA1/ëpir*	Miller and Mekalanos, 1988
Escherichia coli WM6034	BW29427 *ThrB*1004 *pro thi rpsL hsdS lacZ*ΔM15 RP4-1360 Δ(*araBAD*)567 Δ*dapA*1341::[*erm pir*(wt)]	Metacalf, University of Illinois, Urbana, unpublished
Vibrio harveyi BB120	Wildtype	Bassler, *et al.*, 1997
Vibrio harveyi BB120gfp	Wildtype-'Tn7T:eGFP-Cam	Lassak, unpublished
Vibrio harveyi JMH634	Δ*luxM* Δ*luxS cqsA*::cam	Henke and Bassler, 2004a
Vibrio harveyi MR3	BB120 Δ*luxS*	Reiger, 2014
Vibrio harveyi MR3gfp	BB120 Δ*luxS*-'Tn7T:eGFP-Cam	Current thesis
Vibrio harveyi MR13	BB120 Δ*cqsS*	Reiger, 2014
Vibrio harveyi MR13gfp	BB120 Δ*cqsS*-'Tn7T:eGFP-Cam	Current thesis
Vibrio harveyi MR15	BB120 Δ*luxS* Δ*luxM* Δ*cqsS*	Reiger, 2014

Strain	Genotype	Reference
Vibrio harveyi MR15gfp	BB120 Δ*luxS* Δ*luxM* Δ*cqsS*-'Tn7T:eGFP-Cam	Current thesis
Vibrio harveyi MR18	BB120 Δ*luxM*	Reiger, 2014
Vibrio harveyi MR18gfp	BB120 Δ*luxM*-'Tn7T:eGFP-Cam	Current thesis
Vibrio harveyi ΔluxO	BB120 Δ*luxO*	Reiger, 2014
*Vibrio harveyi ΔluxO*gfp	BB120 Δ*luxO*-'Tn7T:eGFP-Cam	Current thesis
Vibrio harveyi EMR2	BB120 Δ*VIBHAR_05206-05205*	Current thesis
Vibrio harveyi EMR2gfp	BB120 Δ*VIBHAR_05206-05205*-'Tn7T:eGFP-Cam	Current thesis
Vibrio harveyi EMR3	BB120 Δ*VIBHAR_06667*	Current thesis
Vibrio harveyi EMR3gfp	BB120 Δ*VIBHAR_06667*-'Tn7T:eGFP-Cam	Current thesis
Vibrio harveyi EMR8	BB120-p*VIBHAR_05206*:GFP	Current thesis
Vibrio harveyi EMR9	BB120-p*VIBHAR_06667*:GFP	Current thesis
Vibrio harveyi EMR12	BB120-VIBHAR_05207:GFP	Current thesis
Vibrio harveyi EMR14	MR3-pBBR1-MSC2-BAD-KLuxS	Current thesis
Vibrio harveyi EMR14gfp	MR3-pBBR1-MSC2-BAD-KLuxS -'Tn7T:eGFP-Cam	Current thesis
Vibrio harveyi EMR16	BB120-VIBHAR_06667:GFP	Current thesis
Vibrio harveyi EMR17	EMR2 reinserted with *VIBHAR_05206-05205*	Current thesis
Vibrio harveyi EMR17gfp	EMR2 reinserted with *VIBHAR_05206-05205* -'Tn7T:eGFP-Cam	Current thesis
Vibrio harveyi EMR18	EMR3 reinserted with *VIBHAR_06667*	Current thesis
Vibrio harveyi EMR18gfp	EMR3 reinserted with *VIBHAR_06667* -'Tn7T:eGFP-Cam	Current thesis
Vibrio harveyi EMR19	MR3 reinserted with *LuxS*	Current thesis
Vibrio harveyi EMR19gfp	MR3 reinserted with *LuxS* -'Tn7T:eGFP-Cam	Current thesis
Vibrio harveyi EMR20	BB120 Δ*VIBHAR_02222-02221*	Current thesis
Vibrio harveyi EMR20gfp	BB120 Δ*VIBHAR_02222-02221*-'Tn7T:eGFP-Cam	Current thesis
Vibrio harveyi EMR21	EMR20 reinserted with *VIBHAR_02222-02221*	Current thesis
Vibrio harveyi EMR21gfp	EMR20 reinserted with *VIBHAR_02222-02221* -'Tn7T:eGFP-Cam	Current thesis
Vibrio harveyi EMR22	BB120 Δ*VIBHAR_02222-02221* Δ*VIBHAR_05206-05205* Δ*VIBHAR_06667*	Current thesis
Vibrio harveyi EMR22gfp	BB120 Δ*VIBHAR_02222-02221*	Current thesis

Strain	Genotype	Reference
	Δ*VIBHAR_05206-05205* Δ*VIBHAR_06667* -'Tn7T:eGFP-Cam	
Vibrio harveyi EMR23	BB120 Δ*VIBHAR_01320*	Current thesis
Vibrio harveyi EMR23gfp	BB120 Δ*VIBHAR_01320*-'Tn7T:eGFP-Cam	Current thesis

2.1.7 Plasmids

Tab. 9: Plasmids

Plasmid	Resistence	Function	Reference
pNPTS138-R6KT	Kan^R	*mobRP4*$^+$*ori*-R6K *sacB*; suicide plasmid for in-frame deletions; Kan^R	Lassak *et al.* (2010)
pUC18R6KT-miniTn7t-eGFP-cm	Cam^R	*Not*I-egfp-Cam^R-*Not*I fragment from pBK-miniTn7-*gfp3* in pUC18-R6KT-miniTn*7*T	Gödeke *et al.* (2011)
pTNS2	Amp^R	ori-R6K; encodes the TnsABC+D specific transposition pathway, Amp^R	Choi *et al.* (2005)
pBBR1-MSC2-BAD	Kan^R	Broad-host range cloning vector by Kovach *et al.* (1995), P_{ara} and *araC* were cloned with *Nsi*I and *BamH*I sites	Reiger, 2014
pNPTS138-R6KT-eGFP	Kan^R	*mobRP4*$^+$*ori*-R6K *sacB*; eGFP was inserted into the multiple cloning site; Kan^R	Lassak, unpublished
pNPTS138R6KT-Δ2222-1	Kan^R	Deletion of *VIBHAR_02222-02221* using *BamH*I and *Nhe*I	this study
pNPTS138R6KT-Δ5206-5	Kan^R	Deletion of *VIBHAR_05206-05205* using *Spe*I and *BamH*I	this study
pNPTS138R6KT-Δ6667	Kan^R	Deletion of *VIBHAR_06667* using *BamH*I and *Nhe*I	this study
pNPTS138R6KT-Δ1320	Kan^R	Deletion of *VIBHAR_01320* using *BamH*I and *Nhe*I	this study
pNPTS138R6KT-UpluxSdown	Kan^R	Knock-in of *LuxS* using *Spe*I and *Nhe*I	this study
pNPTS138R6KT-Up2222-1down	Kan^R	Knock-in of *VIBHAR_02222-02221* using *BamH*I and *Nhe*I	this study
pNPTS138R6KT-Up5206-5down	Kan^R	Knock-in of *VIBHAR_05206-05205* using *Spe*I and *BamH*I	this study
pNPTS138R6KT-Up6667down	Kan^R	Knock-in of *VIBHAR_06667* using *BamH*I and *Nhe*I	this study
pBBR1_MCS2-BAD-KluxS	Kan^R	Complementation in *trans* of *LuxS* using *Spe*I and *Xma*I	this study
pBBR1_MCS2-BAD-K5206-5	Kan^R	Complementation in *trans* of *VIBHAR_05206-05205* using *Spe*I and *Xma*I	this study
pBBR1_MCS2-BAD-K6667	Kan^R	Complementation in *trans* of *VIBHAR_06667* using *Spe*I and *Xma*I	this study
pNPTS138-R6KT-eGFP_5206	Kan^R	GFP-Promoter fusion of *VIBHAR_05206* using BamHI and PspOMI	this study
pNPTS138-R6KT-	Kan^R	GFP-Promoter fusion of *VIBHAR_06667*	this study

Plasmid	Resistence	Function	Reference
eGFP_6667		using BamHI and PspOMI	
pNPTS138-R6KT-eGFP_H5207	Kan^R	GFP-hybrid protein of *VIBHAR_05207* using BamHI and PspOMI	this study
pNPTS138-R6KT-eGFP-H6667	Kan^R	GFP-hybrid protein of *VIBHAR_06667* using BamHI and PspOMI	this study

2.1.8 Oligonucleotides

All oligonucleotides (Tab. 10) used in this thesis were designed using Clone Manager9 Professional Edition by Scientific & Educational Software (Cary, NC, USA) and ordered by Sigma-Aldrich (Munich, Germany).

Tab. 10: Oligonucleotides

Oligonucleotide	Sequence 5‘-3‘
a) Primers for the generation of deletion mutants	
UP5206_RE_s	TGATTTACTAGTTACTTCTAGCTATTTCCCTC
Up_5206_New_OL_as	GCCTGTCATATGATGGACTCAGTACGCAT
Down_5205_new_OL_s	GTCCATCATATGACAGGCAATTCAATGAACG
Down5205_RE_as	ATATCCGGATCCCTCTTGAATGTTTGAAGTGC
Check5206_up	GGGTAAAACGCTTAGAAGACA
Check5205_down	GGATCGGTAGAGCGAAAACGA
UP6667_RE_s	GGGCTTGGATCCCAGAAGCTCTTTCCAATAGTG
UP6667_OL_as	TTCAACGGGCAGATGAACTTATAGTGTGGTTAGCCAT
Down6667_OL_s	TTCATCTGC CCGTTGAAGTGAAAAGCCAA
Down6667_RE_as	TACTTGAGCTAGCCTTGCTCGAAGAAAAAACGCGCCT
Check6667_up_s	AAGGTGTTCTACGCGTTAGAA
Check6667_down_as	TTGTCTCGCGAGGTGGCAAAT
Up2222_RE_s	AAATGGGGATCCACAACCCATTAACCGGCGTA
UP2222_OL_as	AACGAGGTCATCGTTCTCTCCTCGAGCC
Down2221_OL_s	AGAACGATG ACCTCGTTTTTTGGCTAACC
Down2221_RE_as	CATTTAGCTAGCTCAACTTAGCGCTCAAAGCT
Check2222_s_new	TTGATGCCTCTGCAATGGGCCG
Check2221_as_new	CATTAAGCCGTGCGGCGATGCC
Up1320_RE_s	CATTTCGGATCCCATTGGCACTAGATAGAAC
UP1320_OL_as	GATTCACATTATAGTCGTTAACCG
Down1320_OL_s	ATAATGTGAATCATAAGGCTCACGA
Down1320_RE_as	GTCTGTGCTAGCTTCTAGCGCGAACTTTGA
Check1320_up_s	CGGCATTCTTATAGAAGCTCA
Check1320_down_as	TTCGATCAATGCTACCTTGAT
SpeI_6667_s	GGCTTACTAGTCAGAAGCTCTTTCCAATAGTG
Upstream_LuxS_SpeI_s	ACCAAAACTAGTCATTCTTGGCTTTATTCCATGGGGG
Downstream_LuxS_NheI_as	CAACGCGCTAGCCAGCGTATCGGCTTAATTGTCGATG
LuxS_chk_s	AGTAGCTTTCGCCACGACGCT
LuxS_chk_as	CACCTCTGAACGTGCAAATGTTGAAG
6667_XmaI_as	TTTCACCCGGGCGGGGAGTTAGATTATTCAC

Oligonucleotide	Sequence 5‘-3‘
SpeI_LuxS_up_s	AACGTACTAGTGGCGATCATTAAGCAAGAAAG
LuxS_XmaI_as	CTAAAACCCGGGTTAGTCGATGCGTAGCTCTCTC
SpeI_5206_s	CTAGCTATTACTAGTGGAATCAAACTGACCTCCAAA
5205_XmaI_as	ATTGCCCCGGGTTAGAAGAAGCTCTGATCGAT
M13_uni-sense-21	TGTAAAACGACGGCCAGT
M13_reverse-29	CAGGAAACAGCTATGACCATG
b) qRT-PCR primers	
LuxR_118_s	GCG GAT ATT GCA GAG ATC GCT CA
LuxR_266_s	GCG TGG ATG TCT AAG TCG ATG TTA TC
recAq_ER_s	GAT ATC GCT TTG GGT GCT GGT
recAq_ER_as	TGC CTT CAC GTT GCG CAG CA
2222q_s	CTC TGC ATG GGC ACG TAG AG
2222q_as	ATC CAC GGC AGT CGG AAG TGA
5206q_s	GCGTGTTCTACGAAGGTGATG
5206q_as	GTT CAA TTT TAG CCA ACA GGG CAG
6667q_s	TTG CCG TTG CGT TGC TAT CGA
6667q_as	TCA GCA GCA AAA AGG TCG CC
c) Primers for GFP-promoter fusions	
Up5206_gfptag_s	CTAGCTATT GGATCC GGA ATC AAA CTG ACC TCC AAA
Up5206_gfptag_as	TTA TGA GGGCCC CAG TAC GCA TTT GAG CCT GTA
Up6667_gfptag_s	GGCTT GGATCC CAG AAG CTC TTT CCA ATA GTG
Up6667_gfptag_as	ATA GTGGGCCC AGC CAT TAT TTT TAT GTT TCG CCA AG
d) Primers for GFP-hybrid proteins	
Up5207_BamHI_s	CGTGCAGGATCCGATTCATGGATACGAAGAGCT
Down5207_PspOMI_as	GATGGAGGGCCCACGCATTTGAGCCTGTAAATC
new6667_PspOMI_as	TTAGATGGGCCCCTTTTGTAAGCGTAGTTGTAA

M13_uni-sense-21 and M13_reverse-29 are primers annealing just outside of the multiple cloning site of pNPTS138-R6KT and were designed by Lassak (unpublished). The primers LuxR_118_s and LuxR_266_as were designed by Reiger (2014). Up6667_gfptag_s was also used for the generation of the VIBHAR_06667:GFP hybrid protein.

2.2 Methods

2.2.1 Cultivation techniques

2.2.1.1 Cultivation of Escherichia coli and Vibrio harveyi

E. coli was cultured in LB media at 37°C aerobically on the turning wheel TC-7 from New Brunswick Scientific (Edison, USA) while *V. harveyi* was cultured aerobically in AB media for experiments and in LB for mating at 30°C on the same turning wheel.

V. harveyi bioassays were performed by cultivation in 96 well plates aerobically on a Titramax1000 from Heidolph (Schwabach, Germany) at 1,050 rpm at 30°C.

Mating was carried out on 1.5% LB-agar plates supplemented with specific antibiotics or other supplements such as DAP or saccharose o/n or for 2 days.

2.2.1.2 Stock cultures

E. coli cells were mixed with 10% glycerol and stored at -20°C. *V. harveyi* strains were mixed with 75% glycerol freezing media, shock frozen with liquid nitrogen and stored at -80°C.

2.2.2 Molecular biology and genetics

2.2.2.1 Modification of DNA

Standard DNA Techniques were performed if not otherwise mentioned according to Sambrook and Russell (2001). Restrictions and ligations were performed as the manufacturer indicated. Linearized vectors were treated with alkaline phosphatase (NEB, Frankfurt, Germany) to inhibit relegation.

2.2.2.2 Isolation of plasmids

The *E. coli* strain containing the plasmid of interest was cultivated o/n aerobically in test tubes at 37°C on the turning wheel TC-7 and 3 ml were used for plasmid extraction using the HiYield plasmid mini-kit from SLG (Gauting, Germany). Elution was either done with 30-50 µl elution buffer or ddH_2O. The concentration of extracted plasmids was measured using a Nanodrop® Spectrometer ND-1000 UV/vis. Extracted plasmids were stored at -20°C.

2.2.2.3 Isolation of genomic DNA

Genomic DNA was extracted out of 5 ml o/n aerobically grown strains using the Ultra Clean Microbial DNA Isolation-Kit from MO BIO Laboratories Inc. (California, USA) as indicated by the manufacturer. The concentration was measured using a Nanodrop® Spectrometer ND-1000 UV/vis (Peqlab Biotechnologie GmbH, Erlangen, Germany). Extracted DNA was stored at -20°C.

2.2.2.4 Polymerase chain reaction

DNA fragments were amplified using the polymerase chain reaction (Mullis and Faloona, 1987) *in vitro*. The reaction was performed with either Phusion or Q5 polymerase (New England Biolabs, Frankfurt, Germany) using the primer pairs in Tab. 10 in either the Mastercycler nexus or Mastercycler personal from Eppendorf (Hamburg, Germany), for the concentration used in the mastermix see Tab. 10. The protocol was carried out starting with an initial denaturing cycle of 5 min at 98°C, followed by 35-40 cycles of 30 s denaturing at 98°C, 30 s annealing at 50-60°C (depending on the primers) and between 30 s and 6 min elongation at 72°C (depending on the size of the fragment (1 kb per 30 s)), the final step was 10 min elongation at 72°C. The reaction was cooled to 14°C until it was stopped and the PCR reactions were used for gel electrophoresis in either a Mini Sub DNA Cell

GT-agarose gel-running device or a Wide Mini Sub DNA Cell GT-agarose gel-running device in the Power-Pac™ basic system from Biorad (Munich, Germany).

Tab. 11: Mastermix of PCR reactions

Components	50 µl volume	Final concentration
ddH_2O	31.5 µl	
5x Phusion GC Buffer (F-519) or Q5 Standard Buffer	10 µl	
10 mM dNTPs	1 µl	200 µM each
Primer_sense (10 µM)	2.5 µl	0.5 µM
Primer_antisense (10 µM)	2.5 µl	0.5 µM
Template	2 µl	
Phusion or Q5 Polymerase	0.5 µl	0.02 U/µl

2.2.2.5 Colony polymerase-chain reaction

The master mix was set up using a mixture of self-made Taq and Phusion polymerase (1:1 ratio) and the check primer pairs in Tab. 10, and distributed into PCR tubes (for the mastermix see Tab. 11). Genomic DNA from either WT or a mutant strain was used as negative or positive control and colonies were picked from LB plates with specific antibiotics with a toothpick and transferred into the PCR tubes as well as a new LB plate supplemented with the specific antibiotic. The PCR was carried out in the Mastercycler nexus or Mastercycler personal. The protocol started with an initial denaturing cycle of 5 min at 95°C, followed by 35-40 cycles of 30 s denaturing at 95°C, 30 s annealing at 50-60°C (depending on the primers) and between 1 and 6 min. elongation at 72°C (depending on the size of the fragment (1 kb per 30 s)), the final step was 10 min. elongation at 72°C. The reaction was cooled to 14°C until it was stopped and the PCR reactions were used for gel electrophoresis in either a Mini Sub DNA Cell GT-agarose gel-running device or a Wide Mini Sub DNA Cell GT-agarose gel-running device in the Power-Pac™ basic system.

Tab. 12: Mastermix for colony-PCR

Components	20 µl	Final concentration
ddH_2O	13.5 µl	
10x Taq buffer	2.5 µl	
10 mM dNTPs	0.5 µl	250 µM each
Check primer sense (10 µM)	1 µl	0.5 µM
Check primer antisense (10 µM)	1 µl	0.5 µM
Template	1 µl	
Phusion:Taq 1:1	0.5 µl	0.02 U/µl

2.2.2.6 Electrophoretic separation of DNA-fragments

PCR or restricted fragments or plasmids were analysed and separated by gel electrophoresis for 35 min at 120 V. TAE buffer (40 mM Tris; 40 mM glacial acetic acid; 1 mM EDTA) was used for the preparation of the gels and as running buffer. The samples were mixed with loading dye (50% (v/v) Glycerol; 0.1 M EDTA; 1% (w/v) SDS; 0.1% (w/v) Bromophenol blue) and then placed into the wells of a 0.2 µg/ml ethidium bromide stained 2% (w/v) agarose gel. The gels were run in either a Mini Sub DNA Cell GT-agarose gel- running device or a Wide Mini Sub DNA Cell GT-agarose gel-running device in the Power-Pac™ basic system.

Purification of the bands was done using the HiYield Gel extraction kit from SLG (Gauting, Germany) as indicated by the manufacturer.

2.2.2.7 Determination of DNA or plasmid concentration

The concentration of DNA fragments or plasmids from a PCR, a plasmid extraction or after restriction was determined using a Nanodrop® Spectrometer ND-1000 UV/vis. Nucleic acids absorb light at a wavelength between 250-270 nm, however the absorption maximum is at 260 nm.

2.2.2.8 DNA-sequence analysis

The Service Unit in the institute of Genetics at the LMU performed all sequencing experiments. DNA or plasmids were sequenced using an ABI 3730 DNA Analyzer from Applied Biosystems and Hitachi (Foster City, CA, USA) with 50 cm capillary length providing excellent fragment separation and sensitivity. Usually, sequencing was performed via a clean, cycle and run protocol, this is in detail: Between 50-150 ng DNA or 150 – 300 ng plasmid were mixed with a sense or antisense primer (2-10 pmol, see primer Tab. 9) and 10 mM Tris/HCl (pH 8.5). Sequences were analysed using Clone Manager9 Professional Edition by Scientific & Educational Software (Cary, NC, USA) or Chromas Lite 2.1.1 by Technelysium Pty Ltd (South Brisbane, QLD, Australia).

2.2.2.9 qRT-PCR

Cultivation of strains *V. harveyi* WT and JMH634 and RNA extraction at differet time points were performed by Reiger (2014) following the protocol by Wei (2012). The primers were tested in a primer efficiency test using gDNA from the WT in the iQ5 Detectionssystem by Bio-Rad.

The RNA samples were treated with DNaseI following the protocol of the kit “removal of genomic DNA in RNA preparations” by Fermentas/ Thermo Fisher Scientific. This step was controlled by agarose gel electrophoresis. Then, cDNA from the treated RNA samples was synthesized using the “RevertAid H Minus First Strand cDNA Synthesis Kit” Fermentas/ Thermo Fisher Scientific.All samples were adjusted to a concentration of 13 ng/µl using DEPC-treated water by Fermentas/ Thermo Fisher Scientific. A quantitative Real-Time PCR (qRT-PCR) using the specific primer combinations (Tab. 10) was performed with the iQ SYBR® Green Supermix by Bio-Rad in a iQ5 Detectionssystem by Bio-Rad. As controls RNA samples were used for the recA primer combination and DEPC-treated water for all primer combinations were used.

After 40 repeats in a 2-step-cycle, the C_T values were determined by the iQ software by Bio-Rad. Relative expression patterns of the specific genes were normalized with a non-regulated gene which is constitutively expressed, in our case recA, and calcuted using the ΔC_T method (Livak and Schmittgen, 2001).

2.2.2.10 Competent cells and transformation

Two different protocols were used for competent cells, the first transcribed here, was for *E. coli* DH5αλpir cells and the second one described is for *E. coli* WM3064 cells.

First the method of Inoue *et al.* (1990) was modified according to our laboratory standards: *E. coli* DH5αλpir cells were grown o/n in LB media aerobically at 37°C. The cells were diluted in the morning 1:70 into 200 ml fresh LB media and cultivated aerobically at 37°C and 200 rpm for 2 h on a Certomat® from Sartorius (Göttingen, Germany) until an $OD_{600\ nm}$ of 0.6 was reached. Then the cells were put on ice for 10 min, followed by centrifugation at 4°C and 5,000 rpm in pre-cooled falcon tubes for 10 min. The cells were resuspended in 100 ml transformation buffer (50 mM $CaCl_2$, 10 mM PIPES, 15% glycerol, pH 6.6) and left for incubation on ice for 20 min. The cells were then centrifuged at 4°C and 5,000 rpm for 10 min in a Centrifuge 5804R using the A-4-44 rotor and resuspended in 10 ml transformation buffer. This suspension was distributed into pre-cooled 15 ml Eppendorf tubes each containing 200 µl competent cells, shock frozen with liquid nitrogen and stored at -80°C.

Transformation according to the protocol of Sambrook and Russell (2001) with competent *E. coli* DH5αλpir cells was performed as follows: The cells were mixed with either the o/n ligation or 2 µl of a plasmid (100 – 200 ng) and left on ice for 10 – 30 min. Heat shock was performed at 42°C for 90 s and then the cells were cooled on ice for another 2 min. 880 µl LB media was added to the cells and then the cells were aerobically shaken on a ThermoMixer comfort by Eppendorf (Hamburg, Germany) at 37°C, 1,050 rpm for 1 h to 90 min. The cells were then centrifuged at 13,200 rpm in a Centrifuge 5415R with a F45-24-11 rotor from Eppendorf (Hamburg, Germany) and resuspended in 100 µl fresh LB media. These cells were then plated on LB plates with specific antibiotics.

Secondly, according to the method of Dagert and Ehrlich (1979), *E. coli* WM3064 cells were grown o/n aerobically in LB-DAP media and diluted 1:100 in 50 ml fresh LB-DAP media in the morning. The cells were grown aerobically at 37°C until the $OD_{600\ nm}$ of 0.3 – 1 was reached. The cells were left on ice for 15 min and centrifuged in a Centrifuge 5804R using the A-4-44 rotor at 4°C and 800 g for 20 min and then resuspended in 0.1 M $CaCl_2$, followed by an incubation on ice for 20 – 30 min. The cells

were centrifuged again in the Centrifuge 5804R using the A-4-44 rotor at 4°C and 800 g for 20 min and resuspended in 2 ml 0.1 M $CaCl_2$. The cells were stored at 4°C for a max. of 4 weeks.

Transformation according to the protocol of Inoue *et al.* (1990) with competent *E. coli* WM3064 was adjusted as follows: The cells were mixed with either the o/n ligation or 2 µl of a plasmid (100 – 200 ng) and left on ice for 30 min. Heat shock was performed at 42°C for 30 s and 800 µl LB-DAP media was added to the cells and then the cells were aerobically shaken on a ThermoMixer Comfort at 37°C, 1,050 rpm for 60 to 90 min. The cells were then centrifuged at 13,200 rpm in with Centrifuge 5415R with the F45-24-11 rotor and resuspended in 100 µl fresh LB media. These cells were then plated on LB-DAP plates with specific antibiotics.

2.2.2.11 Generation of deletion mutants

To delete a gene in the *V. harveyi* WT, the Up-RE-sense and Up-OL-antisense primers (Tab. 10) were used in a PCR with WT genomic DNA and Q5 or Phusion Polymerase to amplify the 500 bp upstream fragment of the specific gene. The same was done with the Down-OL-sense and Down-RE-antisense primers (Tab. 10) to generate the downstream fragment. Both fragments were fused in an overlap-PCR. The fused fragment and the empty pNPTS138R6KT plasmid were restricted with the specific restriction enzymes listed in Tab. 4 and ligated in a vector:insert ratio of 1:6 with T4 DNA ligase o/n in a water bath starting at 0°C. The competent DH5αλpir cells were transformed with the ligation and plated on LB plates supplemented with kanamycin for outgrowth o/n at 37°C or for 48 h at RT.

The plasmid was extracted using HiYield plasmid mini-kit from SLG (Gauting, Germany) and was control restricted with the restriction enzymes priorly used. If no band was visible after gel electrophoresis, either sequencing and/or PCR was performed with the universal primers M13_uni-sense-21 or M13_reverse-29 or the primers listed in Tab. 10.

Competent *E. coli* WM3064 cells were transformed with the correct plasmids and plated on LB plates supplemented with kanamycin and DAP for cultivation aerobically o/n at 37°C. A single colony was picked and used for mating.

V. harveyi WT was cultivated in LB media with ampicillin o/n at 30°C aerobically and *E. coli* WM3064 pNPTS138R6KT with the fused up and down fragments were cultivated o/n aerobically at 37°C in LB media with kanamycin and DAP. In the morning, all strains were diluted to an $OD_{600\,nm}$ of 2 measured with a Bio-Photometer from Eppendorf (Hamburg) and washed twice in fresh LB media. The pellet of *E. coli* WM3064 pNPTS138R6KT with the fused up and down fragments was first resuspended in 200 µl fresh LB media. This suspension was used to resuspend the pellet of the *V. harveyi* cells. The mix was then plated on a LB-DAP plate and left for a minimum of 3 h at 30°C. The dried mixture was resuspended with 1 ml fresh LB media and diluted up to 1:1,000 and 100 µl of each dilution was plated on LB plates supplemented with Kanamycin. On the next day, 50 colonies were picked and transferred each on a LB plate with kanamycin and secondly on a LB plate with saccharose. On the next day, 2 colonies grown on kanamycin but not on saccharose were transferred to test tubes containing liquid LB media but no antibiotics and grown o/n at 30°C aerobically. From these cultures, a dilution series up to 1:1,000 was performed and from each dilution 100 µl were plated on LB plates containing saccharose. These plates were left at RT to grow for 2 days.

At least 50 cells were then transferred to first a LB plate with carbenicillin and secondly a LB plate with kanamycin. Through this process, the plasmid was removed from the bacterial cells. The cells grown o/n at 30°C on carbenicillin but not kanamycin plates were used in a colony-PCR using the gene-specific check primers (Tab. 10). WT genomic DNA was used as negative control.

The correct clone was grown o/n at 30°C, on the next day mixed with 75% glycerol freezing media, shock frozen with liquid nitrogen and stored at -80°C.

In order to generate double or triple mutants, the specific *V. harveyi* single or double mutant strains were used for mating process instead of the WT.

2.2.2.12 Complementation in trans

In order to complement in *trans*, the deletion mutants *V. harveyi* EMR2 (Δ*VIBHAR_05206-VIBHAR_05205*), EMR3 (Δ*VIBHAR_06667*) and MR3 (Δ*luxS*), new primers were designed using SpeI and XmaI as restriction enzymes (Tab. 4, Tab. 10). The specific genes were amplified using Q5 polymerase and WT DNA. After restriction of the PCR fragments and the plasmid pBBR1-MCS2-BAD, the fragments were ligated to the vector using a vector to insert ratio of 1 to 6 in a water bath starting at 0°C o/n. Competent *E. coli* DH5αλpir cells were transformed with the ligation and plated on LB plates supplemented with kanamycin for outgrowth o/n at 37°C or for 48 h at RT.

The plasmid was extracted using the HiYield plasmid mini-kit and was control restricted with the restriction enzymes priorly used. If no band was visible after gel electrophoresis, either sequencing and/or PCR were performed with the specific primers (Tab. 10).

Competent *E. coli* WM3064 cells were transformed with correct plasmids and plated on LB plates supplemented with kanamycin and DAP for cultivation o/n at 37°C. A single colony was picked and used for mating with the deletion mutant strains and its GFP-tagged copy (for details see chapter 2.2.2.14).

Therefore, the strain was cultivated in LB media with ampicillin o/n at 30°C aerobically and *E. coli* WM3064 pBBR1-MSC2-BAD with the fragment were cultivated overnight aerobically o/n at 37°C in LB media with kanamycin and DAP. In the morning, all strains were diluted to an $OD_{600\ nm}$ of 2 measured with a Bio-Photometer and washed twice in fresh LB media. The pellet of *E. coli* WM3064 pBBR1-MSC2-BAD with the fragment was first resuspended in 200 µl fresh LB media, this suspension was used to resuspend the pellet of the *V. harveyi* cells. This mix was plated on a LB-DAP plate and left for a minimum of 3 h at 30°C. The dried mixture was resuspended with 1 ml fresh LB media and diluted up to 1:1,000. 100 µl of each dilution was plated on LB plates supplemented with kanamycin. Colony-PCR was performed using single colonies grown on these LB-kanamycin plates. Genomic DNA of the specific mutant strain was used as negative control while genomic DNA of the WT was used as positive control. The correct strain was mixed with glycerol freezing media, shock frozen with liquid nitrogen and stored at -80°C.

2.2.2.13 Chromosomal complementation

To complement a deleted gene chromosomally, the Up-RE-sense and the Down-RE-antisense primers prior used for the deletion were used in a PCR with WT genomic DNA and Q5 or Phusion

Polymerase to amplify the target fragment. This fragment and the pNPTS138R6KT plasmid were restricted with the specific restriction enzymes and and ligated using a vector: insert ratio of 1:6 with T4 DNA ligase o/n in a water bath starting with 0°C. Competent *E. coli* DH5αλpir cells were transformed with the ligation and plated on LB plates supplemented with kanamycin for outgrowth o/n at 37°C or for 48 h at RT.

The plasmid was extracted using the HiYield plasmid mini-kit and was control restricted with the restriction enzymes priorly used for the deletion. If no band was visible after gel electrophoresis, either sequencing and/or PCR was performed with the specific primers (Tab. 10).

Competent *E. coli* WM3064 cells were transformed with correct plasmids and plated on LB plates supplemented with kanamycin and DAP for cultivation o/n at 37°C. A single colony was picked and used for mating and homologous recombination of the deletion mutant strains (for details see chapter 2.2.3.10).

The correct strain was mixed with glycerol freezing media, shock frozen with liquid nitrogen and stored at -80°C.

2.2.2.14 Constitutive green fluorescent protein tagging of strains

In order to scan biofilms using the CLSM, either fluorescent strains or staining the strains with a Dye are necessary. For the simplicity, we chose to integrate GFP into the Tn7 site within *V. harveyi*. Here, GFP can be constitutively expressed.

For this procedure, *E. coli* WM3064 pUC18R6KT-miniTn7T-eGFP-cm and *E. coli* WM3064 pTNS2 were cultivated aerobically o/n at 37°C in LB media with the specific antibiotics and DAP, while the specific *V. harveyi* strain was cultivated in LB media with ampicillin o/n at 30°C aerobically. In the morning, all strains were diluted to an $OD_{600\ nm}$ of 2 measured with a Bio-Photometer and washed twice in fresh LB media. The pellet of *E. coli* WM3064 pUC18R6KT-miniTn7T-eGFP-cm was first resuspended in 200 µl fresh LB media, this suspension was used to resuspend the pellet of *E. coli* WM3064 pTNS2 and then finally the *V. harveyi* pellet was resuspended with the *E. coli* suspension. This mix was plated on a LB-DAP plate and left for a minimum of 3 h at 30°C. The dried mixture was resuspended with 1 ml fresh LB media and diluted up to 1:1,000 and 100 µl of each dilution was plated on LB plates supplemented with chloramphenicol. After a maximum of 48 h single colonies were transferred into tubes containing LB media with chloramphenicol and grown aerobically o/n at 30°C.

On the next day, microscopy was performed to check for fluorescence using a Leica DMI6000B microscope with a HXP R120W/45C VIS fluorescence lamp from Leica Microsystems GmbH (Solms, Germany). Correct strains were mixed with glycerol freezing media, shock frozen with liquid nitrogen and stored at -80°C. These strains were used for the creation of 3D biofilms using the flow system and the confocal laser scanning microscope (CLSM, for details see chapter 2.2.5.1).

2.2.2.15 GFP-promoter fusions and GFP-Hybrid proteins

The GFP-promoterfusions were generated using the genes *VIBHAR_05206* and *VIBHAR_06667* and and GFP-hybrid proteins were generated for the genes *VIBHAR_05207* and *VIBHAR_06667*, for both systems the plasmid pNPTS138-R6KT-eGFP (Lassak, unpublished) was used. For the promoterfusion,

500 bp upstream before the start codon were amplified while for generation of the GFP-hybridproteins, 500 bp upstream before the start codon and the gene without the stop codon were amplified. All fragments were restricted and ligated with the plasmid.

Competent DH5αλpir cells were transformed with the ligated plasmid and plated on LB plates supplemented with kanamycin for outgrowth o/n at 37°C or for 48 h at RT. The plasmid was extracted using HiYield plasmid mini-kit from SLG (Gauting, Germany) and was control restricted with the restriction enzymes priorly used. If no band was visible after gel electrophoresis, either sequencing and/or PCR was performed with the universal primers M13_uni-sense-21 or M13_reverse-29 or the primers listed in Tab. 10.

Competent *E. coli* WM3064 cells were transformed with the correct plasmids and plated on LB plates supplemented with kanamycin and DAP for cultivation aerobically o/n at 37°C. A single colony was picked and used for mating.

V. harveyi WT was cultivated in LB media with ampicillin o/n at 30°C aerobically and *E. coli* WM3064 pNPTS138R6KT-eGFP with the specific fragments were cultivated o/n aerobically at 37°C in LB media with kanamycin and DAP. In the morning, all strains were diluted to an $OD_{600\ nm}$ of 2 measured with a Bio-Photometer from Eppendorf (Hamburg) and washed twice in fresh LB media. The pellet of *E. coli* WM3064 pNPTS138R6KT-eGFP with the specific fragments was first resuspended in 200 µl fresh LB media. This suspension was used to resuspend the pellet of the *V. harveyi* cells. The mix was then plated on a LB-DAP plate and left for a minimum of 3 h at 30°C. The dried mixture was resuspended with 1 ml fresh LB media and diluted up to 1:1,000 and 100 µl of each dilution was plated on LB plates supplemented with Kanamycin. On the next day, 50 colonies were picked and transferred each on a LB plate with kanamycin and secondly on a LB plate with saccharose. On the next day, colonies grown on kanamycin but not on saccharose were used in a colony-PCR using the gene-specific check primers (Tab. 10). WT genomic DNA was used as negative control. The correct clone was grown o/n at 30°C, on the next day mixed with 75% glycerol freezing media, shock frozen with liquid nitrogen and stored at -80°C.

V. harveyi cells were cultivated o/n at 30°C aerobically and either diluted 1:5,000 into fresh AB-media supplemented with kanamycin and 5 µl were placed on 1.5% AB-agar plates supplemented with kanamycin. Plates and non-shaking flaskes were incubated over a period of 24 h at 30°C. At different time points, 5 µl of each flasks were placed on AB-slides (5% agarose) and a small fraction of the colony from the plates was streaked onto an AB-slide for microscopy using the Leica DMI6000B microscope with a HXP R120W/45C VIS fluorescence lamp from Leica Microsystems GmbH. *V. harveyi* WT was used as control.

2.2.3 Bioluminescence assays

V. harveyi bioluminescence bioassays were carried out by cultivating in 96 well Costar-plates aerobically on a Titramax1000 from Heidolph (Schwabach, Germany) at 1,050 rpm at 30°C. Overnight cultures of the created strains were diluted into fresh AB media with a start-$OD_{600\ nm}$ of 0.002, AB media was used as a blank. The WT and MR15 strains were used as positive and negative control, respectively. Measurements were carried out every hour from 0 - 9 h and after 24 h. Strains were analysed in triplicates. $OD_{600\ nm}$ was measured using Tecan Infinite F500pro (Crailsheim,

Germany) with an integration time of 0.1 s and bioluminescence was measured with the Berthold plate reader Centro LB 960 (Bad Wildbad, Germany) with shaking for 1 s. The analysis was performed using the MikroWin2000 software from Mikrotek (Overath, Germany). The relative light units (RLU/s) were normalized by dividing the RLU value per $OD_{600\ nm}$ value ($RLU/OD_{600\ nm}$) in Excel (Microsoft Office 2010, Redmond, WA, USA).

2.2.4 Measurements of exopolysaccharide production

Sugars change their colour to yellow or orange if mixed with phenol and sulfuric acid, this can be measured photometrically. This sensitive quantitative method was adapted to our laboratory procedures from the original protocol established by DuBois *et al.* (1956) and Enos-Berlage and McCarter (2000), here in detail:

The strains used in this test were grown in AB media o/n aerobically at 30°C and diluted to an $OD_{600\ nm}$ of 1 using a Bio-photometer in fresh AB media. 100 µl of this dilution was plated on AB plates and left for 24 h at 30°C. Then the cells were scraped from the plates using pipette tips and resuspended in 5 ml PBS buffer (0.801% (w/v) NaCl, 0.02% (w/v) KCl, 0.178% (w/v) $Na_2HPO_4 \cdot 2\ H_2O$, 0.027% (w/v) KH_2PO_4). The suspension was diluted to an $OD_{600\ nm}$ of 0.5 in PBS and vortexed using a Vortex Genie from Scientific Industries (Bohemia, NY, USA) for 1 min before shaking at 1,050 rpm at 30°C for 1 h on a Titramax1000. The cells were centrifuged at 10,000 g in a Sorval® Evolution RC from Kendro Laboratory Products (Langenselbold, Germany) at 4°C for 15 min and the SN was transferred to 50 ml Falcon tubes. 50 µg/ml RNaseA, 50 µg/ml DNaseI and 10 mM $MgCl_2$ were added and the tubes were slewed at 30 rpm for 90 min. Then, 200 µg/ml Proteinase K were added and the tubes were slewed at 30 rpm for 90 min. Precipitation was done by adding 12.5 ml EtOH and centrifugation at 5,000 rpm for 20 min at 4°C in a Centrifuge 5804R using a A-4-44 rotor. The pellet was resuspended in 1 ml ddH_2O and to each tube 25 ml 80% Phenol and 2.5 ml concentrated H_2SO_4 were added and incubated at RT for 10 min. Then, the tubes were put into a water bath at 25 – 30°C until the colour was stable. A D-Glucose gradient (0 – 100 µg/ml) was prepared as standard curve and treated also with phenol and sulfuric acid. Absorption of 1 ml sample was measured at 488 nm in an Ultraspec 2100 pro UV/vis from Amersham Biosciences (GE Healthcare, Little Chalfront, UK).

2.2.5 Biofilm formation

2.2.5.1 Flow systems using confocal laser scanning microscopy

To create biofilms, we established the flow system in our laboratory (Fig. 12). It is made up of media (5 L Schott bottle, Mainz, Germany), a peristaltic pump (Watson Marlow 205S by Th.Geyer, Renningen, Germany), a battery (APC Smart-UPS by 3KV GmbH, Krailing, Germany), bubble traps (Sören Molin, DTU, Denmark), flow chambers (Sören Molin, DTU, Denmark), kitchen and aquarium silicone (Praktiker, Munich, Germany), cover classes 24 x 50 mm (Carl Roth GmbH, Karlsruhe, Germany), a waste container (5 L Schott bottle, Mainz, Germany), silicone tubes 1.5 x 3 mm (VWR, Ismaning, Germany), pump tubes "tygon® 3350 with stopper" 1.65 x 3.35 mm (VWR, Ismaning, Germany), tube connections "Miniadapter" 1.6 mm (VWR, Ismaning, Germany) and silicone tubes 1 x 1 mm (GM GmbH, Munich, Germany).

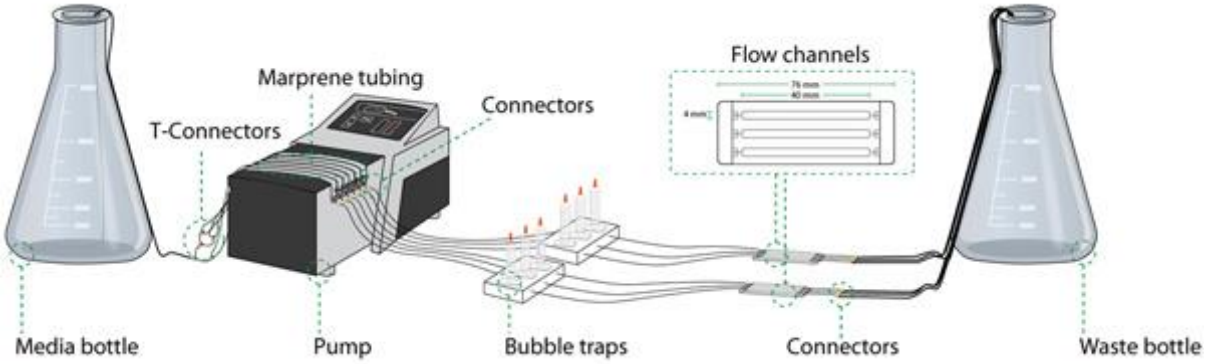

Fig. 12: Experimental set up oft the flow system (Nielsen et al., 2011).

According to the method of Weiss Nielsen *et al.* (2011), the flow system was set up and flushed using ddH_2O for 24 h at a flow rate of 750 rpm (750 µl/min). The system was then rinsed with AB media supplemented with ampicillin for 24 h at the same flow rate. The flow was stopped and the o/n cultures were diluted to an $OD_{600\ nm}$ of 0.5 in fresh AB media. Each cell chamber of the flow channels was inoculated with 3 ml of the specific strain and turned up-side-down w/o flow for 30 min at 30°C. Finally, the flow channels were turned again and the flow was set to 750 rpm and left at 30°C for 18 h.

Scanning of the biofilms was carried out using the Leica TCS SP5 MP (Ti:Sapphire laser) spectral FLIM (2 FLIM detectors) CLSM (Leica DM6000 CS, upright), a 20x magnification lens and an argon-laser at 488 nm wavelength.

After scanning, the flow system was rinsed with 0.5% (v/v) NaClO at 90 rpm for 10 min and dried for storage at RT until the next run.

3D imaging and volume rendering was done using Imaris 7.2 by Bitplane (Zurich, Switzerland).

2.2.5.2 Macrocolonies and Scanning Electron Microscopy

V. harveyi strains were cultivated o/n at 30°C aerobically in AB media in test tubes, the o/n culture was diluted 1:5,000 in fresh AB media and after 6 h 5 µl of each strain were placed on a single 2% AB-Agar plates supplemented with carbenicillin. These plates were stored at 30°C for 8 days in a box together with a beaker filled with ddH_2O to avoid dehydration of the plates. Pictures were taken of the plates daily with a Fusion-SL 3,500 WL from peqlab GmbH (Erlangen, Germany) with light and w/o light and an exposure time of 5 s to check the bioluminescence. Additionally, Professor Gerhard Wanner (collobaration) took pictures of the colonies with a Canon 5D Mark II with a 100 mm macro lens from Canon (Tokio, Japan) to document the formation of the colony.

On the 8^{th} day, the plates were fixed and analysed using a Zeiss Aurega workstation from Carl Zeiss Microscopy GmbH (Munich, Germany) by Professor Wanner and his team. Here, the fixation protocol in detail: First, the samples were overlayed with fixans (2.5% glutaraldehyde in fixans buffer, containing 50 mM Cacodylate, 250 mM NaCl, 100 mM $MgSO_4$, pH 7.5) o/n. Washing was

performed in the morning with fresh fixans buffer for 5, 25 and then for 30 min and finally the samples were washed o/n. On the next day, the samples were put in 1% OsO_4 in fixans buffer for 75 min and then washed in fixans buffer for 5 min, followed by washing in ddH_2O for 5, 25 and then for 90 min. Dehydration was performed with acetone as follows: 10% acetone for 20 min, 20% acetone for 15 min, 40% acetone for 75 min, 60% acetone for 15 min, 80% acetone for 25 min, 100% acetone for 30, 70 min and then o/n. Critical point desiccation was then performed for approximately two hours. The colonies were cut in half, placed on aluminium stubs and were sputtered with platinum.

3 Results

3.1 Effect of quorum sensing on bioluminescence and biofilm formation

3.1.1 Time-dependent biofilm formation of *V.harveyi*

Biofilm formation of the *V. harveyi* WTgfp is shown at different times of incubation (Fig. 13) in order to determine the ideal time point for comparison of the biofilms of the WT to the mutants for later experiments. It is visible that within the first 6 h complete adhesion to the surface occurs (monolayer) and then tower-like structures are formed (12 to 18 h). After 18 h, the biofilm is mature as at this time point the largest volume was measured (Fig. 13and Fig. 14, Tab. 15). This is also the time point when the biofilm appears to be smooth. Disintegration starts between 18 and 24 h as the volume (Fig. 13 and Fig. 14, Tab. 15) decreases and the towers were smaller than at 18 h. This experiment was performed in duplicates.

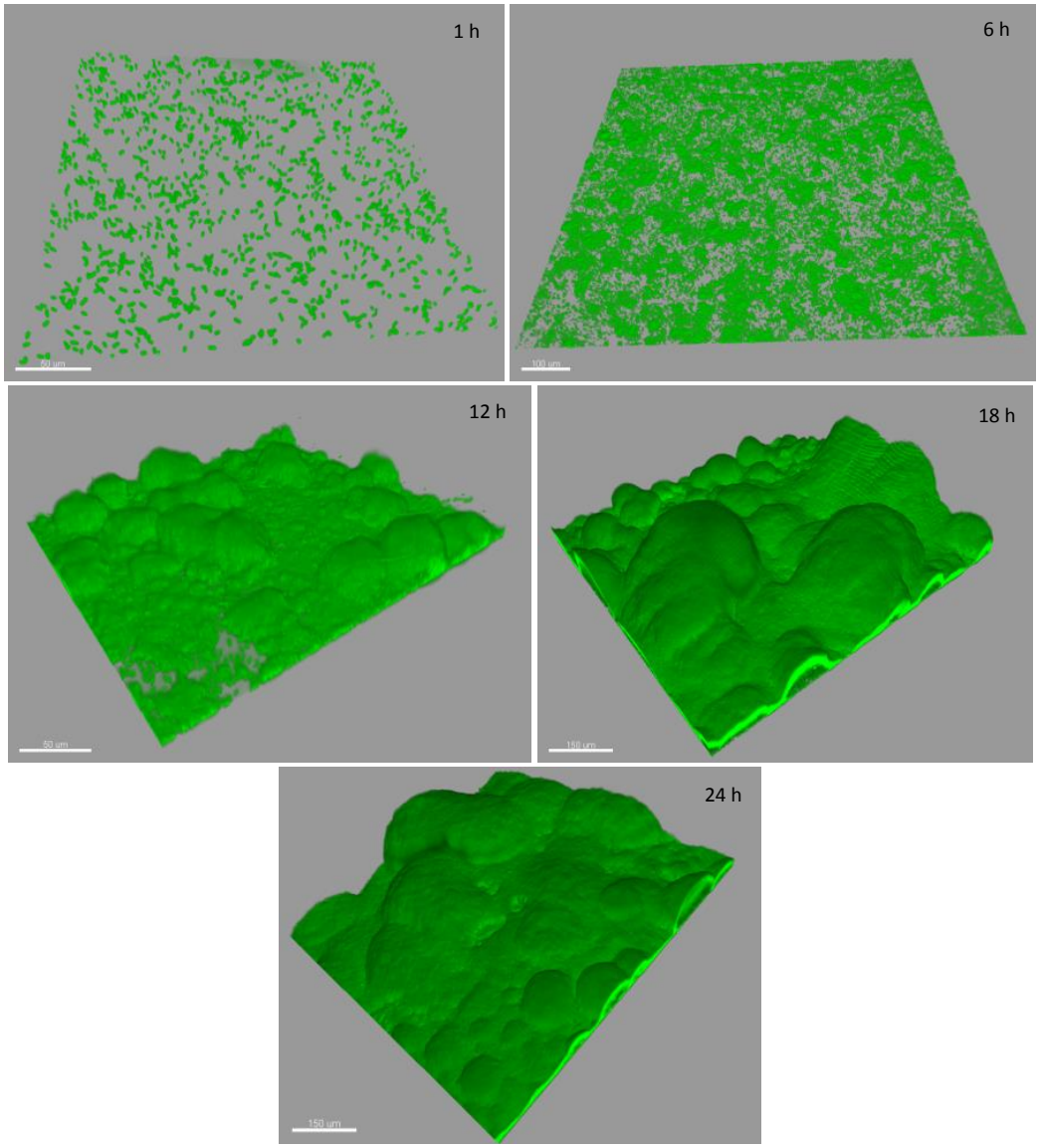

Fig. 13: Time-dependent biofilm formation of *V. harveyi* BB120gfp

After 1 h (scale bar 50 µm), 6 h (scale bar 100 µm), 12 h (scale bar 50 µm), 18 h (scale bar 150 µm) and 24 h (scale bar 150 µm).

As pictured in Fig. 14 (Tab. 15), the largest volume of biomass was measured at 18 h, so this time point was chosen for all other biofilm experiments. The volume of *V. harveyi* WTgfp biofilm after 18 h of incubation was set to 100% for comparison with the biofilms of the mutants.

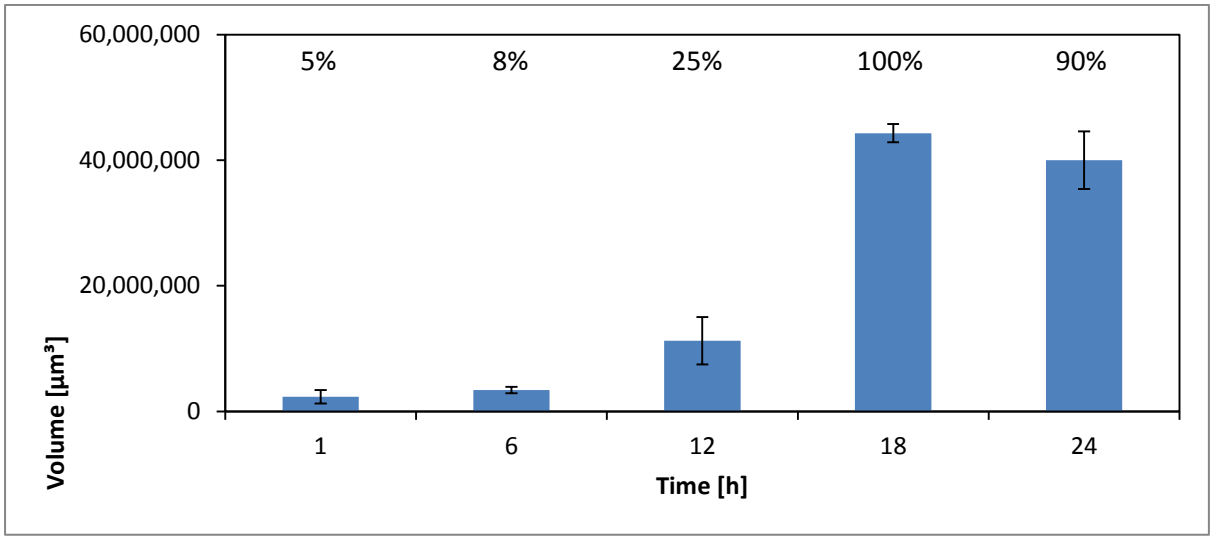

Fig. 14: Volumes of *V. harveyi* BB120gfp biofilms

Volumes of biofilm formation of the WTgfp are shown after different times of incubation. The WTgfp biofilm at 18 h was set to 100%. The experiments were performed in duplicates.

3.1.2 Bioluminescence production and biofilm formation are influenced by QS

As QS has a great effect on biofilm formation, we compared the biofilm of the WTgfp with those of *V. harveyi* Δ*luxO*gfp and *V. harveyi* MR15gfp (Δ*luxS* Δ*cqsA* Δ*luxM*). The deletion of *luxO* results in a constitutive QS ON mutant and has a bright phenotype while the triple synthase deletion mutant MR15 is a QS OFF mutant and has a dark phenotype. First, we performed a bioluminescence assay, bioluminescence production of WT was set to 100% for comparision. The strain Δ*luxO* showed 103% of the WT bioluminescence level while MR15 showed 0% (Fig. 15).

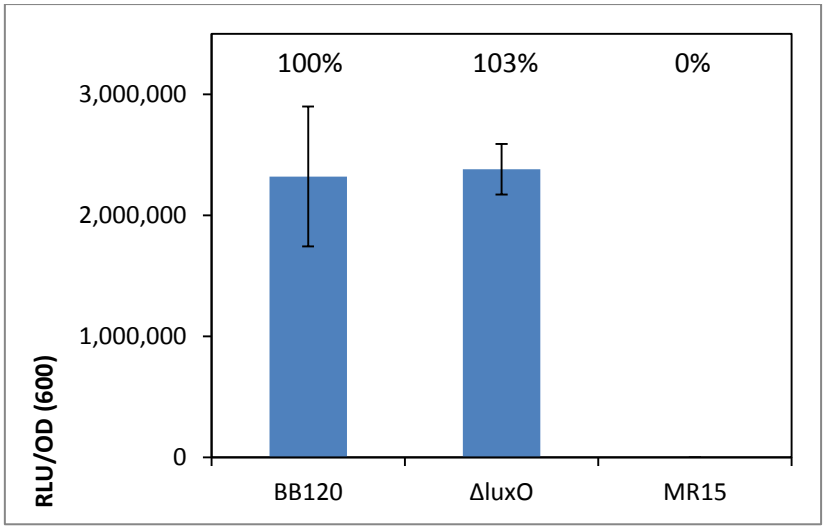

Fig. 15: Bioluminescence assay of WT, Δ*luxO* and MR15

Results are shown after 5 h of cultivation in AB media in a 96-well plate. Measurements were performed in triplicates: *V. harveyi* WT BB120 (positive control), Δ*luxO* and MR15. WT bioluminescence level was set to 100%.

Afterwards, 3D biofilm formation was performed using the flow system. The biofilm of the WTgfp consisted of a monolayer with tower-like structures; mutant strain Δ*luxO*gfp had a monolayer with a few small hill-like structures but only one unstructured tower and strain MR15gfp did not build a monolayer and only a few cells were attached to each other (Fig. 16). These differences are also visible in the volume of the biofilms. The biofilm volume of *V. harveyi* Δ*luxO*gfp was determined to be 37% of the WTgfp biofilm and MR15gfp biofilm volume was determined to be 7% of the WT biofilm (Fig. 17, Tab. 15).

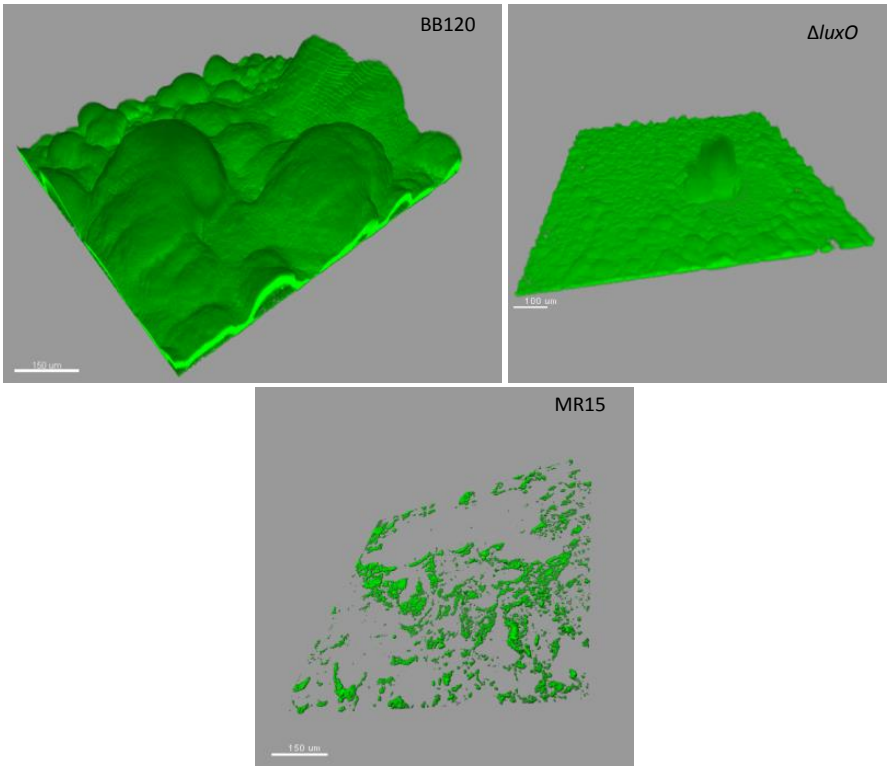

Fig. 16: Biofilm formation of *V. harveyi* strains WTgfp, Δ*luxO*gfp and MR15gfp

Biofilms of BB120gfp (scale bar 150 µm), Δ*luxO*gfp (scale bar 100 µm) and MR15gfp (scale bar 150 µm) are shown after 18 h of incubation.

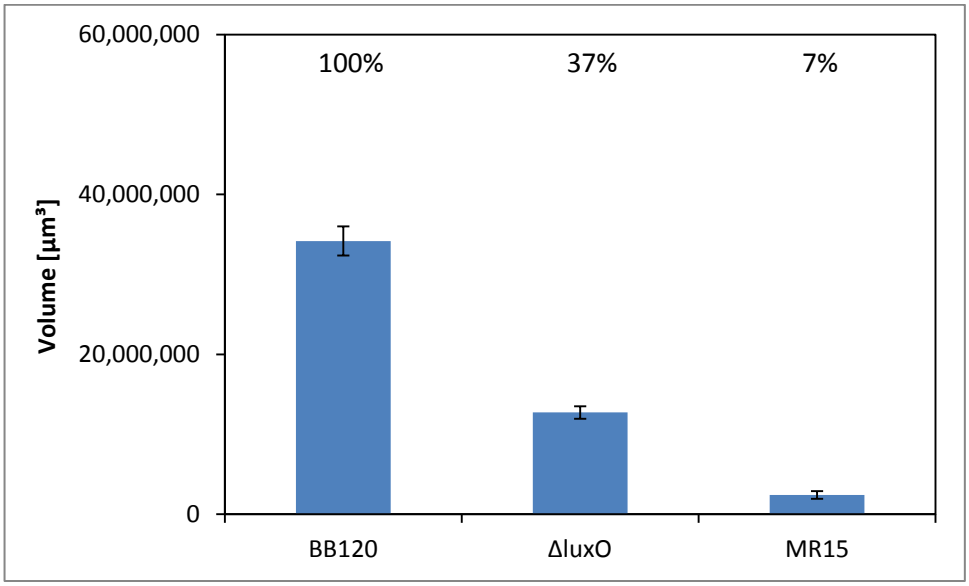

Fig. 17: Volumes of the biofilms of *V. harveyi* strains WTgfp, Δ*luxO*gfp and MR15gfp

Volumes of biofilms of WTgfp, Δ*luxO*gfp and MR15gfp are shown. The experiment was performed in triplicates after 18 h of incubation. The amount of the WT biofilm was set to 100%.

Therefore, it can be concluded that an intact and functioning QS system is required for the formation of a mature biofilm by *V. harveyi*. As a next step, the QS system needed to be investigated in order to determine the AI having the greatest effect on biofilm formation.

3.1.3 Influence of single autoinducers on biofilm formation

V. harveyi WT produces three autoinducers (Fig. 8). AI-2 is produced first, afterwards HAI-1 and CAI-1 are detectable in the supernatant of the WT in batch cultivation.

In the case of a deletion of *luxS* which produces no AI-2 (*V. harveyi* MR3gfp), biofilm formation was completely disrupted and adhesion to the surface was prevented. The effects of the deletion of HAI-1 synthase *luxM* (*V. harveyi* MR18gfp) or CAI-1 synthase *cqsA* (*V. harveyi* MR13gfp) were not as severe as the deletion of *luxS*. The monolayer and also some tower-like structures were still built while this was not the case for the MR3gfp biofilm. However, the overall structure of the biofilms of strains MR13gfp and MR18gfp lack structure and are only show small mushroom shaped towers. Furthermore, the surface appears rougher than the one of the WTgfp biofilm. The triple synthase mutant MR15gfp shows the same effect as strain MR3gfp: no monolayer and no tower-like structures were built (Fig. 18).

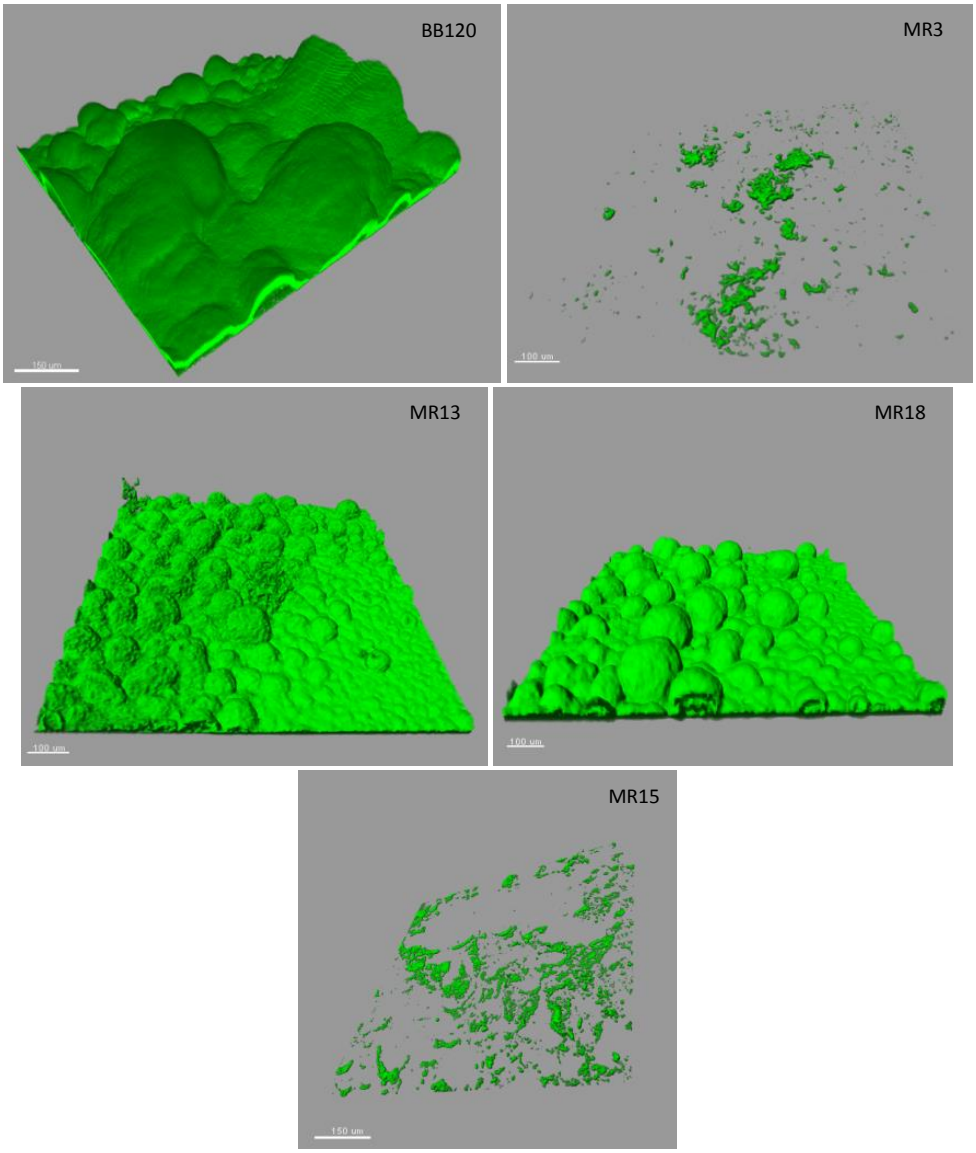

Fig. 18: Biofilm formation of different GFP-tagged *V. harveyi* strains

Biofilms of strains BB120gfp (scale bar 150 µm), MR3gfp, MR13gfp, MR18gfp (scale bars 100 µm) and MR15gfp (scale bar 150 µm) are shown after 18 h of incubation.

All three single deletion mutants showed structural differences (Fig. 18) and differences in volume compared to the WT biofilm (Fig. 19). According to its volume determination, the biofilm of the WT after 18 h was set to 100%. The biofilm of *V. harveyi* MR3gfp (Δ*luxS*) measured only 4% of the WT biofilm volume while *V. harveyi* MR18gfp (Δ*luxM*) volume was 43% of the WT biofilm and *V. harveyi* MR13gfp (Δ*cqsA*) was measured at 70% of the WT biofilm (Fig. 20, Tab. 15). These observations made clear that the deletion of *cqsA* was not significantly influencing biofilm formation.

As described above, lacking all three AI (strain MR15gfp) leads to no biofilm like the biofilm of MR3gfp mutant. Only a few cells were able to adhere to the surface but there are no real cell clusters visible (Fig. 16 and Fig. 18). This is also shown in the volume determination as the biofilm MR15gfp measured only 7% of the WTgfp biomass (Fig. 17 and Fig. 19, Tab. 15).

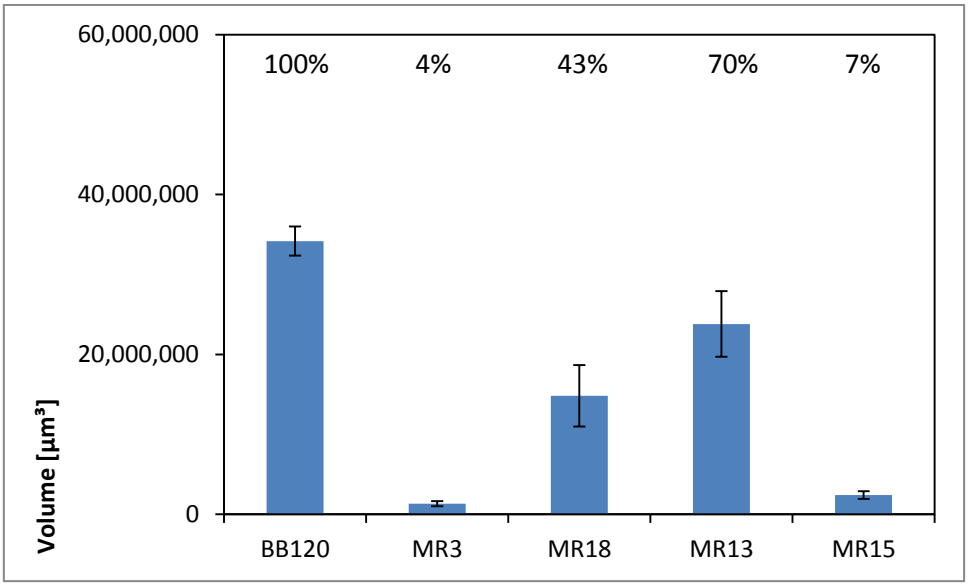

Fig. 19: Volumes of the biofilm of different GFP-tagged *V. harveyi strains*

Biofilm volumes of WTgfp, single synthase deletion mutants *V. harveyi* MR3gfp, MR18gfp and MR13gfp and triple synthase deletion mutant *V. harveyi* MR15gfp are shown after 18 h of incubation, WTgfp biofilm was set to 100%. Experiments were performed in triplicates.

As *V. harveyi* MR3gfp showed the greatest differences compared to the *V. harveyi* WTgfp biofilm, it was necessary to see if complementation in trans and/or chromosomal integration could restore WTgfp levels in both: bioluminescence and biofilm formation. Therefore, MR3 strain was in *trans* complementated (*V. harveyi* EMR14) and chromosomally integrated (*V. harveyi* EMR19).

First, complementation in *trans* using the plasmid pBBR1-MSC2-BAD (EMR14) and chromosomal integration (EMR19) of *luxS* in mutant MR3 were compared to the WT for their bioluminescence levels and then 3D biofilm formation via the flow system was performed.

Strain EMR14 (*luxS* in *trans* complementation) showed 81% of WT bioluminescence (Fig. 20, Tab. 15) and 36% of the WT biofilm level (Fig. 22). The structure of the EMR14gfp strain biofilm is still disrupted but partly a monolayer was build and adhesion of the cells to each other in 3D clearly occurred (Fig. 20).

Strain EMR19 (*luxS* chromosomal integration) showed 76% of WT bioluminescence (Fig. 20, Tab. 15) and 29% of the WT biofilm level (Fig. 22). The biofilm of strain EMR19gfp build partly a monolayer and one unstructured tower (Fig. 21).

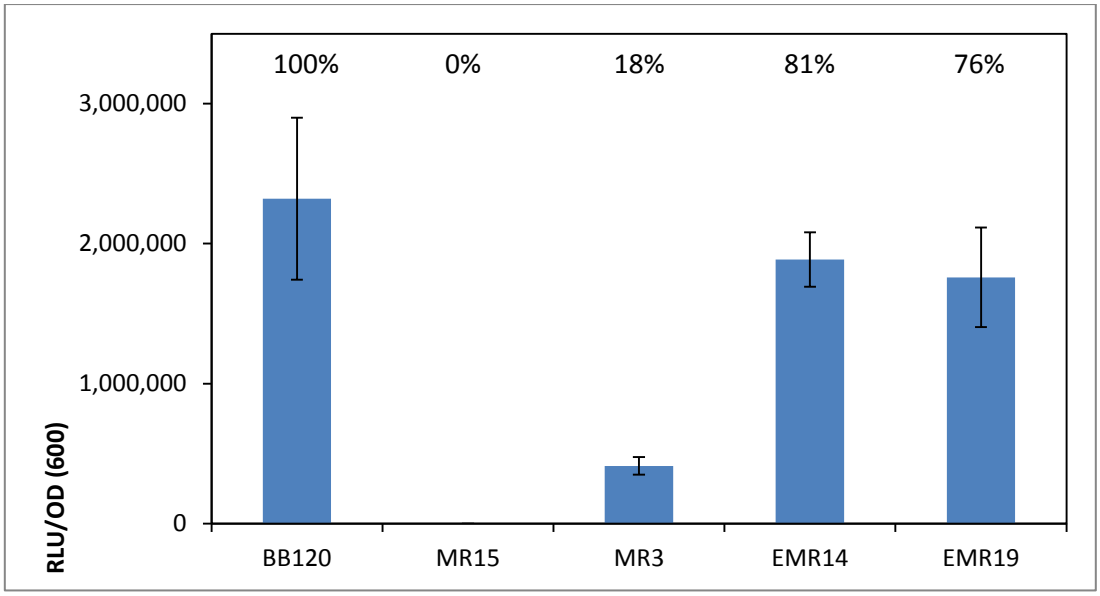

Fig. 20: Bioluminescence assay of *V. harveyi* strains WT, MR15, MR3, EMR14 and EMR19

Results are shown after 5 h of cultivation in AB media in a 96-well plate. Measurements were performed in triplicates of *V. harveyi* strains: WT BB120 (positive control), MR15 (negative control), MR3, EMR14 and EMR19. WT bioluminescence level was set to 100%.

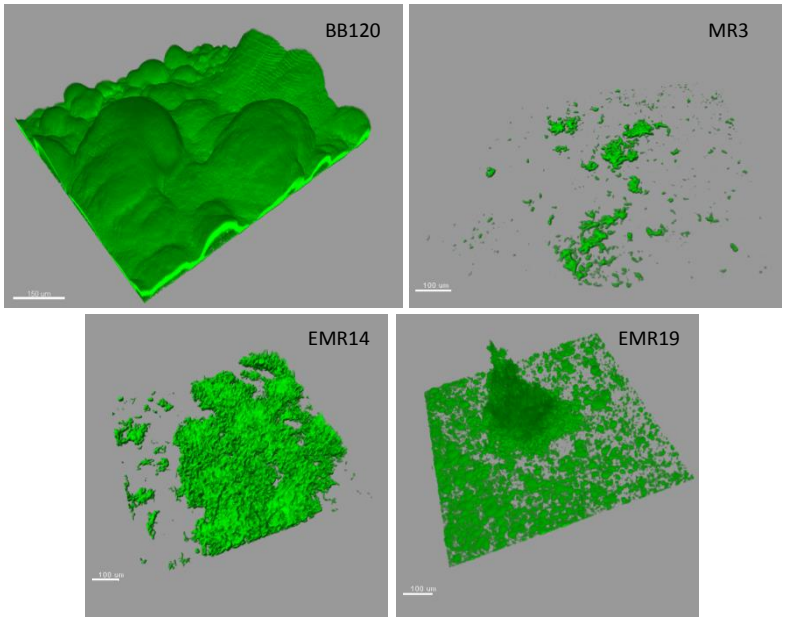

Fig. 21: Biofilm formation of *V. harveyi* strains WTgfp, MR3gfp, EMR14gfp and EMR19gfp

Biofilms of strains WTgfp (scale bar 150 µm), MR3gfp, EMR14gfp and EMR19gfp (scale bars 100 µm) are shown after 18 h of incubation.

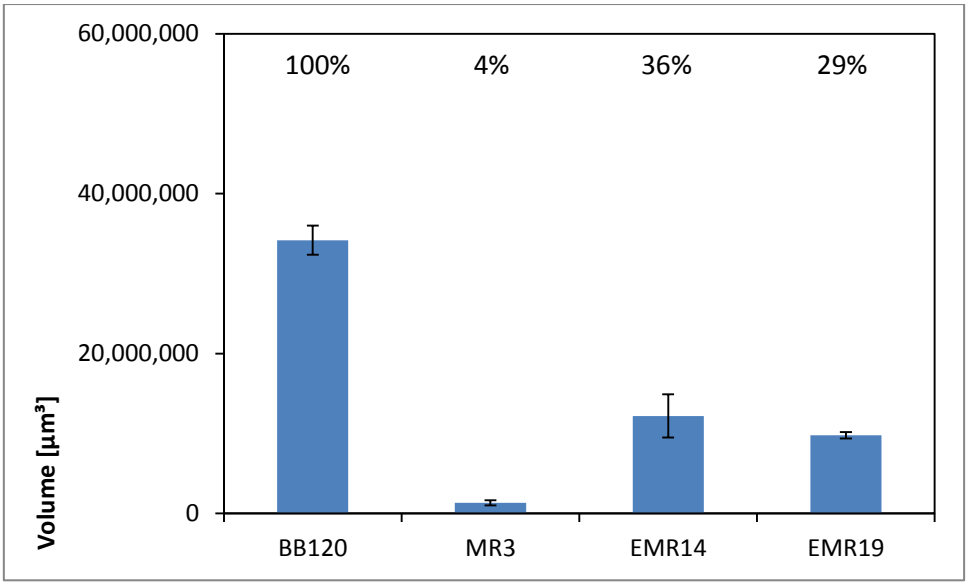

Fig. 22: Volumes of the biofilms of *V. harveyi* strains WTgfp, MR3gfp, EMR14gfp and EMR19gfp

Shown are the different strains after 18 h of incubation. WTgfp biofilm was set at 100% and the experiments were performed in triplicate.

Altogether, AI-2 has the greatest effect on biofilm formation as the lack of it prevents biofilm formation. The other deletion mutants (Δ*luxO*gfp, MR13gfp and MR18gfp) show severe defects, however, each biofilm consists of a monolayer and at least one tower-like structure was built.

Furthermore, in *trans* complementation (strain EMR14) and chromosomal integration (strain EMR19) of *luxS* in mutant strain MR3 showed WT levels in bioluminescence assays and increased biofilm volume and structure when compared to MR3gfp strain.

3.2 Identification of genes involved in the production of biofilms

3.2.1 Bioinformatics: analysis of homology

As detailed in the introduction, exopolysaccharides are used for adhesion to surfaces and affect biofilm formation. Therefore, using www.microbesonline.org (Dehal *et al.*, 2009) for exopolysaccharides synthases and related genes in *V. harveyi* two operons *VIBHAR_02222-02221* and *VIBHAR_05207-05204* as well as one single gene *VIBHAR_06667* were found. Furthermore, a potential nucleoside-diphosphate sugar epimerase (*VIBHAR_01320*) was found. The protein structures of these genes were compared (pBLAST) with known exopolysaccharides of *Vibrio* spp. using the NCBI website (Rockville Pike, Bethesda, MD, USA).

The pBLAST alignment of each protein to the homologue and a family tree of the harveyi group within the family *Vibrionaceae* are shown in the Appendix (Fig. 46 - Fig. 54). The results of homology are shown in Tab. 13.

Tab. 13: Homology studies of putative exopolysaccharide producing proteins found in *V. harveyi* WT

Gene	Function	Homologue	Identity [%] based on protein sequence
VIBHAR_01320	Predicted nucleoside-diphosphate sugar epimerase	*V. sp.* EX25: cell division inhibitor	87
VIBHAR_02222	hypothetical protein	*V. parahaemolyticus* NIHCB0757: glycosyl transferases group 1 family protein	72
VIBHAR_02221	Glycosyltransferase	*V. alginolyticus* NBRC 15630: putative polysaccharide export protein	84
VIBHAR_05207	undecaprenyl-phosphategalactosephosphotransferase	*V. parahaemolyticus* BB220P: capsular polysaccharide synthesis enzyme CpsA sugar transferase	86
VIBHAR_05206	uncharacterised protein	*V. parahaemolyticus* BB220P: capsular polysaccharide biosynthesis CpsB	72
VIBHAR_05205	periplasmic protein involved in polysaccharide export	*V. parahaemolyticus* RIMD 2210633: capsular polysaccharid biosynthesis CpsC polysaccharide export	88
VIBHAR_05204	exopolysaccharide biosynthesis protein	*V. parahaemolyticus* BB220P: capsular polysaccharid synthesis enzyme CpsD exopolysaccharide synthesis	86
VIBHAR_06667	Uncharacterized protein involved in exopolysaccharide biosynthesis	*V. parahaemolyticus* 50: capsular exopolysaccharide family domain protein	87

The sequence identities show that most of the proteins have not been characterized towards their function but suggests involvement in the polysaccharide production. The sequences of *VIBHAR_01320*, *VIBHAR_02221* and *VIBHAR_05207* show predicted functions within polysaccharide production and modification. Bourne and Henrissat (2001) reported a bacterial UDP-*N*-acteylglucosamine 2-epimerase belonging to the family of glycosyltransferases (Wakarchuk *et al.*, 1996). Glycosyltransferases are necessary for the activation of the synthesis of *N*-acetylglucosamine polymers (Karatan and Watnick, 2009) and also for the transfer of sugars to target molecules (Shiabata *et al.*, 2012). Epimerases are involved in the production of carbohydrate polymers; sugars and carbohydrates protect bacteria when located on the cell surface (Allard *et al.*, 2001).

For the first operon (*VIBHAR_02222-02221*) and the single genes (*VIBHAR_01320* and *VIBHAR_06667*) knock-out mutants were generated. For the second operon the middle genes *(VIBHAR_05206-05205,* 1.773 bp*)* were used for deletion as it was not possible to delete the whole operon (*VIBHAR_05207-05204,* 5.358 bp).

The knock-out mutants Δ*VIBHAR_05206-05205* (*V. harveyi* EMR2), Δ*VIBHAR_06667* (*V. harveyi* EMR3), Δ*VIBHAR_02222-02221* (*V. harveyi* EMR20) and Δ*VIBHAR_01320* (*V. harveyi* EMR23) were compared to the WT and MR15 (Δ*luxS* Δ*cqsA* Δ*luxM*) for their bioluminescence levels, their ability for exopolysaccharide (EPS) production and their biofilm formation. This gave an insight in how far the phenotypes are altered when the specific genes were knocked out.

3.2.2 Phenotypic characterization of the deletion mutants

3.2.2.1 Bioluminescence and exopolysaccharide production

For the bioluminescence assay, *V. harveyi* MR15 was used as negative control (0% of the WT bioluminescence level) while BB120 served as positive control and its mean volume was set to 100%. Bioluminescence was not affected by the specified deletions as all knock-out mutants show between 90 and 104% WT bioluminescence levels (Fig. 23, Tab. 14).

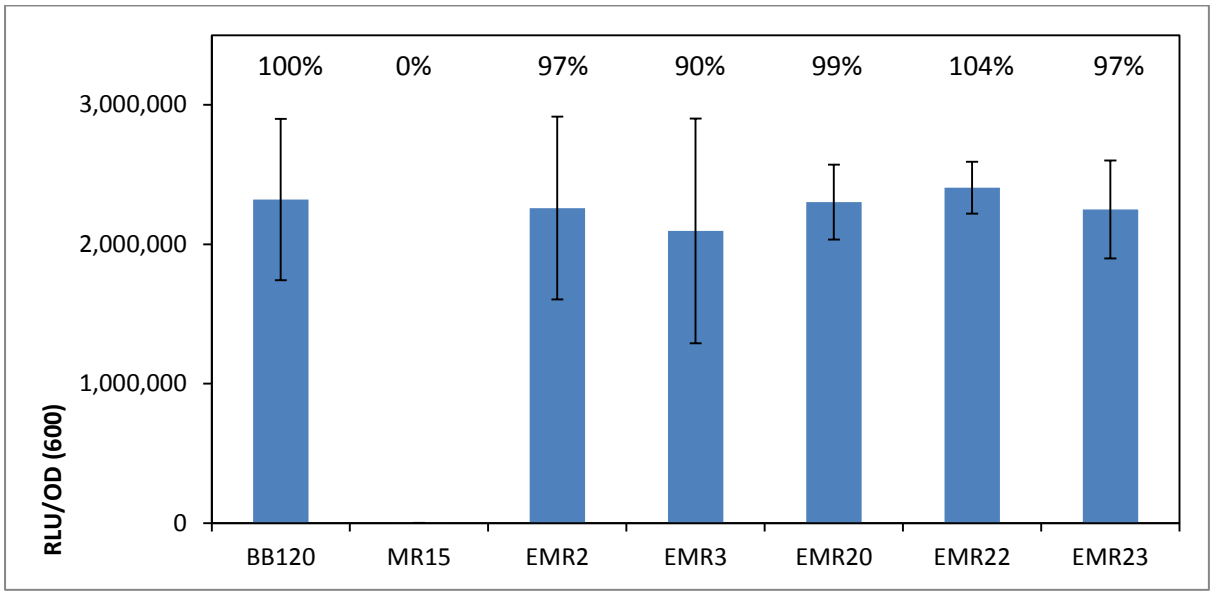

Fig. 23: Bioluminescence assay of different *V. harveyi* strains

Tests were done with the deletion mutants after 5 h of cultivation in AB media in a 96 well plate. Measurements were performed in triplicates. The assayed strains are *V. harveyi* WT BB120 (positive control), MR15 (negative control), EMR2, EMR3, EMR20, EMR22 and EMR23. WT bioluminescence level was set to 100%.

The production of EPS was assayed in triplicate using hydrolysation and measurement of glucose. *V. harveyi* MR15 (38% of the WT glucose level) was used as negative control while BB120 was the positive control and its mean volume was set to 100%. Glucose levels were determined to be severely reduced in the deletion mutants *V. harveyi* EMR2, EMR3 and EMR20 (39 to 44% of the WT glucose level, Fig. 23). The triple exopolysaccharide deletion mutant *V. harveyi* EMR22 showed 48% of the WT glucose level (Fig. 24, Tab. 16). Deletion mutant EMR23 was included in this experiment due to time restriction.

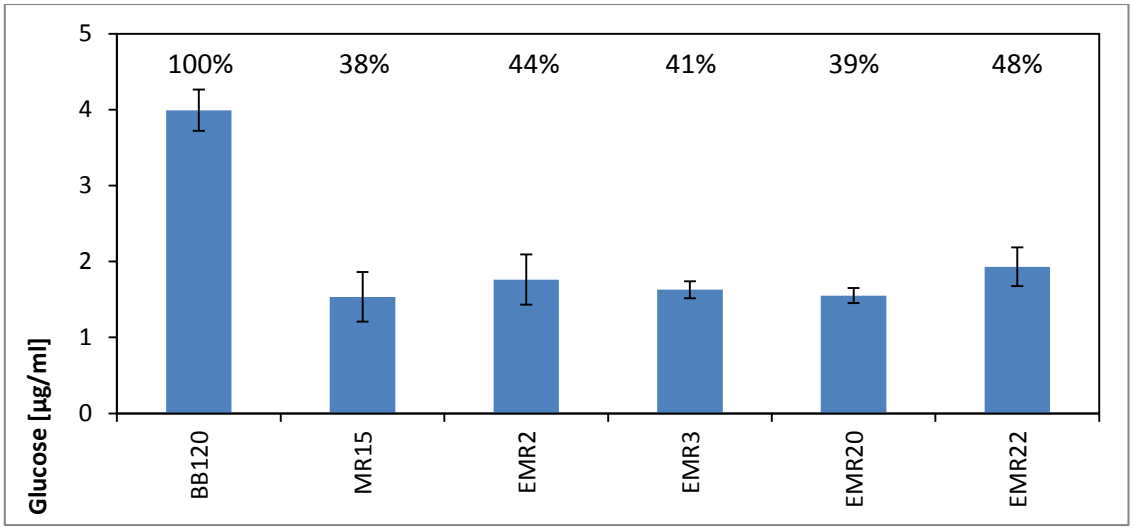

Fig. 24: EPS determination via glucose hydrolysation of different *V. harveyi* strains

The experiment was measured after 24 h in triplicate. Assayed strains are *V. harveyi* WT BB120 (positive control), MR15 (negative control), EMR2, EMR3, EMR20 and EMR22. WT glucose level was set at 100%.

The data concludes that the selected genes for knock-out mutants are involved in EPS production but bioluminescence production is not affected by the gene deletions.

3.2.2.2 Impact of putative EPS genes on biofilm formation

Biofilm formation experiments were performed using the flow system. The deletion of *VIBHAR_02222-02221* (EMR20gfp), *VIBHAR_05206-05205* (EMR2gfp) and *VIBHAR_01320* (EMR23gfp) resulted in a flat biofilm as only the formation of a monolayer occurred. The greatest effect was seen by the deletion of *VIBHAR_02222-VIBHAR_02221* (EMR20gfp) as even the monolayer is disrupted and not constantly spread over the whole surface. Also, the deletion of *VIBHAR_06667* (EMR3gfp) resulted in a destructured biofilm, such that elevated structures were built but were deformed and low, the biofilm appears to be like waves. This is also correlated with the volume determinations (Fig. 26, Tab. 15). The triple exopolysaccharide deletion mutant (EMR22gfp) showed a flat biofilm as the mutants EMR2gfp and EMR23gfp (Fig. 25). These results are clearly reflected by the volumes. The deletion mutants only showed volumes between 15% and 23% of the WTgfp biofilm volume (Fig. 26, Tab. 15).

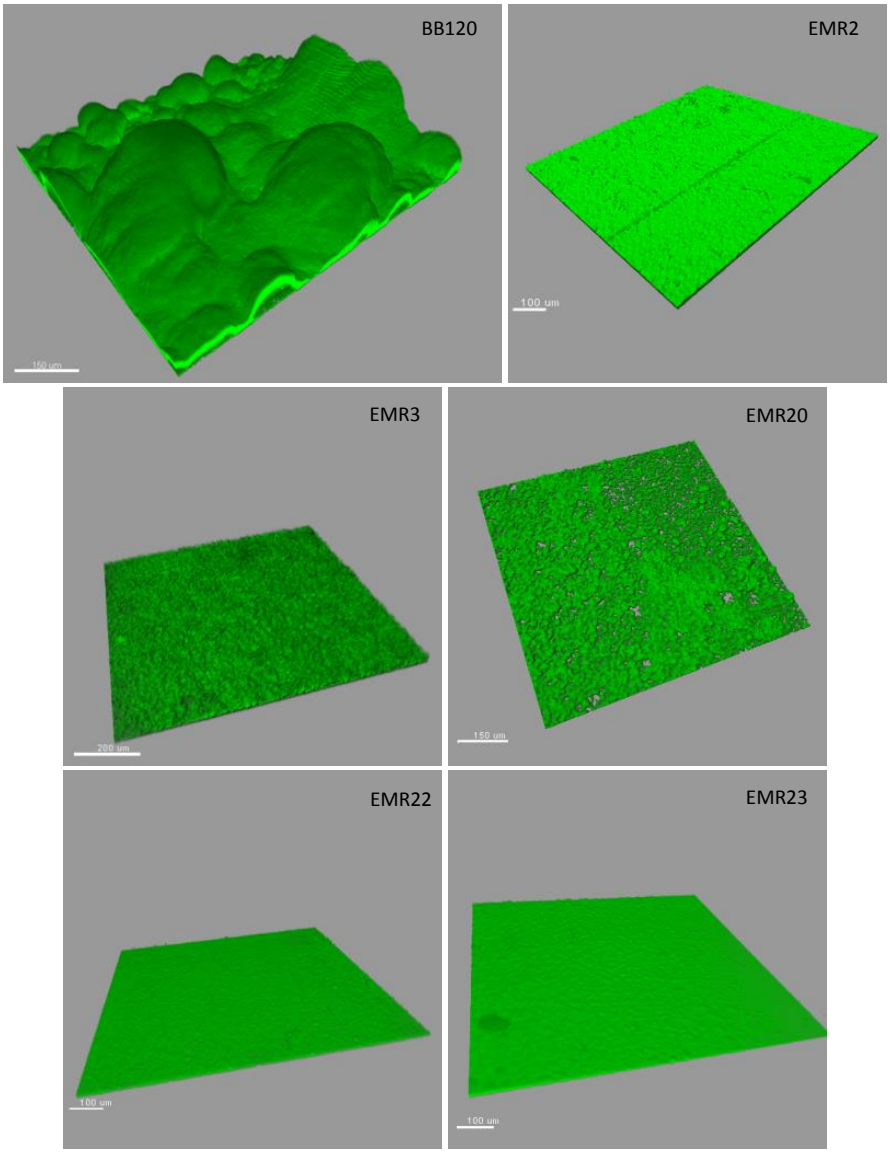

Fig. 25: Biofilm formation of different *V. harveyi* strains

Biofilms of strains BB120gfp (scale bar 150 µm), EMR2gfp (scale bar 100 µm), EMR3gfp (scale bar 200 µm), EMR20gfp (scale bar 150 µm), EMR22gfp and EMR23gfp (scale bars 100 µm) are shown after 18 h of incubation.

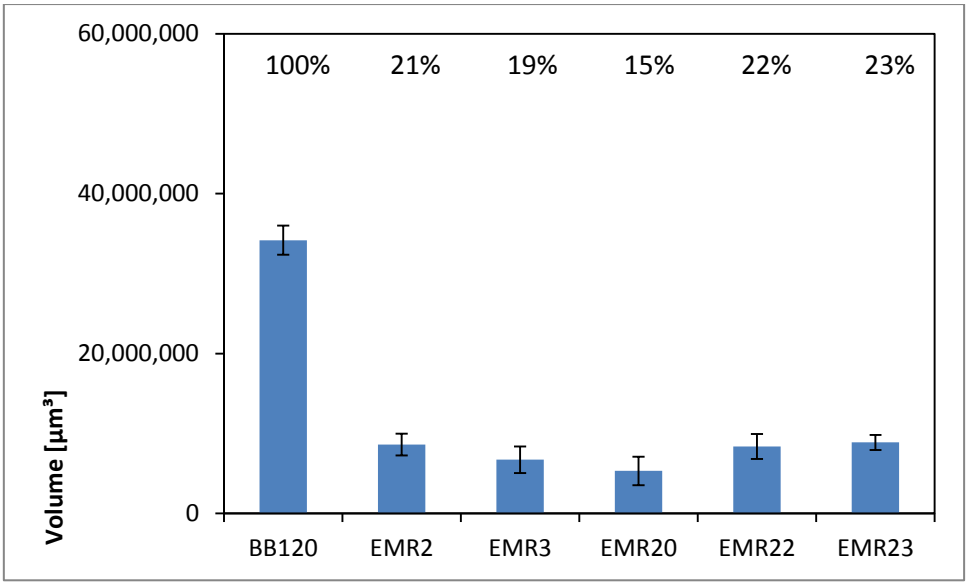

Fig. 26: Volumes of the biofilms of different *V. harveyi* strains

Volumes of the biofilms of strains BB120gfp, EMR2gfp, EMR3gfp, EMR20gfp, EMR22gfp and EMR23gfp are shown after 18 h of incubation. The WT biofilm was set to 100%, experiments were performed in triplicate.

This data suggests that the selected genes for the generation of knock-out mutants are involved in EPS production within *V. harveyi*. All mutants show similar phenotypes: no effect on bioluminescence production but severely reduced glucose levels and severely reduced biofilm formation in biomass and structure when compared to WT.

3.2.2.3 Phenotypic characterization of the knock-in mutant strains

As all three single deletion mutants show severely reduced biofilms, single deletion mutants were chromosomal integrated (knock-in) with their missing genes (*VIBHAR_05206-05205* into *V. harveyi* EMR2, EMR17; *VIBHAR_06667* into *V. harveyi* EMR3, EMR18; *VIBHAR_02222-02221* into *V. harveyi* EMR20, EMR21). Bioluminescence assays, exopolysaccharide measurements and biofilm formation experiments were performed in triplicate with the new strain set: EMR17, EMR18 and EMR21.

Bioluminescence production was not affected by the integration of the deleted genes (88 - 95% of the WT bioluminescence, Tab. 14), glucose levels could be restored by the integrated strains (95 - 103% of WT glucose level, Fig. 27, Tab. 16) and biofilm formation could be partially restored (Fig. 28). The volume of the biofilms of the knock-in strains was more than doubled compared to the biofilm of the deletion mutants (38 - 63% WT biofilm volume, Fig. 29, Tab. 15). Also, knock-in strains showed more structure and build up mostly small and flat towers, however the towers have the appearance of small mushrooms (Fig. 28). The biofilm of EMR18gfp appears to be similar to the biofilms of MR13gfp (Δ*cqsA)* and MR18gfp (Δ*luxM,* Fig. 18*)*.

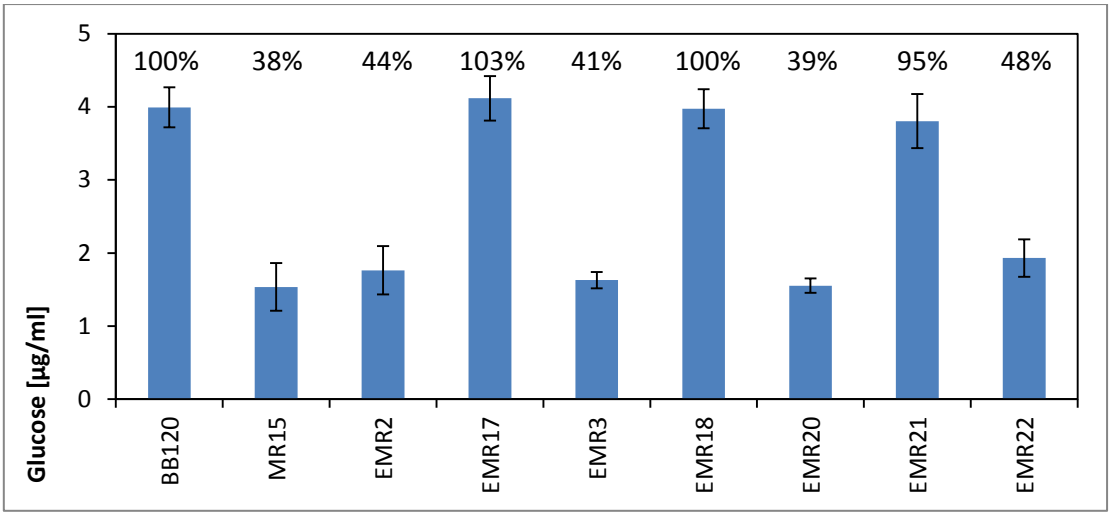

Fig. 27: EPS determination via glucose hydrolysation of *V. harveyi* WT, knock-out and knock-in mutants

Results measured after 24 h in triplicate of nine strains: *V.harveyi* WT BB120 (positive control), MR15 (negative control), EMR2, EMR17, EMR3, EMR18, EMR20, EMR21 and EMR22. The WT glucose production was set to 100%.

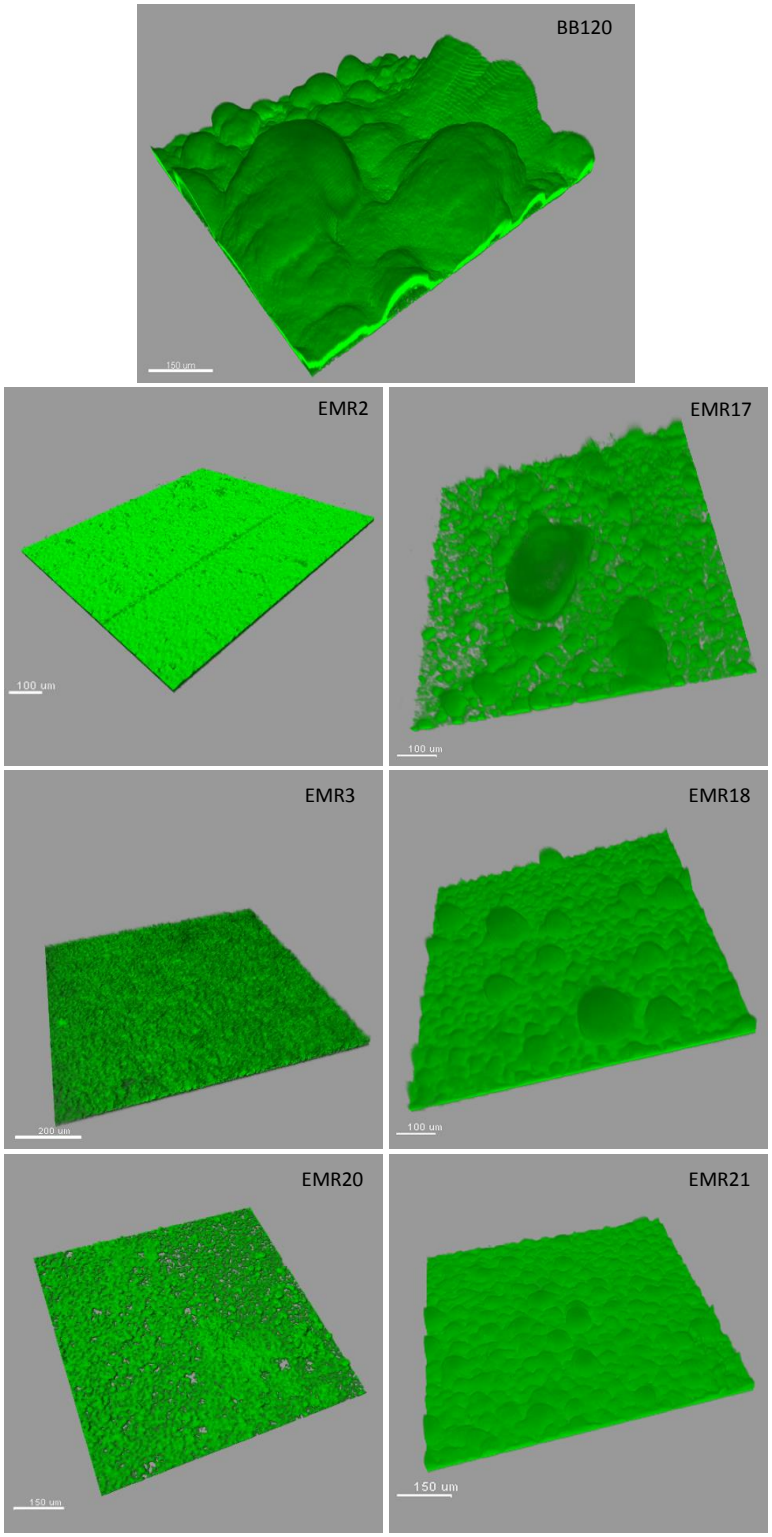

Fig. 28: Biofilm formation of *V. harveyi* WT, knock-out and knock-in mutant strains

Biofilms of BB120gfp (scale bar 150 µm), EMR2gfp, EMR17gfp (scale bars 100 µm), EMR3gfp (scale bar 200 µm), EMR18gfp (scale bar 100 µm), EMR20gfp and EMR21gfp (scale bar 150 µm) are shownafter 18 h of incubation.

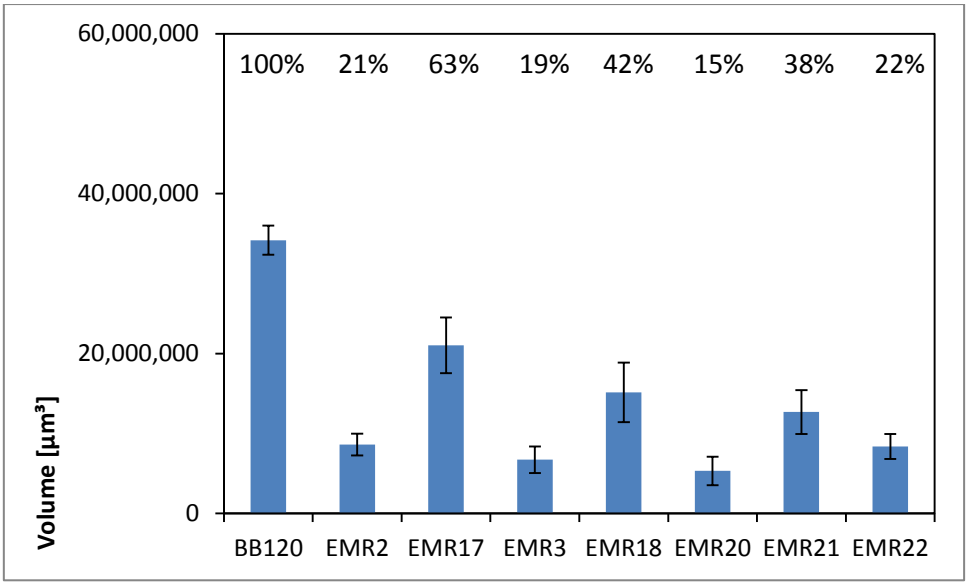

Fig. 29: Volumes of the biofilms of *V. harveyi* WT, knock-out and knock-in mutant strains

Volumes of biofilms of WT BB120gfp, EMR2gfp, EMR17gfp, EMR3gfp, EMR18gfp, EMR20gfp, EMR21gfp and EMR22gfp were measured after 18 h of incubation. The WT biofilm was set to 100% and all experiments were performed in triplicates.

To summarize, the genes selected for the knock-out mutants showed severe defects in EPS production and biofilm formation which could be restored fully towards EPS production and partially in biofilm formation when the genes were knocked in again.

3.2.2.4 Transcriptional and translational expression of putative exopolysaccharide genes

V. vulnificus has a lipopolysaccharide and three exopolysaccharides involved in biofilm formation. All of these are expressed at different time points within the biofilm formation (Lee *et al.*, 2013). In order to determine, if QS has an influence on gene expression; RNA extraction, cDNA synthase and qRT-PCR were performed on the potential exopolysaccharide genes comparing *V. harveyi* WT with strain JMH634 (QS OFF mutant, Δ*luxS* Δ*luxM cqsA*:cm^r). All expression profiles were below 10% of the house keeping gene *recA* at all time points tested (exponential growth phase - $OD_{600\ nm}$ of 0.6, early stationary growth phase - $OD_{600\ nm}$ of 1.3 and late stationary growth phase - $OD_{600\ nm}$ of 2, (Tab. 17).

However, the data obtained from the RNA extraction in the late stationary growth phase is depicted below as an example (Fig. 30, Tab. 17). Expression of *VIBHAR_06667* shows the greatest difference between the WT (9.15% *recA*) and the QS OFF mutant (0% *recA*). The blue columns show WT gene expression and the red columns show gene expression obtained from strain JMH634 (Fig. 30, Tab. 17).

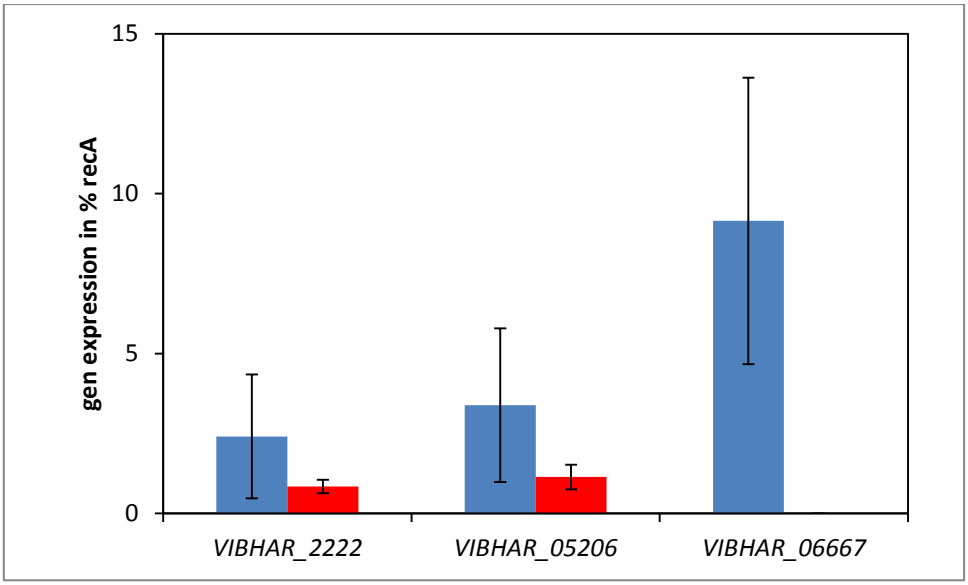

Fig. 30: Transcriptional expression of the putative exopolysaccharide genes comparing WT (blue columns) and JMH634 (red columns)

Furthermore, GFP-promoter fusions and GFP-hybrid proteins of the potential exopolysaccharide genes *VIBHAR_05206 and VIBHAR_06667* were generated and microscopy at different time points using cultivation in non-shaking flakes and on plates was performed. The expression profiles were really low as can be seen below in an example of *V. harveyi* EMR8 (BB120-p*VIBHAR_05206:gfp)* after 18 h of cultivation on an AB-agar plate (Fig. 31).

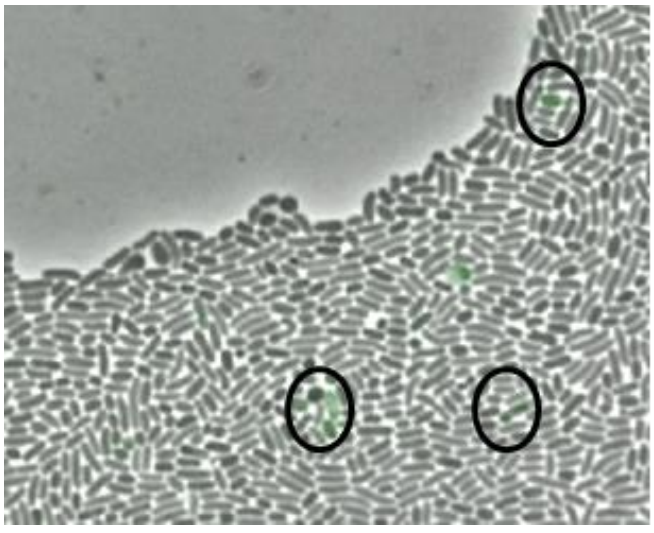

Fig. 31: Microscopy of EMR8 after 18 h of cultivation on an AB-agar plate was performed. Black circles indicated GFP-expression

In conclusion, transcriptional and translational expression profiles were too low in all performed experiments to investigate this matter further.

3.2.3 Putative LuxR binding sites

LuxR is one of two master regulators within the QS ascade of *V. harveyi* (Kessel *et al.*, 2013a). As described above LuxR can activate or repress gene expression and also influence gene expression directly or indirectly (Kessel *et al.*, 2013b). *luxR* is maximally transcribed at high cell density (Kessel *et al.*, 2013a). Pompeani *et al.* (2008) described a 21 bp consensus (Fig. 32) to be a *luxR* binding site and Kessel *et al.* (2013b) identified 1,165 *luxR* binding sites.

The genes selected within this thesis for knock-out mutants were manually checked for this consensus and upstream of *VIBHAR_05207*, *VIBHAR_01320* and *luxS* possible *luxR* binding sites were discovered.

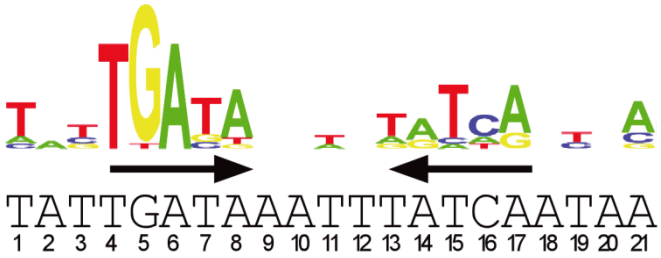

Fig. 32: LuxR binding site consensus (Pompeani *et al.*, 2008)

Here, are the putative *luxR* binding sites manually found:

- TATTGAGATATGACACTCAAT is located 32 bp upstream of *VIBHAR_05207* (start of operon *VIBHAR_05207 to VIBHAR_05204*),
- CATTGATATGATCATGCAAGA is located 15 bp upstream of *VIBHAR_01320* and
- AATTGACTTTTAGGTGAGGGA is located 61 bp upstream of *luxS*.

This data suggests that the genes above are directly regulated by LuxR. However, in this thesis, it was not established in which way the genes are regulated (active expression or repression at LCD or HCD).

3.3 Colony morphology of macrocolonies

Biofilms are most often grown in flow systems (Serra *et al.*, 2013), however, another possibility for biofilm formation is the outgrowth of macrocolonies on agar plates. This technique of macrocolony biofilms allows the analysis on macro level (colony structure and formation patterns) and also on micro level as single cells can be viewed under microscopes (Serra *et al.*, 2013; Serra and Hengge, 2014).

3.3.1 Bioluminescence and structure of macrocolonies

First, the formation of rings, the structure and the bioluminescence appearance of the macrocolonies were compared to each other. Therefore, the following strains were used: *V. harveyi* WT BB120, *V. harveyi* Δ*luxO*, *V. harveyi* MR15 (Δ*luxS* Δ*cqsA* Δ*luxM*), *V. harveyi* MR3 (Δ*luxS), V. harveyi* MR13 (Δ*cqsA), V. harveyi* MR18 (Δ*luxM), V. harveyi* EMR14 (Δ*luxS* – pBBR1-MSC2-BAD-*luxS) V. harveyi* EMR19 (chromosomal integrated *luxS* in Δ*luxS), V. harveyi* EMR2 (Δ*VIBHAR_05206-05205*), *V. harveyi* EMR3 (Δ*VIBHAR_06667*), *V. harveyi* EMR20 (Δ*VIBHAR_02222-02221*) and *V. harveyi* EMR23 (Δ*VIBHAR_01320*).

The colonies formed so called ring-structures from the center to the edge (Fig. 33). Visible, is that the ring formation of each strain is present from day 1 and with each day the number of rings increases. Furthermore, the structure of the macrocolonies changes shape: the edge of the macrocolonies of WT and strain Δ*luxO* change from round (day 1 to 3) to radial and bloomy (day 5 and 8), respectively. MR15 strain remains a round colony although on day 5 and 8 the edge of the colony appears to be fuzzy (Fig. 33).

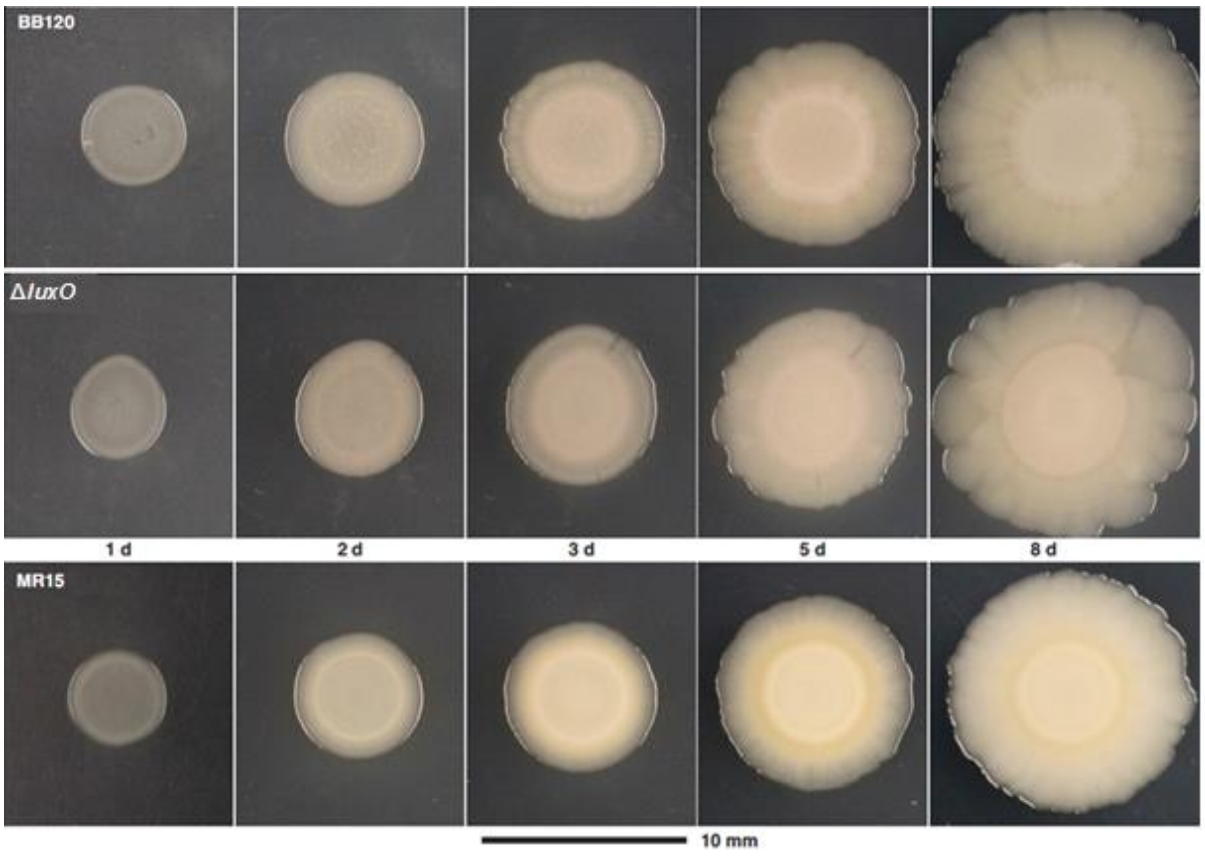

Fig. 33: Timeline of the macrocolonies of *V. harveyi* strains WT (top row), *V. harveyi* Δ*luxO* (middle row) and *V. harveyi* MR15 (bottom row)

Images were taken with a Canon 5D Mark II and a 100 mm macro lens from Canon (Tokio, Japan) by Prof. Wanner.

Furthermore, after 8 days of cultivation on AB-agar plates, pictures were taken with a Samsung galaxy S4 mobile phone GT-I950 from 2013 (panel A, Fig. 34 - Fig. 37) and also with a Fusion-SL 3.500 WL by peqlab GmbH (Erlangen, Germany) with light exposure to visualize colony morphology (panel B, Fig. 34 - Fig. 37) and without light exposure to visualize bioluminescence production (panel C, Fig. 34 - Fig. 37).

Below, BB120 shows the formation of 4 rings while Δ*luxO* strain shows 6 rings and MR15 shows 3 rings. The shape of Δ*luxO* strain is bloomy and the WT colony is rather radial while MR15 strain appears to be round (panel A-C, Fig. 34). Also, clearly visible is the lack of bioluminescence of MR15 compared to WT and Δ*luxO* strain, however, also parts of the macrocolony of Δ*luxO* strain lack bioluminescence (panel C, Fig. 34).

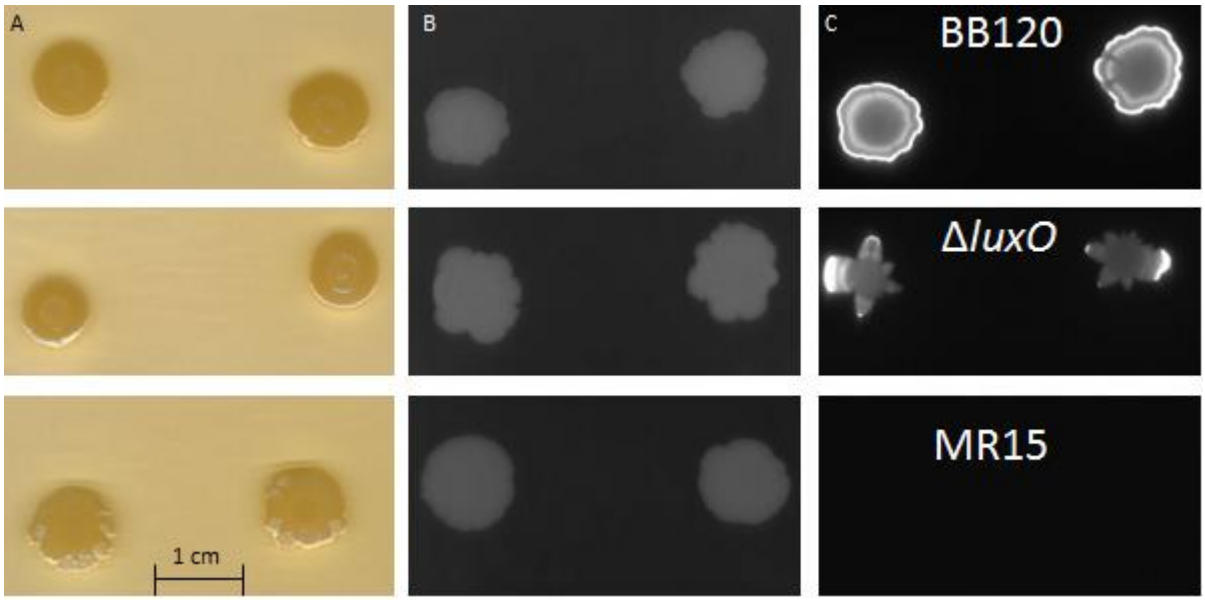

Fig. 34: Macrocolonies of *V. harveyi* strains WT (top row), *ΔluxO* (middle row) and MR15 (bottom row) after 8 days of cultivation

Panel A: Images were taken with a Samsung galaxy S4 mobile phone, Panel B: Images were taken with a Fusion-SL 3.500 WL to visualize bioluminescence production by *V. harveyi* strains after 8 days light and panel c shows the image from Panel B without light, exposure time was 5 s. Images of panel A are not the same as in panel B and C.

Next, the WT was compared to the single synthase deletion mutants: *V. harveyi* MR3 (Δ*luxS), V. harveyi* MR13 (Δ*cqsA)* and *V. harveyi* MR18 (Δ*luxM)*. The colonies of strains MR13 and MR18 have a round shape while BB120 and MR3 colonies are rather radial of shape. MR13 and MR18 display the formation of 4 and 5 rings, respectively, while WT colony shows 4 rings and MR3 shows the formation of 2 rings (panel A-C, Fig. 35). The bioluminescence of MR13 strain is weaker in the center of the colony which is not the case for MR18 strain, MR3 colony is only bioluminescent on the edge of the colony and all strains show a greater bioluminescence on the edge of the colony than in the center (panel C, Fig. 35).

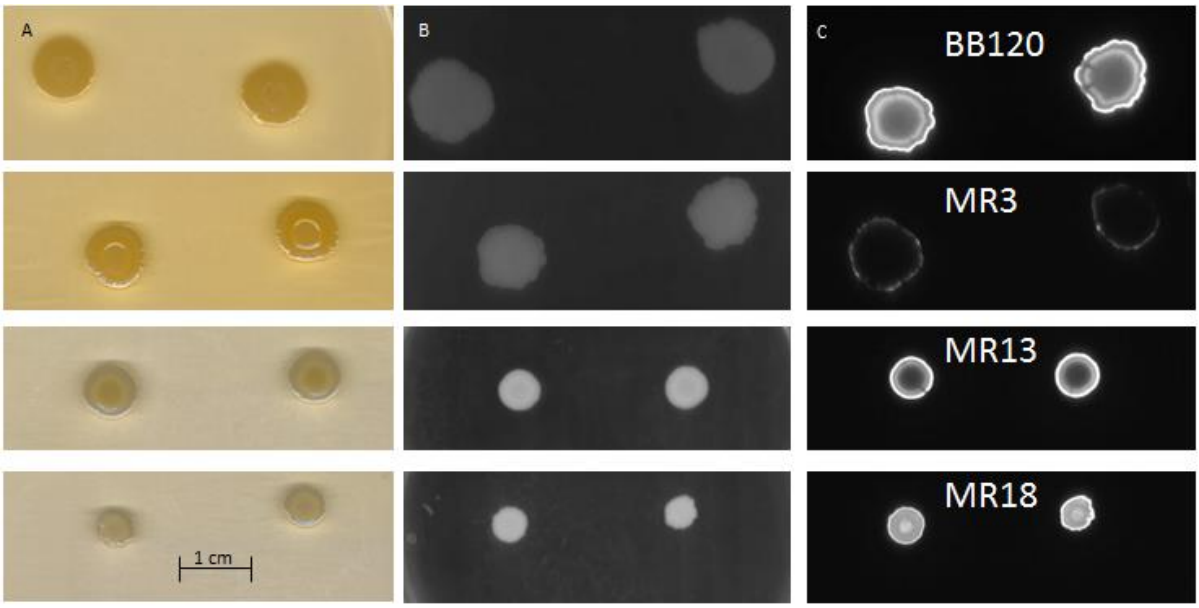

Fig. 35: Macrocolonies of *V. harveyi* strains WT (top row), MR3 (second to top row), MR13 (second to bottom row) and MR18 (bottom row) after 8 days of cultivation

Panel A: Images were taken with a Samsung galaxy S4 mobile phone, Panel B: Images were taken with a Fusion-SL 3.500 WL to visualize bioluminescence production by *V. harveyi* strains after 8 days light and panel c shows the image from Panel B without light, exposure time was 5 s. Images of panel A are not the same as in panel B and C..

Below, are the in *trans* complementation (EMR14) and chromosomal integration of *luxS* (EMR19) in MR3 strain (Δ*luxS*) shown in comparision with the WT. The macrocolony of the WT shows the formation of 4 rings, MR3 shows 2 rings while EMR14 and EMR19 show each 5 rings and radial structures on the edge of the colony (panel A-C, Fig. 36). Clearly, MR3 strain only displays bioluminescence on the the edge of the colony while EMR14 and EMR19 nearly show WT bioluminescence levels (panel C, Fig. 36). Also, all mutant strains depicted below show a similar colony shape: a round shape which becomes fuzzy on the edge of the colony while the WT and MR3 colony are of a rather radial shape (panel A-C, Fig. 36).

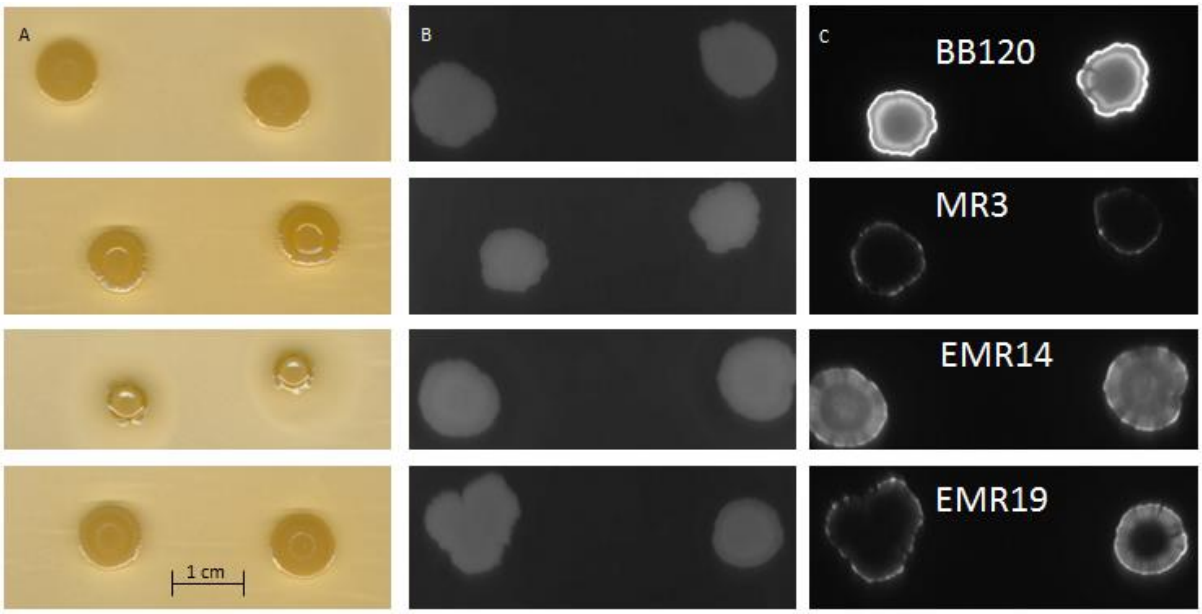

Fig. 36: Macrocolonies of *V. harveyi* strains WT (top row), MR3 (second to top row), EMR14 (second to bottom row)and EMR19 (bottom row) after 8 days of cultivation

Panel A: Images were taken with a Samsung galaxy S4 mobile phone, Panel B: Images were taken with a Fusion-SL 3.500 WL to visualize bioluminescence production by *V. harveyi* strains after 8 days light and panel c shows the image from Panel B without light, exposure time was 5 s. Images of panel A are not the same as in panel B and C.

Also, the colony morphologies and the ring formation of the macrocolonies of the putative exopolysaccharide deletion mutants were compared to the WT macrocolony (panel A-C, Fig. 37). WT shows 4 rings and EMR2 shows 7 while EMR3, EMR20 and EMR23 show the formation of 4 rings. All strains including the WT show a greater bioluminescence at the edge of the colony (panel C, Fig. 37). Also, EMR2 has a round shape of the colony while WT is of a radial shape and the other mutant strains show a bloomy shape (panel A-C, Fig. 37).

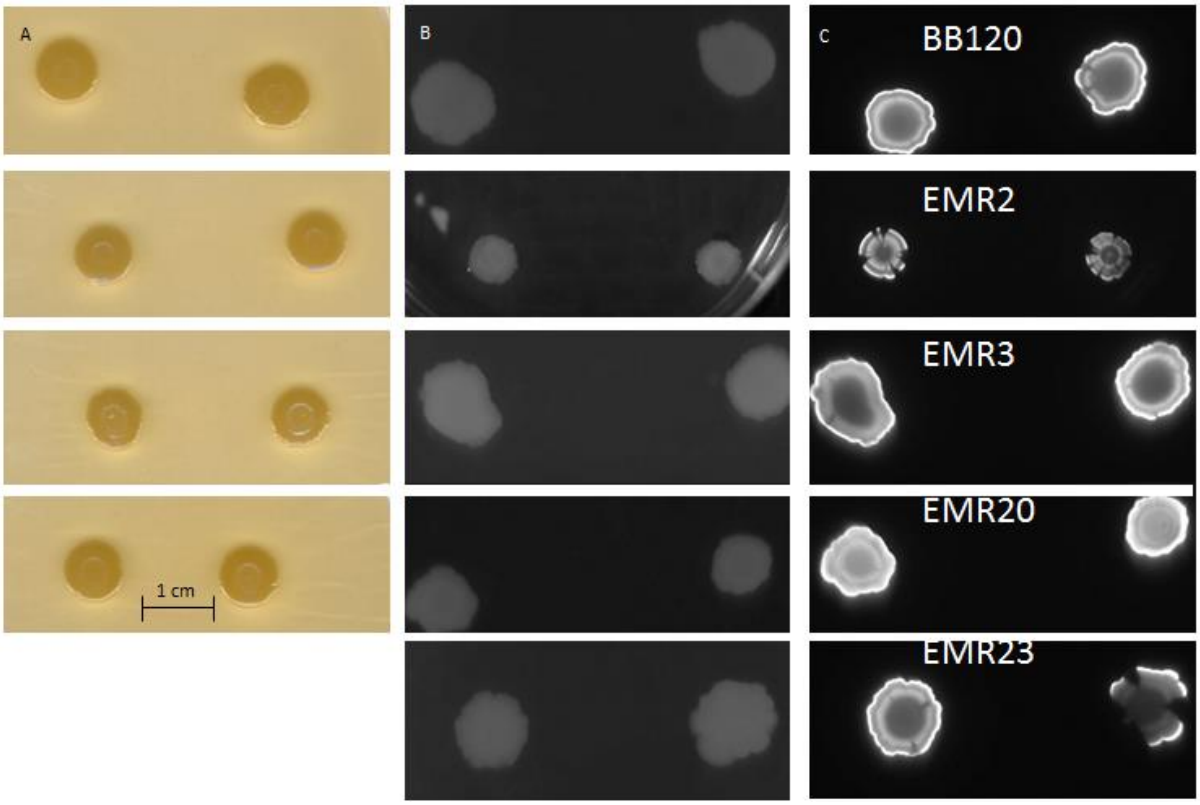

Fig. 37: Macrocolonies of *V. harveyi* strains WT (top row), EMR2 (second to top row), EMR3 (middle row), EMR20 (second to bottom row) and EMR23 (bottom row) after 8 days of cultivation

Panel A: Images were taken with a Samsung galaxy S4 mobile phone, Panel B: Images were taken with a Fusion-SL 3.500 WL to visualize bioluminescence production by *V. harveyi* strains after 8 days light and panel c shows the image from Panel B without light, exposure time was 5 s. Images of panel A are not the same as in panel B and C.

In conclusion, MR15 strain lacks the bioluminescence completely while MR3 strain shows a strongly reduced bioluminescence which was restored to WT levels by in *trans* complementation (EMR14) and knock-in mutant EMR19. The other mutant strains show WT bioluminescence levels. The colonies of the WT and the mutants display different ring formation patterns: minimal 2 rings were formed and maximal 7. Also, different shapes of the macrocolony were visible while the WT and MR3 colonies rather show a radial shape, the colonies of strains MR15, MR13, MR18, EMR14, EMR19 and EMR2 are round and Δ*luxO*, EMR3, EMR20 and EMR23 formed colonies of a bloomy shape.

3.3.2 Analysing of the macrocolonies via Scanning Electron Micrsocopy

Additionally, *V. harveyi* WT was compared to the strains Δ*luxO* and MR15 using Scanning electron Microscopy to analyse the macrocolony on single cell level. After the process of fixation, the ring structures are even better to be seen. On macrocolony of MR15 strain, 14 rings can be counted (left part of picture) now (Fig. 38).

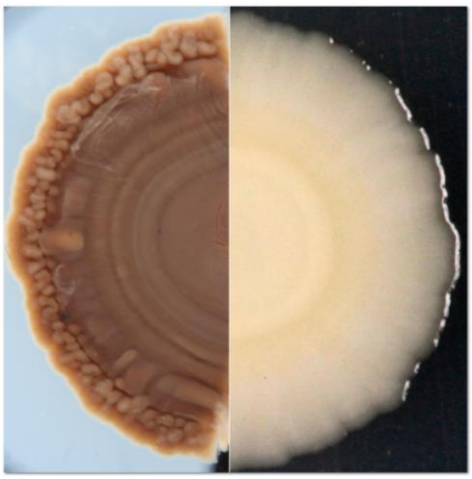

Fig. 38: Macrocolony of strain MR15 before (right image) and after (left image) fixation

Fused image shown after (left) and before (right) fixation of a 8 day old *V. harveyi* MR15 macrocolony. Images were taken with a Canon 5D Mark II and a 100 mm macro lens from Canon (Tokio, Japan) by Prof. Wanner.

Here, an overview of the center of a 8 day cultivated *V. harveyi* WT macrocolony is shown (Fig. 39). It can be assumed that the wave-like structures depicted below are due to the growth of the colony. The parts of the colony which are thicker than the parts next to it on the colony are what we determined as rings.

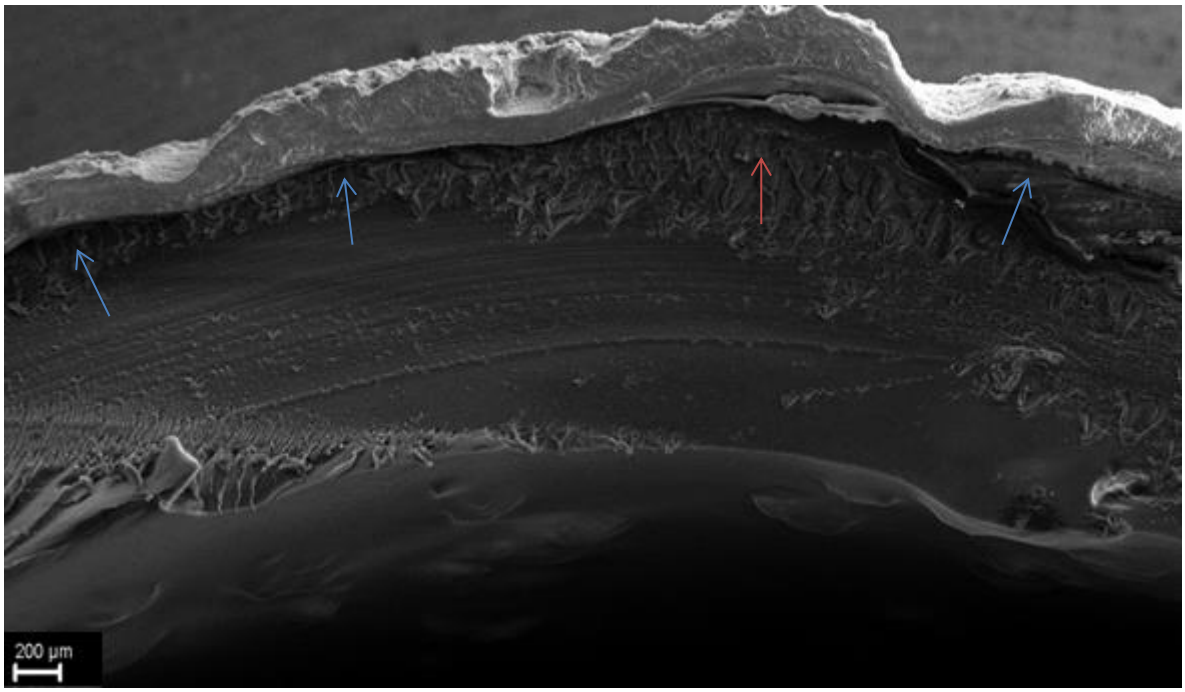

Fig. 39: Overview of a *V. harveyi* WT macrocolony, blue arrows indicate rings and red arrow indicates the center

Below are images shown from the center and the edge of the WT macrocolony and visible is an elongation of the cells on the edge compared to the center (Fig. 40).

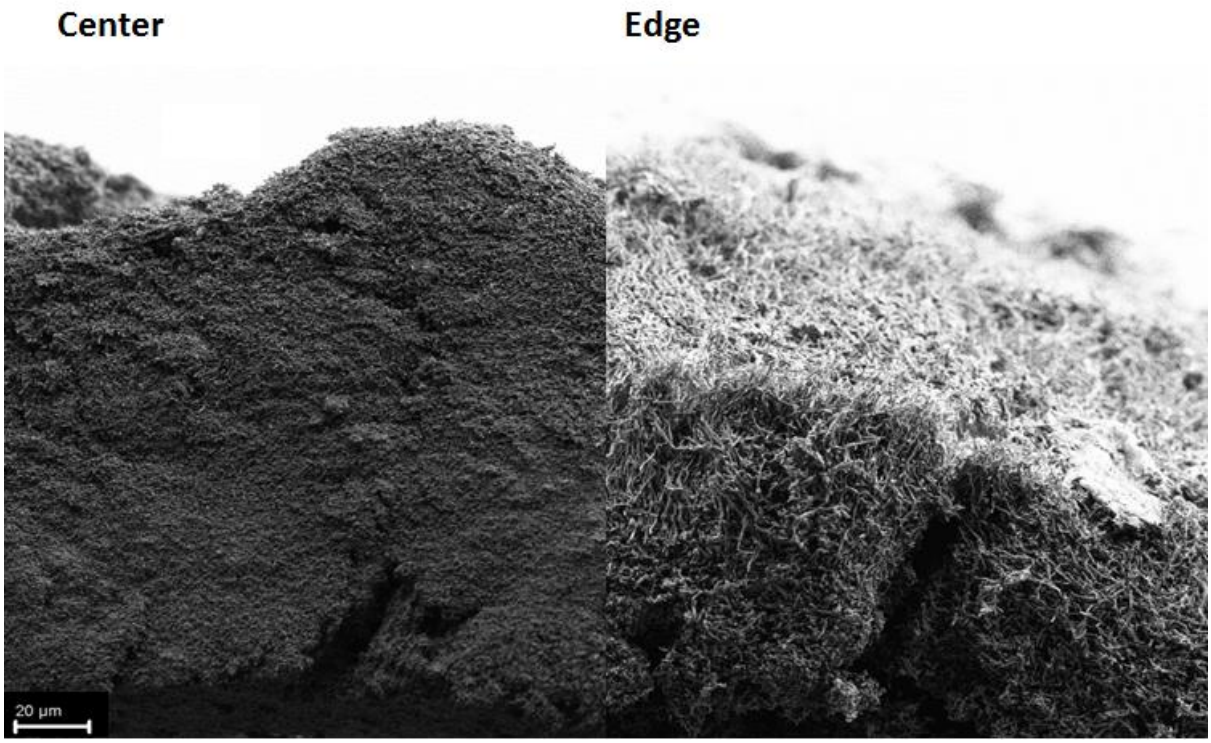

Fig. 40: Left side shows the center of the WT macrocolony and right side shows the right edge of the macrocolony

Single cells from the colony are round and rod-shaped from the center of the colony to the rings but on the edge enlarged rod-shaped cells were visible (Fig. 41).

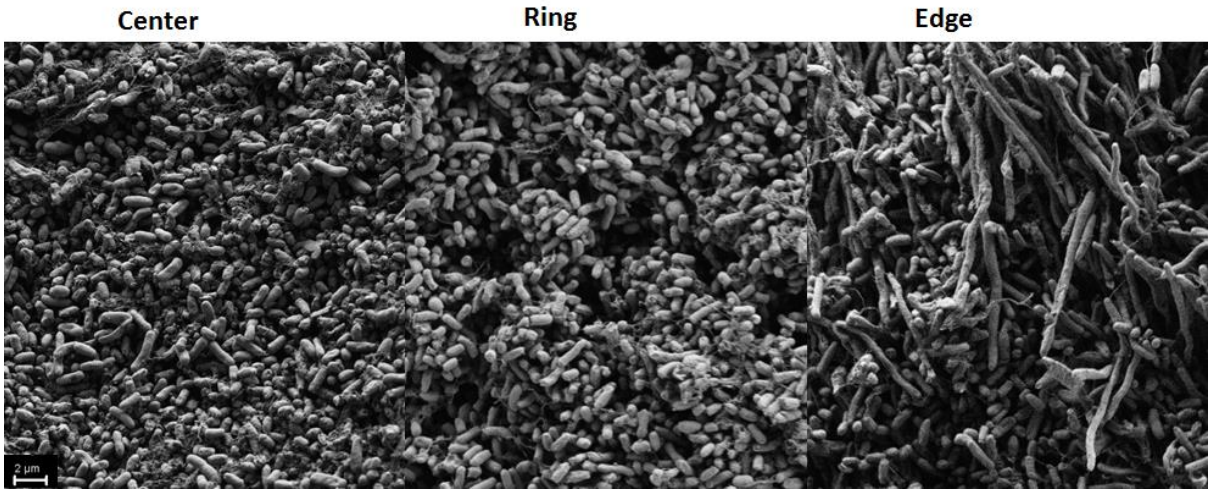

Fig. 41: WT macrocolony from the center to the first left ring and right edge (left to right images)

Below, are the center and the edge shown of a macrocolony formed by *V. harveyi* Δ*luxO.*The edge is broken due to the fixation process. It appears that the cells all have the same shape (Fig. 42).

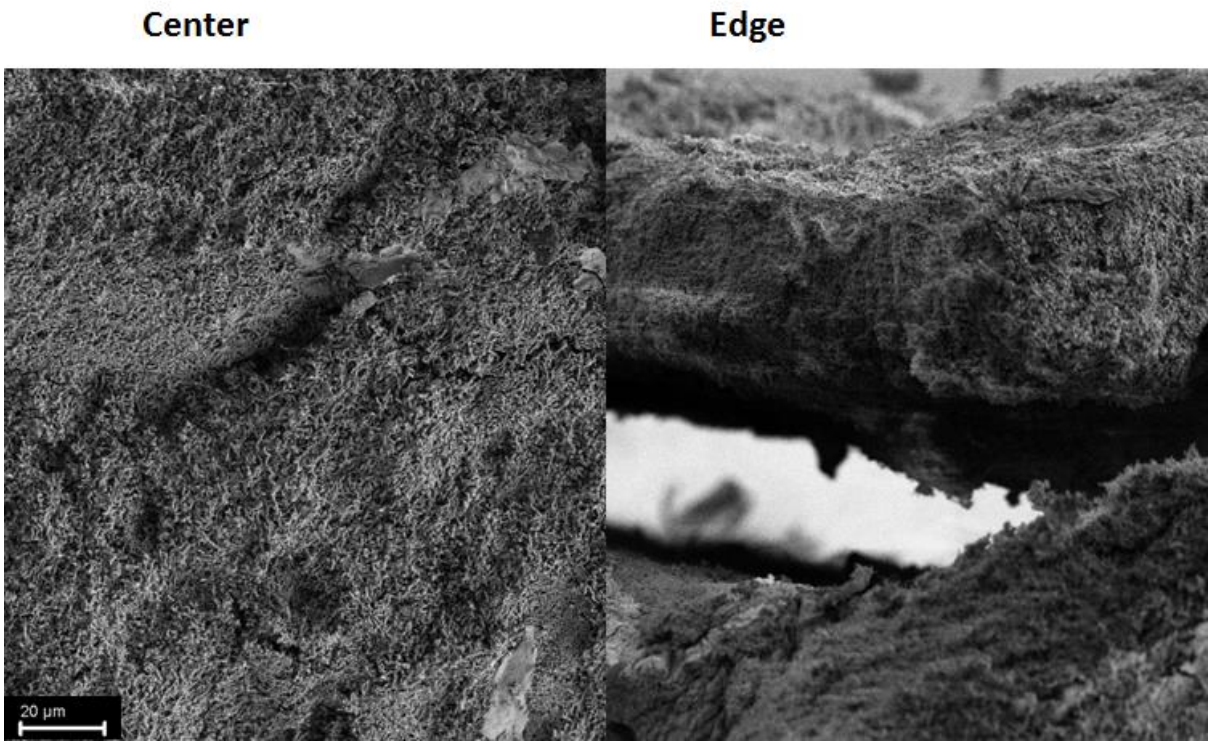

Fig. 42: Center (left image) and left edge (right image) of a Δ*luxO* strain macroyolony

The center, a ring as well as the edge of a Δ*luxO* macrocolony shows that the cells have all the same shape: round and rod-shaped, however, more cells seem to be rod-shaped (Fig. 43).

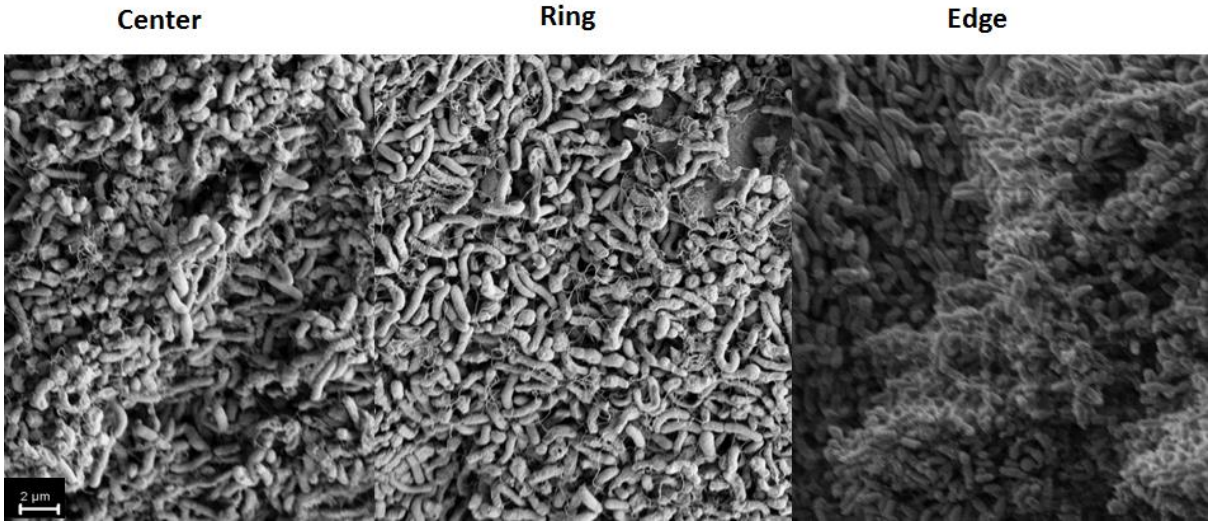

Fig. 43: Macroyolony of a Δ*luxO* strain from the center to the second ring left and the left edge (left to right images)

The center and the edge of a MR15 strain macrocolony indicate the same cell shape (Fig. 44).

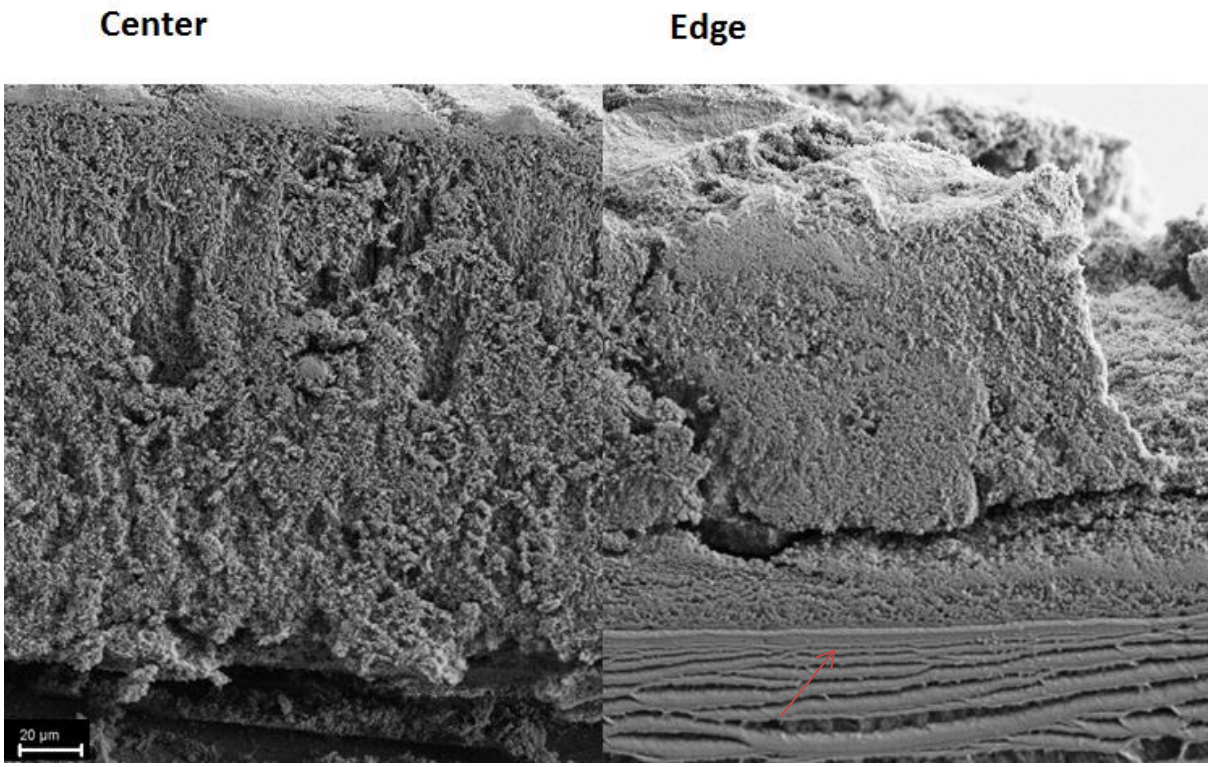

Fig. 44: Center (left image) and left edge (right image) of a MR15 strain macrocolony, red arrow indicates agar

The cells in the center, a ring and on the edge of a MR15 macrocolony appear to be mostly rod-shaped and a smaller amount of the cells is round (Fig. 45).

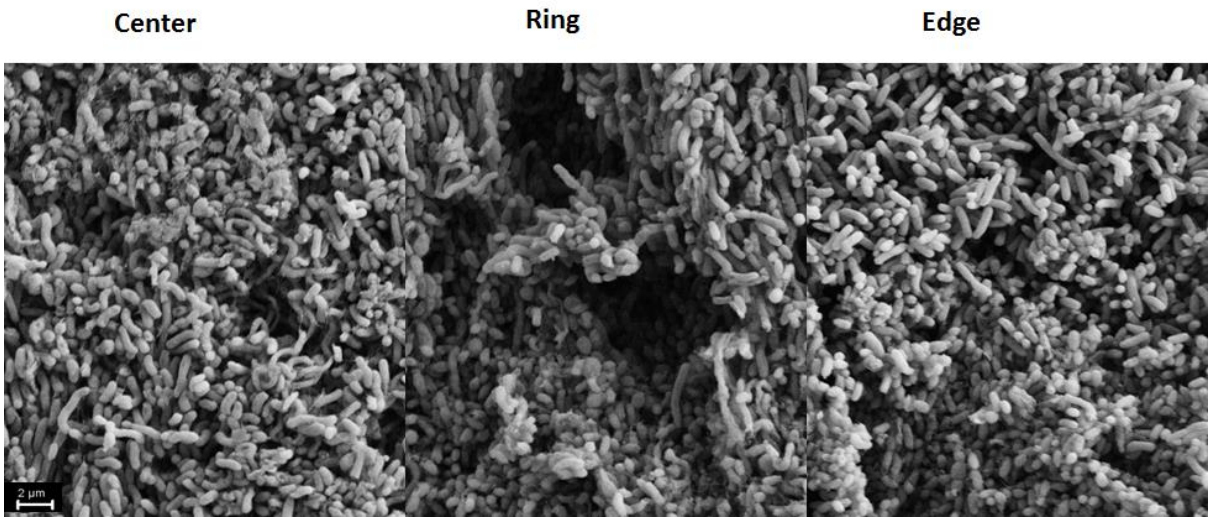

Fig. 45: MR15 strain macrocolony from the center, the second ring right and the left edge (left to right images)

The images above show that only the edge of the WT macrocolony displays elongated cells but neither the Δ*luxO* nor MR15 cells show this phenotype. It is assumed that this phenotype is influenced by QS.

4 Discussion

4.1 The influence of QS on bioluminescence and biofilm formation in *V. harveyi*

In order to determine *V. harveyi´*s ability to form biofilms, biofilm formation of the WT in a flow system was analysed. After 18 h of cultivation, the highest level of biomass was measured and therefore, biomass at this time point was set as 100%. The bacteria showed the common steps of biofilm formation within 24 h (Davey and O´Toole, 2000, Stoodley *et al.*, 2002, Fong and Yildiz, 2007, Nadell *et al.*, 2010, Parsek and Greenberg, 2005, Aguilar *et al.*, 2010): Initial attachment after 1 h (5% biomass level), microcolony formation after 6 h (8% biomass level), maturation after 18 h of cultivation (100% biomass level) and detachment began to occur between 18 and 24 h (90% biomass level, Fig. 13 and Fig. 14). The detachment step within the biofilm usually occurs due to nutrient depletion or via QS, e.g. *V. cholerae* upregulates enzymes via QS in order to disperse the cells from the biofilm at high cell density (Nadell *et al.*, 2010). Within our system, QS is the likely reason for detachment since nutrient availability was guaranteed through the constant flow rate, and also along with the constant flow rate the AI concentration within the system is diluted.

4.1.1 QS affects bioluminescence and biofilm formation

The constitutive QS ON mutant Δ*luxO* showed a flat biofilm with various clusters of microcolonies and one unstructured tower, producing 37% biomass of the WT (Fig. 16 and Fig. 17). One reason for this result could be that because QS is switched on constitutively, it can only use its energy to produce slightly more bioluminescence (103% WT level, Fig. 15, Tab. 14) but it is unable to overproduce all WT phenotypes. The data described above is consistent with data shown in Anetzberger *et al.* (2009), however, in that publication a *luxO*:cam^r strain was used instead of a *luxO* knock-out mutant.

The QS OFF mutant MR15 showed no bioluminescence at all (Tab. 14, 0% WT Level). Furthermore, the QS OFF mutant MR15 was unable to form a surface coated biofilm. Instead this mutant showed only minorly attachment of cells to the surface, and was able to produce a biomass of only 7% of the WT level (Fig. 16 and Fig. 17, Tab. 15). Therefore, it can be concluded that a complete and intact QS is necessary for the formation of a mature biofilm of *V. harveyi*.

4.1.2 AI-2 influences the adhesion of *Vibrio harveyi* on surfaces

As described above, AI-2 is the first AI produced within *V. harveyi* during batch cultivation (Fig. 8). In the time scale biofilm formation by the WT (Fig. 13 and Fig. 14), adhesion to a surface takes place in the time frame when only AI-2 is detectable in the supernatant. When HAI-1 and CAI-1 are detectable in the supernatant during batch cultivation, microcolonies start to develop in the biofilms. Therefore, cells lacking AI-2 production (MR3, Δ*luxS)* lead to decreased attachment on surfaces and no biofilm is detected (4% WT level, Fig. 18 and Fig. 19, Tab. 15). Lacking HAI-1 results still in 43% of the WT level (MR18, Δ*luxM*), so there is a severe decrease in biomass while lacking CAI-1 (MR13, Δ*cqsA*) causes the least difference in biofilm formation with respect to WT biofilms, as this mutant still made 70% of the WT biomass. The MR13 and MR18 biofilms seem to be off less

structure than the WT biofilm but still built up small mushroom shaped towers (Fig. 18 and Fig. 19, Tab. 15).

As reviewed in Tab. 2, lack of AI-2 causes severe defects in normal bacterial lives. In view of the results in this thesis, for *V. harveyi*, it is clear that AI-2 is the most important AI for *V. harveyi´*s biofilm formation as it affects the adhesion of the cells to the surface which is the starting point of biofilm formation.

Methodologies not yet tested include the effect of AI-2 in supernatant and the effect of artificial AI-2 added in the flow systems. However, the addition of DPD, SAM, cysteine or methionine could not restore biofilm formation in a *luxS* mutant of *S. enterica* serovar Typhimurium (Doherty *et al.*, 2006). Similarly, Lebeer *et al.* (2007) reported that AI-2 conditioned media fails to restore the WT biofilm level of a *luxS* mutant of *Lactobacillus reuteri* strain 100-23.

Also, Auger *et al.* (2006) found that addition of AI-2 (1 to 6.8 µM) to the cultures inhibits biofilm formation of *B. cereus*. So, one possibility could be that complemented in *trans* MR3 (EMR14) and chromosomal integrated MR3 (EMR19) mutants produce too much AI-2 to be able to form a WT biofilm. Both show similar bioluminescence levels as the WT (76 to 81% of the WT bioluminescence level, Fig. 20, Tab. 14). Further, biofilms increased in biomass and structure compared to their knock out copies, however, compared to WT biofilm, there are still severe differences in the structures of the knock in biofilms (36 and 29% of the WT biomass level, respectively, Fig. 21 and Fig. 22). A LuxP-FRET-Reporter assay (Rajamani *et al.*, 2007) could determine the AI-2 levels compared to the WT to ensure that the production is sufficient. Furthermore, both strains could be tested with qRT-PCR on *luxS* expression and also a Western Blot could show the protein levels of LuxS of these strains.

4.2 Identification of EPS genes involved in the production of biofilms

Adhering to biotic or abiotic surfaces is promoted by the extracellular polysaccharides present on bacterial cell surfaces (Shibata *et al.*, 2012). In this context, *Vibrio harveyi´*s polysaccharides were investigated. Genes found contributing to extracellular polysaccharide formation were: a gene coding for an epimerase (*VIBHAR_01320*, EMR23); an operon coding for a glycosyltransferase and a hypothetical protein coding for a glycosyltransferase in *V. parahaemolyticus* (*VIBHAR_02222-VIBHAR_02221*, EMR20); an operon containing a galactosephosphotransferase and three uncharacterized proteins all coding for genes being involved in the capsular polysaccharide synthesis within *V. parahaemolyticus* (*VIBHAR_05206-VIBHAR_05205*, EMR2); and a single uncharacterized gene coding for a protein involved in polysaccharide synthesis (*VIBHAR_06667*, EMR3) were identified by homology search (Tab. 13). For all these genes, novel deletion mutants were generated and their phenotypes for bioluminescence, EPS production and biofilm formation were characterized and compared to the WT.

Bioluminescence levels were not affected by the deletions (90 to 104% of the WT bioluminescence level, Fig. 23, Tab. 14). The EPS production of the mutants EMR2, EMR3, EMR20 and their triple deletion mutant EMR21 was done by glucose determination after hydrolysation, the mutants showed between 39% and 48% of the WT glucose production (Fig. 24, Tab. 16). The WT equivalent glucose level could be restored by chromosomal integration (95 to 103% of the WT level, Fig. 27, Tab. 16).

As a first inquiry into biofilm formation of the mutants generated in this thesis, biofilm formation via crystal violet staining was performed on all mutants (results not shown). These mutants were then later used in the CLSM experiments with the flow systems.

Deletion of the predicted nucleoside-diphosphate sugar epimerase (EMR23, Δ*VIBHAR_01320*) resulted in a flat monolayered biofilm with no tower or hill structures and a biomass of 26% of the WT level (Fig. 25 and Fig. 26). Therefore, it was shown that this epimerase is essential for the maturation of the biofilm. Epimerases are involved in the production of carbohydrate polymers, sugars and carbohydrates to protect bacteria when located on the cell surface (Allard *et al.*, 2001). Sialic acid, which also serves as a carbon source and is found outside on bacterial cells, is used to mask the pathogens from the host immune systems. *H. influenzae* among other pathogens and commensals uses the epimerase NanE for the biosynthesis of sialic acid (Almagro-Moreno and Boyd, 2009) which is a component of *H. influenzae* biofilms (Greiner *et al.*, 2004). Within *V. vulnificus* the *gne* gene coding for an UDP-*N*-acetylgalactosamine 4-epimerase is involved in the biosynthesis of O-antigen within lipopolysaccharides. A *V. vulnificus gne* mutant lacks the O-antigen on the surface which resulted in decreased biofilm formation in gill mucus of eels, this has also been described for *V. cholerae*. Furthermore, the O-antigen is required for swarming, swimming and colony expansion (Valiente *et al.*, 2008). As the predicted epimerase is not characterized, it would be necessary in order to determine its function to better understand the phenotype of the deletion mutant.

Bourne and Henrissat (2001) reported a bacterial UDP-*N*-acteylglucosamine 2-epimerase belonging to the family of glycosyltransferases. Furthermore, meningococcal lipopolysaccharide biosynthesis requires UDP-glucose-4-epimerase and three glycosyltransferases: two galactosyltransferases, lgtB and lgtE, and one *N*-acetylglucosaminyltransferase, lgtA (Wakarchuk *et al.*, 1996).

The deletion mutants EMR2 (Δ*VIBHAR_05206-VIBHAR_05205*), EMR20 (Δ*VIBHAR_02222-VIBHAR_02221)* and EMR22 (Δ*VIBHAR_05206-VIBHAR_05205* Δ*VIBHAR_06667* Δ*VIBHAR_02222-VIBHAR_02221*) developed only flat biofilms with volumes of 21%, 15% and 22% of the WT biofilm level, respectively (Fig. 25 and Fig. 26). The biofilm of the deletion mutant EMR3 (Δ*VIBHAR_06667)* resulted in 19% of the WT biofilm volume and showed an unstructured monolayer biofilm. A flat biofilm was also found by deleting the glycosyltransferases *gftB* and *gftC* in *S. mutans* (Xiao *et al.*, 2012). Also, *Shibata et al.* (2012) found six genes coding for glycosyltransferases and six genes partly being involved in polysaccharide modification, among others, within the symbiosis polysaccharide (*syp*) locus of *A. fischeri*. This locus is required for biofilm formation and the structural proteins are involved in polysaccharide production and export. Mutations in the predicted glycosyltransferase genes resulted in defect biofilms. A mutation in *sypR* gene in *A. fischeri* is predicted to have the same function as *VIBHAR_05207* (operon includes genes *VIBHAR_05207* to *VIBHAR_05204*) and resulted in a severely reduced biofilm compared to the WT. Furthermore, Xiao *et al.* (2012) compared single to mixed species biofilms and found increased glycosyltransferase activity in biofilms of mixed species. Glycosyltransferases were increasingly expressed during the steps of microcolonisation of the surface. A biofilm of *S. oralis* with *S. mutans,* having double deletions of the glycosyltransferase genes *gftB* and *gftC,* was rather flat without clear 3D structure (Xiao *et al.*, 2012). A mutation in the undecaprenyl-phosphate-α-*N*-acetyl-glucosaminyltransferase (*wecA*) of *H. influenzae* resulted in little or no biofilm. *wecA* is homologous to *E. coli´*s *wecA*, which is involved in polysaccharide

synthesis (Greiner *et al.*, 2004). The characterization of the proteins would be necessary to fully understand their function and role in biofilm formation of *V. harveyi*.

Furthermore, all the biofilms mentioned above show a monolayered biofilm. Lee *et al.* (2013) described that EPS in *V. vulnificus* enhance maturation of biofilms as the cells attach to each other like glue. Thus, some polysaccharides are necessary for the attachment on surfaces and between the cells. In view of the fluid flow experiment performed EPS may stabilize cell aggreagates into 3D structures and pillar formations to resist shear forces (Young, 2006). Which exact gene is deleted, may be a key factor for bacteria to remain attached to each other, and the specific gene product may play a role of a different magnitude than other factors. Key protein RbmA of *V. cholerae* is coded by a gene located within the *vps* locus and this protein coats cell surfaces, thereby promoting cell-cell adhesion (Guttenplan and Kearns, 2013). Stodley *et al.* (2002) replaced this type of function by using a polysaccharide intercellular adhesin to form *S. epidermidis* microcolonies and mature a biofilm, so adhering cells together. In order to determine similar functions for the genes studied in this thesis, localization studies of their coded proteins should be performed.

As the mutants showed severe reduction of glucose levels and only monolayered biofilms, chromosomal integration (knock in) of the mutants EMR2, EMR3 and EMR20 was performed and EPS production and biofilm formation experiments were performed. The WT glucose levels could be restored by the knock in mutant strains (95 to 103% of the WT glucose level, Fig. 27, Tab. 15) and as expected, there was no change in bioluminescence levels (88 - 95% of the WT bioluminescence, Tab. 14). However, it was not possible to restore WT biofilm formation but there was a great increase in biofilm formation compared to the deletion mutants. The mutants showed biofilms with biomass ranging from 15 to 21% of the WT level while their complemented counterparts grew biofilms from 38 to 63% of the WT level (Fig. 28 and Fig. 29). The biofilms of the complemented strains also showed more tower-like structures (Fig. 28).

In addition, *V. vulnificus* has a lipopolysaccharide and three exopolysaccharides involved in biofilm formation. All of these are expressed at different time points within the biofilm formation (Lee *et al.*, 2013). Therefore, qRT-PCR on *VIBHAR_02222*, *VIBHAR_05206* and *VIBHAR_06667* was performed and also GFP-Promoter fusions for *VIBHAR_05206* and *VIBHAR_06667* and GFP-hybrid proteins were generated for *VIBHAR_05207* and *VIBHAR_06667.* Neither transcriptional nor translational expression gave further insights on the genes tested as all data obtained from these experiments were too low (Fig. 30, Fig. 31 and Tab. 17). One explanation for the qRT-PCR data could be that incorrect cultivation methods have been chosen as the RNA extraction was performed during batch cultivation. However, the harvest of biofilm cells currently presents technical difficulties to be overcome. As the fusion and hybrid mutant strains were tested using non-shaking flakes and plate cultivation, it can be only assumed that alternative cultivation methods or different time points then selected here need to be explored. Also, there is the possibility that the gene expression for each gene is only active at a very distinct time point during cultivation and time lapse experiments were not performed in this study.

In conclusion, the deletion of the putative exopolysaccharide genes resulted all in decreased EPS production and only in monolayered biofilms. Knock in mutants could restore WT glucose levels fully and partially WT biomass levels and showed similar to WT biofilm structures. However, there was no

information for transcriptional or translational expression profiles for the selected genes and proteins gained.

4.3 Colony morphology is affected by QS and EPS production

Biofilm formation can also occur when colonies are grown on agar plates over a long period of time (Serra *et al.,* 2013). This is the first description to date of colony formation using macrocolony biofilms of *V. harveyi*. Macrocolonies of the WT were compared with the different mutant strains Δ*luxO*, MR15 (Δ*luxS* Δ*cqsA* Δ*luxM*), MR3 (Δ*luxS)*, MR13 (Δ*cqsA)*, MR18 (Δ*luxM)*, EMR14 (Δ*luxS* – pBBR1-MSC2-BAD-*luxS)*, EMR19 (knock in of *luxS* in Δ*luxS)*, EMR2 (Δ*VIBHAR_05206-05205*), EMR3 (Δ*VIBHAR_06667*), EMR20 (Δ*VIBHAR_02222-02221*) and EMR23 (Δ*VIBHAR_01320*) for their colony morphology and ring pattern formation.

First, as in batch cultivation (Fig. 15), MR15 macrocolony lacks bioluminescence completely while MR3 strain shows reduced bioluminescence on the edges of the macrocolony after 8 days of cultivation on agar plates. The bioluminescence of MR3 could be restored by *luxS* in *trans* complementation (EMR14) and knock in of *luxS* (EMR19). The other mutant strains show similar to WT bioluminescence levels (Fig. 34 to Fig. 37).

Secondly, colony morphology varies when the WT macrocolony is compared with the other mutant strains. Ring formation is reduced from 4 rings (WT) to 2 and 3 rings for MR3 and MR15, respectively (Fig. 33, Fig. 34 and Fig. 35). MR13, EMR3, EMR20 and EMR23 each formed 4 visible rings which is constitent to the WT ring formation (Fig. 33, Fig. 35, Fig. 36 and Fig. 37). Macrocolonies of strains MR18, EMR14 and EMR19 show each the formation of 5 rings while Δ*luxO* macrocolony formed 6 rings and EMR2 macrocolony displays 7 rings (Fig. 33, Fig. 34 to Fig. 37). However, after fixation the ring patterns are stronger visible and MR15 macrocolony displays 14 rings after fixation (Fig. 38). Currently, to fully categorize ring pattern formation, all strains need fixation. Even if *E. coli* macrocolonies displayed by Serra *et al.* (2013) showed different ring formations when *E. coli* WT macrocolonies are compared to mutant strains, the ring formations were not further described. Therefore, it can only be assumed that ring formation is a mode of growth of the colony.

Furthermore, the colonies grown on agar plates vary in their shape: WT and MR3 macrocolonies form rather radial colonies (Fig. 33, Fig. 35) while macrocolonies of strains MR15, MR13, MR18 and EMR2 (Fig. 33, Fig. 34, Fig. 35 and Fig. 37) show round colonies and EMR14 and EMR19 macrocolonies show round colonies with fuzzy edges (Fig. 36). Also, the shapes of the macrocolonies of strains Δ*luxO*, EMR3, EMR 20 and EMR23 are bloomy (Fig. 33, Fig. 34 and Fig. 37). These colony morphologies have not been described for other bacteria to date. It would be necessary to analyse colony shape of other mutant strains for a full conclusion. However, it appears that with a gene deletion in either the QS cascade or putative EPS production, a different mode of growth is triggered.

Wrinkled structures being determined as swarming were observed when *V. parahaemolyticus* WT was grown on agar plates (Linda *et al.*, 1998). However, none of the distinct swarming structures were seen, that were described by Kearns (2010). Also, *E. coli* macrocolonies of all strains displayed by Serra *et al.* (2013) are of a round shape.

On day 8, the macrocolonies of strains Δ*luxO* and MR15 were compared with the WT macrocolony on single cell level using Scanning Electron Micrsocopy (Fig. 33). The data gained here suggests a QS triggered morphological change in cell shape as only WT macrocolonies show long filamentous cells on the edge of the macrocolonies while the cells of the QS ON and OFF mutants were rod-shaped and coccoid on the edge of the colonies (Fig. 39 and Fig. 45).

Serra and Hengge (2014) describe the rod-shaped cells to be in exponential growth phase and the ovoid cells to be in stationary growth phase when cells in macrocolony biofilms are compared with cells in batch culture. Furthermore, Serra *et al.* (2013) also described *E. coli* cells on the top of a macrocolony to be ovoid and rod-shaped and elongated cells are visible on the edge of the macrocolony. However, Boles and McCarter (2002) found that expression of an operon affected swarming ability in *V. parahaemolyticus*. They suggested that there is an advantage for elongated cells on the edge of a colony and advantages for normal-sized cells during colonization. This may also be the case for *V. harveyi* as this elongation is affected by QS.

In contrast, Farmer and Janda (2005) reported that *Vibrio* rods convert to coccoids when starved on nutrients, form filaments when starved of nitrogen, and form large swollen rods during phosphorus starvation. Nutrient depletion could be occurring internally within the colony, but there must be another reason for filamentation of rods on the edge of macrocolonies as nitrogen and phosphorus starvation are not likely to be occurring. Notably also, the filamentation occurred only in the WT and therefore, the change of cell shape is QS triggered.

In conclusion, the ring patterns and colony shapes visible can not be determined as swarming but it can be assumed that QS and putative EPS production influence ring pattern formation and colony shape. Bioluminescence production is consistant with the bioluminescence assays in batch cultivation. However, it can be assumed that the elongation of the cells on the edge of the WT macrocolony is affected by QS.

4.4 Outlook

WT levels of biofilm formation via *luxS* in *trans* complementation or *luxS knock in* the *luxS* deletion mutant were not to fully restored, it might be possible tofully complement WT biofilms levels by directly using catalytic products of *luxS* downstream activity, or analogues of these products. It has shown that only genetic recombination of *luxS* could restore WT phenotypes in *Listeria monocytogenes* and *Lactobacillus reuteri* but not addition of synthetic AI-2 (Choudhary and Schmidt-Dannert, 2010). Hypothetically, in *V. harveyi* it could be vice-versa.

Additionally, exopolysaccharides from *V. harveyi* could be purified and and tested for their ability to inhibit or disrupt the formation of biofilms by bacteria. As precedents, each of the following: an exopolysaccharide from *Vibrio* sp. QY101 (Jiang *et al.*, 2011); an exopolysaccharide of *B. licheniformis*; a polysaccharide of *Vibrio* sp. (Lee *et al.*, 2013) and a group II CPS of *E. coli* were able to inhibit formation of biofilmy by other species (Lee *et al.*, 2013, Jiang *et al.*, 2011).

For the predicted epimerase gene, it would be desirable to construct a fluorescent hybrid protein and/ or fluorescent promoter fusion and monitor its activity by a time lapse experiment. Also, it would be interesting if WT biofilm formation could be restored via complementation of the epimerase gene as this was not completely possible with the other genes used in this study.

Characterisation of all the proteins coding for putative exopolysaccharide genes used in this study could lead to new conclusions on biofilm formation.

In order to determine if the behavior observed in the macrocolony formation is actual swarming, it would be necessary to monitor the cells on single cell level closely over time, not only in the late stage. Swarming behavior is defined as vegetative rods that elongate being aseptate and multinucleate. Also, swarmer cells can initiate biofilm formation (Young, 2006). Macrocolony formation was examined over a time frame of 8 days but colonies were only analysed on single cell level using Scanning Electron Microscopy on day 8. On that day, the WT showed long filamentous cells on the edges of the colony but neither Δ*luxO* nor MR15 showed this behavior. In order to determine when this morphological change begins, it would be necessary to examine the colonies with the Scanning Electron Microscope each day.

5 References

Aguilar, C., Carlier, A., Riedel, K., Eberl, L. (2010): Chapter 2: Cell-cell communication in biofilms of Gram-negative bacteria in Bacterial Signaling, edited by Krämer, R. and Jung, K., WILEY-VCH Verlag GmbH & Co. KGaA. Weinheim, ISBN: 978-3-527-32365-4

Allard, S.T.M., Giraud, M.-F., Naismith, J.H. (2001): Epimerases: structure, function and mechanism. Cell Mol Life Sci 58, 1650-1665

Almagro-Moreno, S. and Boyd, E.F. (2009): Insights into the evolution of sialic acid catabolism among bacteria. BMC Evol Biol 9 (118), doi: 10.1186/1471-2148-9-118

Anetzberger, C., Pirch, T., Jung, K. (2009): Heterogeneity in quorum sensing-regulated bioluminescence of *Vibrio harveyi*. Mol Microbiol 73 (2), 267-277

Anetzberger, C., Reiger, M., Fekete, A., Schell, U., Stambrau, N., Plener, L., Kopka, J., Schmitt-Kopplin, P., Hilbi, H., Jung, K. (2012): Autoinducers act as biological timers in *Vibrio harveyi*. PLoS One 7 (10), e48310

Annous, B.A., Fratamico, P.M., Smith, J.L. (2009): Quorum Sensing in biofilms: Why bacteria behave the way they do. J Food Sci 74 (1), R24-R37

Auger, S., Krin, E., Aymerich, S., Gohar, M. (2006): Autoinducer 2 affects biofilm formation by *Bacillus cereus*. Appl and Envrion Microb 72 (1), 937-941

Bassler, B.L., Greenberg, E.P., Stevens, A.M. (1997): Cross-species induction of Luminescence in the quorum-sensing bacterium *Vibrio harveyi*. J Bacteriol 179 (12), 4043-4045

Bassler, B.L. (2002): Small talk: Cell-to-cell communication in bacteria. Cell 109, 421-424

Bassler, B.L. and Losick, R. (2006): Bacterially speaking. Cell 125, 237-246

Blokesch, M. and Schoolnik, G.K. (2007): Serogroup conversion of *Vibrio cholerae* in aquatic reservoirs. PLoS Pathog 3 (6): e81

Boles, B.R. and McCarter, L.L. (2002): *Vibrio parahaemolyticus* scrABC, a novel operon affecting swarming and capsular polysaccharide regulation. J Bacteriol 184 (21), 5946-5954

Bourne, Y. and Henrissat, B. (2001): Glycoside hydrolases and glycosyltransferases: families and functional modules. Curr Opin Struc Biol 11 (5), 593-600

Bowers, R.M., Sullivan, A.P., Costello, E:K., Collett Jr., J.L., Knight, R., Fierer, N. (2011): Sources of bacteria in outdoor air across cities in the midwestern United States. Appl Environ Microbiol 77 (18): 6350

Cao, J.-G. and Meighen, E.A. (1989): Purification and structural identification of an Autoinducer for the luminescence system of *Vibrio harveyi*. J Biol Chem 264 (36), 21670-21676

Chen, X., Schauder, S., Potier, N., Dorsselaer, A.V., Pelczer, I., Bassler, B.L., Hughson, F.M. (2002): Structural identification of a bacterial quorum-sensing signal containing boron. Nature 415 (6871), 545-549

Choi, K.*H.,* Gaynor, J.B., White, K.G., Lopez, C., Bosio, C.M., Karkhoff-Schweizer, R.R., Schweizer, H.P. (2005): A Tn7-based broad-range bacterial cloning and expression system. Nat Methods, 2 (6): 443-8

Choudhary, S. and Schmidt-Dannert, C. (2010): Applications of quorum sensing in biotechnology. Appl Microbiol Biotechnol 86, 1267-1279

Cuadra-Saenz, G., Rao, D.L., Underwood, A.J., Belapure, S.A., Campagna, S.R., Sun, Z., Tammariello, S., Rickard, A.H. (2012): Autoinducer-2 influences interactions amongst pioneer colonizing streptococci in oral biofilms. Microbiology 158, 1783-1795

Dagert, M. and Ehrlich, S.D. (1979): Prolonged incubation in calcium chloride improves the competence of *Escherichia coli* cells. Gene 6 (1): 23-8

Davey, M.E. and O´Toole, G.A. (2000): Microbial biofilms: from ecology to molecular genetics. Microbiol Mol Biol R 64 (4), 847-867

Defoirdt, T., Boon, N., Sorgeloos, P., Verstraete, W., Bossier, P. (2008): Quorum Sensing and quorum quenching in *Vibrio harveyi*: lessons learned from *in vivo* work. The ISME Journal 2, 19-26

Dehal, P.S., Joachimiak, M.P., Price, M.N., Bates, J.T., Baumohl, J.K., Chivian, D., Friedland, G.D., Huang, K., Keller, K., Novichkov, P.S., Dubchak, I.L., Alm, E.J., Arkin, A.P. (2009): MicrobesOnline: an integrated portal for comparative and functional genomics. Nucl Acids Res Doi: 10.1093/nar/gkp919

Dogsa, I., Brloznik, M., Stopar, D., Mandic-Mulec, I. (2013): Exopolymer diversity and the role of levan in *Bacillus subtilis* biofilms. PLoS One 8 (4), e60244

Doherty, N., Holden, M.T.G., Qazi, S.N., Williams, P., Winzer, K. (2006): Functional analysis of *luxS* in *Staphylococcus aureus* reveals a role in metabolism but not quorum sensing. J Bacteriol 188 (8), 2885-2897

DuBois, M., Gilles, K.A., Hamilton, J.K., Rebers, P.A., Smith, F. (1956): Colorimetric method for determination of sugars and related substances. Anal Chem, 28 (3), 350-356

Enos-Berlage, J.L. and McCarter, L.L. (2000): Relation of capsular polysaccharide production and colonial cell organization to colony morphology in *Vibrio parahaemolyticus*. J Bacteriol, 182, 5513-20

Farmer, J.J. III and Janda, J.M. (2005): Familiy I. Vibrionaceae. In Bergey´s Manual® of Systematic Bacteriology, Volume 2: The Proteobacteria, Part B The Gammaproteobacteria, edited by G. Garrity, Spinger, originally published by Williams & Wilkins, 1984

Fenley, A.T., Banki, S.K., Kulkarni, R.V. (2011): Computational modeling of differences in the quorum seinsing induced luminescence phenotypes of *Vibrio harveyi* and *Vibrio cholera*. J Theor Biol 274, 145-153

Fong, J.C.N. and Yildiz, F.H. (2007): The rbmBCDEF gene cluster modulates development of rugose colony morphology and biofilm formation in *Vibrio cholerae*. J Bacteriol 189 (6), 2319-2330

Fong, J.C.N., Syed, K.A., Klose, K.E., Yildiz, F.H. (2010): Role of *Vibrio* polysaccharide (vps) genes in VPS production, biofilm formation and *Vibrio cholerae* pathogenesis. Microbiology 156, 2757-2769

Geier, H., Mostowy, S., Cangelosi, G.A., Behr, M.A., Ford, T.E. (2008): Autoinducer-2 triggers the oxidative stress response in *Mycobacterium avium*, leading to biofilmformation. Appl Environ Microbiol 75 (6), 1798-1804

Gibbs, K.A. and Greenberg, E.P. (2011): Territoriality in *Proteus*: Advertisement and aggression. Chem. Rev. 111 (1), 188-194

Gode-Potratz, C.J. and McCarter, L.L. (2011): Quorum sensing and silencing in *Vibrio parahaemolyticus*. J Bacteriol 193 (16), 4224-4237

Gödeke, J., Paul, K., Lassak, J., Thormann, K.M. (2011): Phage-induced lysis enhances biofilm formation in *Shewanella oneidensis* MR-1. ISME J, 5 (4): 613-26

Greenberg, E.P., Hastings, J.W., Ulitzur, S. (1979): Induction of luciferase synthsis in *Beneckea harveyi* by other marine bacteria. Arch Microbiol. 120, 87-91

Greiner, L.L., Watanabe, H., Phillips, N.J., Shao, J., Morgan, A., Zaleski, A., Gibson, B.W., Apicella, M.A. (2004): Nontypeable *Haemophilus influenza* strain 2019 produces biofilm containin N-acetylneuraminic acid that may mimic sialylated O-linked glycans. Infect Immun 72 (7), 4249-4260

Guttenpland, S.B. and Kearns, D.B. (2013): Regulation of flagellar motility during biofilm formation. FEMS Microbiol Rev 37 (6), 849-871

Güvener, Z.T. and McCarter, L.L. (2003): Multiple regulators control capsular polysaccharide production in *Vibrio parahaemolyticus*. J Bacteriol 185 (18), 5431-5441

Henares, B.M., Higgins, K.E., Boon, E.M. (2012): Discovery of a nitric oxide response quorum sensing circuit in *Vibrio harveyi*. ACS Chem Biol 17; 7 (6), 1331-1336

Henarees, B.M., Xu, Y., Boon, E:M. (2013): A nitric oxide-responsive quorum sensing circuit in *Vibrio harveyi* regulates flagellar production and biofilm formation. Int J Mol Sci 14, 16473-16484

Henke, J.M. and Bassler, B.L. (2004a): Three parallel quorum-sensing systems regulate gene expression in *Vibrio harveyi*. J Bacteriol 186 (20), 6902-6914

Henke, J.M. and Bassler, B.L. (2004b): Bacterial social engagements. Trends Cell Biol 14 (11), 648-655

Hildago-Cantabrana, C., Sanchez, B., Milani, C., Ventura, M., Margolles, A., Ruas-Madiedo, P. (2014): Genomic overview and biological functions of exopolysaccharide biosynthesis in *Bifidobacterium* spp. Appl Environ Microbiol 80 (1), 9-18

Huq, A., Whitehouse, C.A., Grim, C.J., Alam, M., Colwell, R.R. (2008): Biofilms in water, its role and impact in human disease transmission. Curr Opin Biotech 19, 244-247

Inoue, H., Hiroshi, N., Hiroto, O. (1990): High efficiency transformation of *Escherichia coli* with plasmids. Gene 96, 23-28

Jiang, P., Li, J., Han, F., Duan, G., Lu, X., Gu, Y., Yu, W. (2011): Antibiofilm activity of an exopolysaccharide from marine bacterium *Vibrio* sp. QY101. PLoS One 6 (4), e18514

Kaper, J.B. and Sperandio, V. (2005): Bacterial cell-to-cell signaling in the gastrointestinal tract. Infect Imm 73 (6), 3197-3209

Karatan, E. and Watnick, P. (2009): Signals, regulatory networks, and materials that build and break bacterial biofilms. Microbiol Mol Biol R 73 (2), 310-347

Kavita, K., Mishra, A., Jha, B. (2013): Extracellular polymeric substances from two biofilm forming *Vibrio* species: Characterisation and applications. Carbohyd Polym 94, 882-888

Kearns, D.B. (2010): A field guide to bacterial swarming motility. Nature Rev 8, 634-644

Kessel van, J.C., Rutherford, S.T., Shao, Y., Utria, A.F., Bassler, B.L. (2013a): Individual and combined roles of the master regulators AphA and LuxR in control of the *Vibrio harveyi* Quorum-Sensing regulon. J Bacteriol 195 (3), 436-443

Kessel van, J.C., Ulrich, L.E., Zhulin, I.B., Bassler, B.L. (2013b): analysis of activator and repressor functions reveals the requirements fro transcriptional control by LuxR, the master regulator of quorum sensing in *Vibrio harveyi*. mBio Vol. 4(4), e00378-13

Labbate, M., Queck, S.Y., Koh, K.S., Rice, S.A., Givskov, M., Kjelleberg, S. (2004): Quorum Sensing-controlled biofilm development in *Serratia liquefaciens* MG1. J Bacteriol 186 (3), 692-698

Lassak, J., Henche, A.L., Binnenkade, L., Thormann, K.M. (2010): ArcS, the cognate sensor kinase in an atypical Arc system of *Shewanella oneidensis* MR-1. Appl Environ Microbiol 76 (10): 3263-74

Lebeer, S., de Keersmaecker, S.C.J., Verhoeven, T.L.A., Fadda, A.A., Marchal, K., Vanderleyden, J. (2007): Functional analysis of *luxS* in the probiotic strain *Lactobacillus rhamnosus* GG reveals a central metabolic role important for growth and biofilm formation. J Bacteriol 189 (3), 860-871

Lee, K.J., Kim, J.A., Hwang, W., Park, S.J., Lee, K.H. (2013): role of capsular polysaccharide (CPS) in biofilm formation and regulation of CPS production by quorum-sensing in *Vibrio vulnificus*. Mol Microbiol 90 (4), 841-857

Leewenhoek, M. and Graaf de, R. (1673): A specimen of some observations made by a microscope, contrived by M. Leewenhoeck in Holland, lately communicated by Dr. Regnerus de Graaf. Phil. Trans. 1673 8

Lin, B., Wang, Z., Malanoski, A.P., O´Grady, E.A., Wimpee, C.F., Vuddhakul, V., Alves Jr, N., Thompson, F.L., Gomez-Gil, B., Vora, G.J. (2010): Comparative genomic analysis identify *Vibrio harveyi* genome sequenced strains BAA1116 and HY01 as *Vibrio campbellii*. Environ Microbiol Rep. 2 (1), 81-89

Livak, K.J. and Schmittgen, T.D. (2001): Analysis of relative gene expression data using real-time quantitative PCR and the $2^{-\Delta\Delta C(T)}$ method. Methods 25: 402-408

Manandhar, S., Vidhate, S., D´Souza, N. (2009): Water soluble levan polysaccharide biopolymer electrospun fibers. Carbohyd Polym 78, 794-798

McCarter, L.L. (1998): OpaR, a homolog of *Vibrio harveyi* LuxR, controls opacity of *Vibrio parahaemolyticus*. J Bacteriol 180 (12), 3166-3173

McMahon, M. (2014): What should I know about bacterial identification. Edited by O. Wallace, copyright protected by 2003-2014 Conjecture Corporation. http://www.wisegeek.com/what-should-i-know-about-bacterial-identification.htm, download 28th July 2014

Messing, N. and Metz, H. (2006): Hefen und Bakterien stärken unsere Gesundheit – Mikroorganismen als Wirkstoff-Produzenten und Veredler von Lebensmitteln. Verlag Ganzheitliche Gesundheit, 3. Auflage

Miller, V.L. and Mekalanos, J.J. (1988): A novel suicide vector and its use in construction of insertion mutations: osmoregulation of outer proteins and virulence determinants in *Vibrio cholerae* requires toxR. J Bacteriol, 170, 2575-2583

Miyashiro, T. and Ruby, E.G. (2012): Shedding light on bioluminescence regulation in *Vibrio fischerii*. Mol Microbiol 84 (5), 795-806

Nadell, C.D., Xavier, J.B., Foster, K.R. (2009): The sociobiology of biofilms. FEMS Microbiol Rev 33, 206-224

Nakhamchik, A., Wilde, C., Rowe-Magnus, D.A. (2008): Cyclic-di-GMP regulates extracellular polysaccharide production, biofilm formation and rugose colony development by *Vibrio vulnificus*. Appl Environ Microbiol 74 (13), 4199-4209

Natrah, F.M.I., Ruwandeepika, H.A.D., Pawar, S., Karunasagar, I., Sorgeloos, P., Bossier, P., Defoirdt, T. (2011): Regulation of virulence factors by quorum sensing in *Vibrio harveyi*. Vet Med 154, 124-129

Nealson, K.H., Platt, T., Hastings, J.W. (1970): Cellular control of the synthesis and activity of the bacterial luminescent system. J Bacteriol 104 (1), 313-322

Ng, W.-L., Perez, L., Wei, Y., Kraml, C., Semmelhack, M.F., Bassler, B.L. (2011): Signal production and detection in *Vibrio* CqsA/CqsS quorum-sensing systems. Mol Microbiol 79 (6), 1407-1417

Ng, W.-L., Perez, L., Cong, J., Semmelhack, M.F., Bassler, B.L. (2012): Broad spectrum pro-qourum-sensing molecules as inhibitors of virulence in vibrios. PLoS Pathogens 8 (6), e1002767

Nijvipakul, S., Wongratana, J., Suadee, C., Entsch, B., Ballou, D.P., Chaiyen, P. (2008): LuxG is a functioning flavin reductase for bacterial luminescence. J Bacteriol 190 (5), 1531-1538

Nilsson, M., Chiang, W.-C., Fazli, M., Gjermansen, M., Givskov, M., Tolker-Nielson, T. (2011): Influence of putative exopolysaccharide genes on *Pseudomonas putida* KT2440 biofilm stability. Environ Microbiol 13 (5), 1357-1369

Parsek, M.R. and Greenberg, E.P. (2005): Sociomicrobiology: the connections between quorum sensing and biofilms. Trends Microbiol 13 (1), 27-33

Pereira, C.S., Thompson, J.A., Xavier, K.B. (2012): AI-2-mediated signaling in bacteria. FEMS Microbiol Rev. 37 (2), 156-81

Pérez, P.D. and Hagen, S.J. (2010): Heterogeneous response to a quorum-sensing signal in the luminescence of individual *Vibrio fischerii*. PLoS One 5 (11): e.15473

Pérez-Núñez, D., Briandet, R., David, B., Gautier, C., Renault, P., Hallet, B., Hols, P., Carballido-López, R., Guédon, E. (2011): A new morphogenesis pathway in bacteria: unbalanced activity of cell wall synthesis machineries leads to coccus-to-rod transistion and filamentation in ovococci. Mol Microbiol 79 (3), 759-771

Pompeani, A.J., Irgon, J.J., berger, M.F., Bulyk, M.L., Wingreen, N.S., Bassler, B.L. (2008): The *Vibrio harveyi* master quorum-seninsing regulator, LuxR, a TetR-type protein is both an activator and a repressor: DNA recognition and binding specificity at target promoters. Mol Microbiol 70 (1), 76-88

Rajamani, S., Zhu, J., Pei, D., Sayre, R. (2007): A luxP-FRET-based reporter assay for the detection and quantification of AI-2 bacterial Quorum-Sensing signal compunds. Biochemistry 46, 3990-3997

Reiger, M. (2014): Regulation der Autoinduktoren von *Vibrio harveyi*. Dissertation. Faculty of Biology. LMU München

Rendueles, O., Kaplan, J.B., Ghigo, J.-M. (2013): Antibiofilm polysaccharides. Environ Microbiol 15 (2), 334-346

Rickard, A.H., Palmer Jr, R.J., Blehert, D.S., Campagna, S.R., Semmelhack, M.F., Egland, P.G., Bassler, B.L., Kolenbrander, P.E. (2006): Auotinducer-2: a concentration-dependent signal for mutualistic bacterial biofilm growth. Mol Microbiol 60 (6), 1446-1456

Rui, F., Marques, J.C., Miller, S.T., Maycock, C.D., Xavier, K.B., Ventura, M.R. (2012): Sterochemical diversity of AI-2 analogs modulates quorum sensing in *Vibrio harveyi* and *Escherichia coli*. Bioorg Med Chem 20, 249-256

Ryan, R.P. and Dow, J.M. (2008): Diffusible signals and interspecies communication in bacteria. Microbiol 154, 1845-1858

Ryder, C., Byrd, M., Wozniak, D.J. (2007): Role of polysacchardies in *Pseudomonas aeruginosa* biofilm development. Curr Opin Microbiol 10 (6), 644-648

Sambrook, J. and Russell, D.W. (2001): Molecular cloning – a laboratory manual, books 1 – 3, 3rd Edition, CSHL Press

Seper, A., Pressler, K., Kariisa, A., Haid, A.G., Roier, S., Leitner, D.R., Reidl, J., Tamayo, R., Schild, S. (2014): Identification of genes induced in *Vibrio cholerae* in a dynamic biofilm system. International J Med Microbiol 304 (5-6), 749-763

Serra, D.O., Richter, A.M., Klauck, G., Mika, F., Hengge, R. (2013): Microanatomy at cellular resolution and spatial order of physiologiacal differentiation in a bacterial biofilm. mBio Vol. 4(2, e00103-13

Serra, D.O. and Hengge, R. (2014): Stress responses go three-dimensioin – the spatial order of physiological differentiation in bacterila macrocolony biofilms. Environ Microbiol 16 (6), 1455-1471

Shibata, S., Yip, E.S., Quirke, K.P., Ondrey, J.M., Visick, K.L. (2012): Roles of the structural symbiosis polysaccharide (*syp*) genes in host colonization, biofilm formation, and polysaccharide biosynthesis I *Vibrio fischeri*. J Bacteriol 194 (24), 6736-6747

Stoodley, P., Sauer, K., Davies, D.G., Costerton, J.W. (2002): Biofilms as complex differentiated communities. Ann Rev Microbiol 56, 187-209

Sudhamani, S.R., Tharanathan, R.N., Prasad, M.S. (2004): Isolation and characterization of an extracellular polysaccharide from *Pseudomonas caryophylli* CFR 1705. Carbohyd Polym 56, 423-427

Suginata, W., Chumjan, W., Mahendran, K.R., Schulte, A., Winterhalter, M. (2013): Chitoporin from *Vibrio harveyi*, a channel with exceptional sugar specificity. J Biol Chem 288 (16), 11038-11046

Surette, M.G., Miller, M.B., Bassler, B.L. (1999): Quorum sensing in *Escherichia coli*, *Salmonella typhimurium* and *Vibrio harveyi*: A new family of genes responsible for autoinducer production. Proc Natl Acad Sci 96, 1639-1644

Thompson, F.L., Iida, T., Swings, J. (2004): Biodiversity of Vibrios. Microbiol Mol Biol R 68 (3), 403-431

Valiente, E., Jimenez, N., Merino, S., Tomas, J.M., Amaro, C. (2008): *Vibrio vulnificus* biotype 2 serovar E *gne* but not *galE* is essential for lipopolysaccahride biosynthesis and virulence. Infect Immun 76 (4), 1628-1638

Vendeville, A., Winzer, K., Heurlier, K., Tang, C.M., Hardie, K.R. (2005): Making “sense“ of metabolism: Autoinducer-2, LuxS and pathogenic bacteria. Nature Reviews, Microbiology 3, 383-396

Wakarchuk, W., Martin, A., Jennings, M.P., Moxons, E.R., Richards, J.C. (1996): functional relationships of the genetic locus encding the glycosyltransferase enzymes involved in expression of the lacto-*N*-neotetraose terminal lipopolysaccharide structure in *Neisseria meningitides*. J Bio Chem 271 (32), 19166-19173

Wang, Y., Wang, H., Liang, W., Hay, A.J., Zhong, Z., Kann, B., Zhu, J. (2013): Qourum sensing regulatory cascade control *Vibrio fluvialis* pathogenesis. J Bacteriol 195 (16), 3583-3589

Watnick, P. and Kolter, R. (2000): Minireview - Biofilms, city of microbes. J Bacteriol 182 (10), 2675-2679

Wei, Y., Perez, L.J., Ng, W.-L., Semmelhack, M.F., Bassler, B.L. (2011): Mechanism of *Vibrio cholerae* Autoinducer-1 biosynthesis. ACS Chem Biol 6 (4), 356-365

Wei, Y. (2012): A simple preparation of RNA from yeastr by hot phenol for Northern Blo. Bio-protocol 2(9): e209. http://www.bio-protocol.org/e209

Weiss Nielsen, M., Sternberg, C., Molin, S., Regenber, B. (2011): *Pseudomonas aeruginosa* and *Saccharomyces cerevisiae* Biofilm in flow cells. J Vis Exp, 47, e2383

Xiao, J., Klein, M:I., Falsetta, M.L., Lu, B., Delahunty, C.M., Yates III, J.R., Heydorn, A., Koo, H. (2012): The exopolysaccharide matrix modulates the interaction between 3D architecture and virulence of a mixed species oral biofilm. PLoS Pathogens 8 (4), e1002623

Yajima, A. (2011): Synthesis of microbial signaling molecules and their stereochemistry-activity relationships. Biosci Biotechnol Biochem 75 (8), 1418-1429

Ye, L., Zheng, X., Zheng, H. (2014): Effect of *sypQ* gene on poly-*N*-acetylglucosamine biosynthesis in *Vibrio parahaemolyticus* and its role in infection process. Glycobiology 24 (4), 351-358

Young, K.D. (2006): The selective value of bacterial shape. Microbiol Mol Bio R 70 (3), 660-703

6 Appendix

6.1 pBLAST results of all proteins analysed in this thesis

glycosyl transferases group 1 family protein [Vibrio parahaemolyticus]

Sequence ID: ref|WP_021822864.1| Length: 374 Number of Matches: 1

▶ See 1 more title(s)

Range 1: 1 to 374 GenPept Graphics ▼ Next Match ▲ Previous Match

Score	Expect	Method	Identities	Positives	Gaps
577 bits(1487)	0.0	Compositional matrix adjust.	270/376(72%)	313/376(83%)	3/376(0%)

```
Query  1    MTDIVVFGEDFGGLPSSSQHLIKHLAKNHRILWVNSIGLRQPTPTTKDAKRLVAKLSGSV  60
            MTDIVVFGEDFGGLPSS+QH+++ LA NHRILWVNSIGLRQP PT KD +RLV+K+S ++
Sbjct  1    MTDIVVFGEDFGGLPSSTQHIVQRLATNHRILWVNSIGLRQPKPTGKDIQRLVSKISRAI  60

Query  61   KQKDDKAQTAFSHHDDSD-IHTITLLTIPAPRSAWARRVATQMMKYQLSKKLNELGFQHT  119
                    T   H D  D I T+ LLTIPAP SA++R+VA +MM++QL K L  L F +
Sbjct  61   SNTGSDKPTM--HCDAVDNIFTVNLLTIPAPHSAFSRKVAAKMMQHQLEKHLKALNFDNP  118

Query  120  VFWTSLPTAVDICKEMSAKGIVYYCGDDFGALAGVDHQTVLEHETELVDCADLVLAASER  179
            +FWTSLPTA D+C  M+ +G++YYCGDDFGALAGVDHQTV+EHE  LVD AD +LAAS++
Sbjct  119  LFWTSLPTAADVCNAMNKRGLIYYCGDDFGALAGVDHQTVMEHERTLVDNADCILAASDK  178

Query  180  LAANFPHEKTVTIPHGVDFSLFSKSVDKAEDMPNNGRKVLGFYGSLSEWLDYQLVEQVAE  239
            LAA FP  KT T+PHGVDFSLFS   +KA D+PNNGRK+LGFYGSLS+WLDY+L++QVA+
Sbjct  179  LAARFPDNKTTTLPHGVDFSLFSTPAEKASDLPNNGRKILGFYGSLSDWLDYRLIDQVAQ  238

Query  240  QAQDWDLVFIGPNELPHNSLPQRSNVHYLGARAHHDLPRYSQHWDASWLPFVDNAQIQAC  299
             A DWDLVFIGPNE  HN LPQR NVHYLG RAHH LP YSQHWDASWLPFVDNAQI+AC
Sbjct  239  HAPDWDLVFIGPNEFAHNPLPQRDNVHYLGTRAHHLLPSYSQHWDASWLPFVDNAQIKAC  298

Query  300  NPLKLLEYLATGTPVISTPFPALKPYQHMLHVVTDVEDVCASLNHLLPPPEGSLSLIQQQ  359
            NPLKLLEYLATGTPVISTPFPAL PY+HMLH+V DVEDVCASLNHLLPPP GS S +QQQ
Sbjct  299  NPLKLLEYLATGTPVISTPFPALMPYKHMLHIVADVEDVCASLNHLLPPPNGSTSYVQQQ  358

Query  360  SWESRARQIERLVRAL  375
            SWE+RA Q+E+LVRAL
Sbjct  359  SWEARADQVEKLVRAL  374
```

Fig. 46: pBLAST of VIBHAR_02222

putative polysaccharide export protein [Vibrio alginolyticus NBRC 15630 = ATCC 17749]

Sequence ID: ref|YP_008534891.1| Length: 477 Number of Matches: 1

See 3 more title(s)

Range 1: 1 to 475 GenPept Graphics Next Match Previous Match

Score	Expect	Method	Identities	Positives	Gaps
794 bits(2050)	0.0	Compositional matrix adjust.	397/475(84%)	444/475(93%)	0/475(0%)

```
Query  1    MSDLRDNLTLLLLHGAWRRRYLLVIPMIVLPILGFLISKAVPTKYVAHTSMLIQETAKMNP  60
            M+DLR+NL++LLHG WRRRY++VIPM+VLP+LGF++SK VPT YVAHTSMLIQETAKMNP
Sbjct  1    MNDLRENLSVLLHGTWRRRYMIVIPMLVLPVLGFIVSKLVPTTYVAHTSMLIQETAKMNP  60

Query  61   FLQDLAVSTMLKDRLSALSTLLKSRHVLYSVAKEQGLIDDTMDANEQEFIIKDLANRLTV  120
            FLQDLAVSTMLKDRLSALSTLLKSRHVLYSVAKEQ LI+D M A EQEFIIKDLA+RL+V
Sbjct  61   FLQDLAVSTMLKDRLSALSTLLKSRHVLYSVAKEQSLINDEMSAKEQEFIIKDLASRLSV  120

Query  121  QQLGKDFIQIQLTSSQSEGMEAVLSSVSNHFVEQLLAPERSSIKDSSHFLTIHIDKRREE  180
            Q LGKDFIQIQL S +SEGME++L SV  HFVEQLLAPERSSIKDSSHFLTIHI+KRREE
Sbjct  121  QPLGKDFIQIQLQSGKSEGMESMLLSVREHFVEQLLAPERSSIKDSSHFLTIHINKRREE  180

Query  181  LDKAEQAFAEYKNAYSHATPAMQAQSLTRLASLKQTLAEKEAELAGVKRSLGSLDQQLSK  240
            LDKAEQAFAEYKN YS ATP MQAQSLTRLASLKQTLAEKEAELAGV RSLGSLDQQLSK
Sbjct  181  LDKAEQAFAEYKNTYSDATPEMQAQSLTRLASLKQTLAEKEAELAGVSRSLGSLDQQLSK  240

Query  241  TNPVIGKIEEQIIEIRSELTLLRARYTEAHSSVQGKLRELNRLEQERSVLLNSKQPEMNS  300
            TNPVIGK+EEQII+IRSELTLLRA+YTEAHS VQGKLRELNRLEQERSVLLNSKQPE+NS
Sbjct  241  TNPVIGKLEEQIIDIRSELTLLRAKYTEAHSLVQGKLRELNRLEQERSVLLNSKQPELNS  300

Query  301  DQLWDIASTTTISTIGDAQPLLVSQLRQLQIMRGRYESLEEETISLRNMIQELESDANRF  360
             QLWDIAS TT++++G+AQPLLVSQL QLQ+MRGR+E+L EET SLR+MIQELE +A++F
Sbjct  301  AQLWDIASNTTVNSLGEAQPLLVSQLHQLQMMRGRFEALTEETNSLRDMIQELERNAHQF  360

Query  361  GSTATEINRLARDVAVKRELYDDLVERYEMAQLTGSLGVFEENKRVKVIDEPYTPTLPAN  420
            GSTATEINRLARDVAVKRE+YD+LVERYEMAQLTGSLG FEENKRVK+IDEP+TPT+P N
Sbjct  361  GSTATEINRLARDVAVKREMYDELVERYEMAQLTGSLGEFEENKRVKIIDEPFTPTIPTN  420

Query  421  LPAIIFVLLGLIGGAGLGIGLATIAELADNSIRSRKALEKHLGAPVITTIPKIIF  475
            LP+ +FV+LG IGGAGLGIGLATI ELADNSIRS++ALEKHLG PVITT+P +++
Sbjct  421  LPSFVFVILGFIGGAGLGIGLATILELADNSIRSKRALEKHLGVPVITTLPNVVY  475
```

Fig. 47: pBLAST of VIBHAR_02221

Capsular polysaccharide synthesis enzyme CpsA sugar transferase [Vibrio parahaemolyticus BB22OP]

Sequence ID: ref|YP_007301305.1| Length: 383 Number of Matches: 1

See 2 more title(s)

Range 1: 1 to 383 GenPept Graphics Next Match Previous Match

Score	Expect	Method	Identities	Positives	Gaps
711 bits(1835)	0.0	Compositional matrix adjust.	330/383(86%)	361/383(94%)	0/383(0%)

```
Query  84   ISWLVTCTFLFMVLYFSQVHQIFDKNILAMWLLLTPVLLLSWRSIFRVGLAYMRKLGYNT  143
            +SWL+T   LFMVLYFS+V+ +FD++ILA+W+ +TP LLL+WR  FR  LAY+RK+G+NT
Sbjct  1    MSWLMTSALLFMVLYFSEVYPLFDRSILALWVTIITPALLLAWRVTFRTVLAYLRKMGFNT  60

Query  144  RTAIIIGQTPHGLTLANELENHTEHGVLFDGFYDERSQDRLPESDYPIKGNVRLALERAK  203
            RTAIIIGQTPHG+TLANE++NHTEHGVLFDGFYDERS DRLP S+YPIKG V  ALERAK
Sbjct  61   RTAIIIGQTPHGITLANEIQNHTEHGVLFDGFYDERSSDRLPSSEYPIKGAVNQALERAK  120

Query  204  RGEVDYVYIAMPMHANERIALFLNQFSDTTANTYLIPDFFTYNLLHSRWDQIGQVQTLSV  263
            RGEVDYVYIAMPMHA ERIA  LNQFSDTTANTYLIPDFFTYNLLHSRWDQIGQVQTLSV
Sbjct  121  RGEVDYVYIAMPMHAKERIASILNQFSDTTANTYLIPDFFTYNLLHSRWDQIGQVQTLSV  180

Query  264  FDTPFAGISSWVKRLEDIVLSSIILLLISPVLLAISLGIKLTSKGPVIFKQYRYGLDGRK  323
            FDTPFAG+SSW+KR EDI+ SSIIL+LISP+LLAI++GIKLTSKGPVIFKQ+RYGLDGRK
Sbjct  181  FDTPFAGVSSWIKRFEDILFSSIILVLISPILLAIAIGIKLTSKGPVIFKQHRYGLDGRK  240

Query  324  IEVWKFRSMTTMEQGNDVKQATKNDPRITPFGGFLRRTSLDELPQFINVLQGTMSIVGPR  383
            IEVWKFRSMTTM+QG ++KQATKNDPRITPFGGFLRRTSLDELPQFINVLQGTMSIVGPR
Sbjct  241  IEVWKFRSMTTMDQGPNIKQATKNDPRITPFGGFLRRTSLDELPQFINVLQGTMSIVGPR  300

Query  384  PHAVSHNEEYRQIVDRYMLRHKVKPGITGWAQINGYRGETDTLDKMEKRVEFDLDYIHHW  443
            PHAV+HNEEYRQIV RYMLRHKVKPGITGWAQINGYRGETDTLDKMEKRVEFDLDYIHHW
Sbjct  301  PHAVAHNEEYRQIVARYMLRHKVKPGITGWAQINGYRGETDTLDKMEKRVEFDLDYIHHW  360

Query  444  SVWMDIKIIFLTIFKGFTGSNAY  466
            SVWMDIKIIFLT+FKGFTGSNAY
Sbjct  361  SVWMDIKIIFLTVFKGFTGSNAY  383
```

Fig. 48: pBLAST of VIBHAR_05207

Capsular polysaccharide synthesis enzyme CpsB [Vibrio parahaemolyticus BB22OP]

Sequence ID: refIYP_007301306.1| Length: 402 Number of Matches: 1

▶ See 3 more title(s)

Range 1: 1 to 402 GenPept Graphics ▼ Next Match ▲ Previous Match

Score	Expect	Method	Identities	Positives	Gaps
643 bits(1659)	0.0	Compositional matrix adjust.	291/402(72%)	357/402(88%)	0/402(0%)

```
Query  7    IMKVIPITVAIAMSSASVLAEPMAYKTDSGIEFIPTLGVFYEGDDNINKADRGKNIESVN  66
            +MK     +A+A+ S + LAEPMAY+T+SGIEFIP +  FYEGDDNINKA++ ++IESVN
Sbjct  1    MMKTTTPALALALCSTATLAEPMAYQTESGIEFIPLVKAFYEGDDNINKAEKSQDIESVN  60

Query  67   IWGIEPALLAKIERNQYRANVLYKLSAGFSSDDQNDYDDHAFQFTNFFEFNHRNRLVIDY  126
            IWG+EP+LLA+IERNQYRA++ YKL AGFSSDD+NDYDDH FQFTNFFEFNHR+RLV+DY
Sbjct  61   IWGLEPSLLARIERNQYRADIQYKLKAGFSSDDKNDYDDHTFQFTNFFEFNHRHRLVVDY  120

Query  127  QFRAQHEEKGEDFTEGQGSLPNSPVEFHRNDLRTNYVFGSEGSKGRLEFGIGYIDKTYQN  186
            +F+A HE +GED TEGQG+L +SP+EF+RNDL+TNYVFGS G+KGR EFG+GY DK YQN
Sbjct  121  RFQALHEIRGEDITEGQGNLLDSPIEFYRNDLKTNYVFGSAGAKGRFEFGLGYSDKAYQN  180

Query  187  YRDGMPGKPDAKTKYNDFRAPNAHIEFYLRATPRTYWLVGTQQMSTNYLSDHPSVPSKDS  246
            YR+G+PGKP+AKTKYNDFRAPNAH+EFYLRATP+TYWLVGT+Q+ T YL+ +P   SKDS
Sbjct  181  YRNGLPGKPNAKTKYNDFRAPNAHVEFYLRATPKTYWLVGTKQVFTEYLNKNPRAASKDS  240

Query  247  YSGFYYTGAQWEVTGKTKGIARLGYQVKDFDSHQRETFNGFSWDIGLEWQPQEQSLITLK  306
             + FYYTGA+WE++GKT+GIARLGYQVKDFDS QRETF GFSWDIG EW PQEQ+L+T+K
Sbjct  241  DTSFYYTGAEWEISGKTQGIARLGYQVKDFDSEQRETFKGFSWDIGFEWLPQEQTLVTVK  300

Query  307  TTQAAVSPDQDGDYDLQTRYFIDLKHDWNSYLATRLEALYQQDAYTGITRNEDRYALSAG  366
            TTQAAV+PDQDGDY+LQTRY +D+KHDWNSYLATRL  +YQ+D YTGITRN++RY LSAG
Sbjct  301  TTQAAVNPDQDGDYNLQTRYRLDIKHDWNSYLATRLGGIYQEDDYTGITRNDERYTLSAG  360

Query  367  LDYQIKRWVLLQADWRYLDKDSDWQGYSFEQNIWSLSARFSL  408
            +DYQI+RW+ L+ADW+Y DK S+  GYS++QN+W+LSA+FSL
Sbjct  361  VDYQIRRWIQLKADWQYQDKTSNRSGYSYDQNVWILSAQFSL  402
```

Fig. 49: pBLAST of VIBHAR_05206

polysaccharide export-like protein [Vibrio parahaemolyticus RIMD 2210633]

Sequence ID: refINP_800915.1| Length: 177 Number of Matches: 1

▶ See 40 more title(s)

Range 1: 1 to 177 GenPept Graphics ▼ Next Match ▲ Previous Match

Score	Expect	Method	Identities	Positives	Gaps
314 bits(805)	9e-107	Compositional matrix adjust.	156/177(88%)	162/177(91%)	0/177(0%)

```
Query  1    MNLLATLFSLVLVLLSTPSFASANEQDYLLDTGDTISVQVYGEEDLSIKNILITSDGYFD  60
            MN L  L  L L+L ST   A++NEQDYLLDTGDTISVQVYGEEDLSIKNILITSDGYFD
Sbjct  1    MNPLFKLIGLALLLFSTFVSANSNEQDYLLDTGDTISVQVYGEEDLSIKNILITSDGYFD  60

Query  61   YPYLGRIKAINKTPKQLKYEIETGLKGDYLINPKVMVAINSFRLFYVNGEVRKPGGFEYQ  120
            YPYLGRIKAINKTPKQLKYEIETGLKGDYLINPKVMV IN FRLFYVNGEVRKPGGFEY+
Sbjct  61   YPYLGRIKAINKTPKQLKYEIETGLKGDYLINPKVMVTINYFRLFYVNGEVRKPGGFEYR  120

Query  121  PGLTIEKAIALAGGLTDRASRKSINLIQHATGNTVESVSMQRSVEPGDIVFIDQSFF  177
            PGLTIEKAIALAGGLTDRASRKSINLT+H TG TVE VSMQR+VEPGDIVFIDQSFF
Sbjct  121  PGLTIEKAIALAGGLTDRASRKSINLTKHKTGKTVEGVSMQRTVEPGDIVFIDQSFF  177
```

Fig. 50: pBLAST of VIBHAR_05205

Capsular polysaccharide synthesis enzyme CpsD exopolysaccharide synthesis [Vibrio parahaemolyticus BB22OP]

Sequence ID: ref|YP_007301308.1| Length: 726 Number of Matches: 1

▶ See 3 more title(s)

Range 1: 1 to 726 GenPept Graphics ▼ Next Match ▲ Previous Match

Score	Expect	Method	Identities	Positives	Gaps
1305 bits(3378)	0.0	Compositional matrix adjust.	626/726(86%)	684/726(94%)	0/726(0%)

```
Query  6    MNETHSTQAPTNQVPLIRFGHHFRTLKKNWLSILAFTIIFSLTCTWYIYSKKSVYQATAI  65
            MN TH      N+V LIRFGHHF+TLKKNWLSI AFT+IFSLTCTWYIYSK S+YQATAI
Sbjct  1    MNGTHPNNFQMNKVELIRFGHHFKTLKKNWLSIAAFTLIFSLTCTWYIYSKTSIYQATAT  60

Query  66   LLIQEEQKSALSIEEVYGVDTTKKEYFQTQIAILKSNHIADKVITKLNLVNHPDFTSSSG  125
            LLIQEEQKSALSIEEVYGVDTTKKEYFQTQIAILKSNHIADKVI +LNL  HP+FTSS G
Sbjct  61   LLIQEEQKSALSIEEVYGVDTTKKEYFQTQIAILKSNHIADKVINELNLTQHPEFTSSGG  120

Query  126  IKQKIDEIKAIPFVQDLLHVAPNPKETSQHTKPYYQALQTFKRKLDIEPVRNTQLVKIRF  185
            +KQKID+IKA+P VQDLL+V+P+PKETSQ+++ YYQALQ FKRKL+IEPVRNTQLV+I F
Sbjct  121  LKQKIDDIKAVPLVQDLLNVSPSPKETSQYSESYYQALQAFKRKLEIEPVRNTQLVRISF  180

Query  186  RSTDPQLATTIANAIGQAYIDANFEAKLVVTQNAATWLTNNSQKLEERLRASEQALQDFL  245
            RS DP+LAT +ANA+GQAYIDANFEAKLVVTQNAATWLTNNSQKLEERL+ SE ALQ+FL
Sbjct  181  RSADPKLATRVANAVGQAYIDANFEAKLVVTQNAATWLTNNSQKLEERLKKSEHALQEFL  240

Query  246  MQEGLIDINGIDDIYANELEELNRKLNAAVNNRIEAQTLIQLLKRKSTQDIDSLLSIDEF  305
            ++EGLIDINGIDDIYANELEELNRKLN AVN RIEAQTLIQLLKRKS+Q++DSLLSIDEF
Sbjct  241  LKEGLIDINGIDDIYANELEELNRKLNTAVNKRIEAQTLIQLLKRKSSQNLDSLLSIDEF  300

Query  306  ANQAQIRDLKMSEAQAAKSVSELSQRYGPKHDRMIQAKAQLASIQARTEQLIREISFSKQ  365
            ANQAQIRDLK+SEAQAAK+VSEL+QRYGPKHDRM+QAKAQLASIQ RT+QLIREISFSKQ
Sbjct  301  ANQAQIRDLKLSEAQAAKNVSELAQRYGPKHDRMVQAKAQLASIQERTQQLIREISFSKQ  360

Query  366  QDLLAAKAQEDMLRAELDNKKSDFQMLGSQKARYEQLKREVESNKDLYEAFLNREKETNA  425
            QDLLAAKAQEDMLR ELD KKSDFQ LGSQKARYEQLKREVESNKDLYEAFLNREKET+A
Sbjct  361  QDLLAAKAQEDMLREELDRKKSDFQSLGSQKARYEQLKREVESNKDLYEAFLNREKETSA  420

Query  426  TSDYKNVTARFTDPAIVPLFPIAPQRMKLVLIATFFGFAIACALLIILETLREVIRTSSD  485
            TSDYKNVTARFTD AI+PLFP+APQRMKLVLIATFFGFAIACAL+IILETLREVIRTS+D
Sbjct  421  TSDYKNVTARFTDKAIIPLFPVAPQRMKLVLIATFFGFAIACALVIILETLREVIRTSND  480

Query  486  VQDKLGVTCLGTIPKVKKRALCQKGVTYSAYLDQDEKLFSEACRSVRTSLLLRLTNSKQK  545
            VQDKLGVTCLG IP VKKR L + GV+Y+AYLD+DEKLFSEACRSVRTSLLLRLTN+KQK
Sbjct  481  VQDKLGVTCLGVIPMVKKRTLRKNGVSYTAYLDKDEKLFSEACRSVRTSLLLRLTNTKQK  540

Query  546  ILPFTSAIPEEGKTSTSINMAVSFSTMEKVLLIDCDLRKPSLAKRFNLPESSPGLTNILT  605
            ILPFTSAIPEEGKTSTSINMAVSFSTMEKVL+IDCDLR+PSLAKRFN+PES PGLTNILT
Sbjct  541  ILPFTSAIPEEGKTSTSINMAVSFSTMEKVLIIDCDLRRPSLAKRFNIPESQPGLTNILT  600

Query  606  MDTPLSECIIKKEEANLDVLPAGIIPPNPQELLASDRFEKLLEYLASKYDRIIIDTPPLL  665
            MDT + +CI++ ++ANLDVLPAG+IPPNPQELLAS+RF+KLL++    +YDRIIIDTPPLL
Sbjct  601  MDTAIKDCIVRIDDANLDVLPAGLIPPNPQELLASNRFKKLLDHFQDRYDRIIIDTPPLL  660

Query  666  SVSDALILGQKANGLITVIRSESTKASLVNVALSKQIQHSIPSLGVLITQAKSKEGETLY  725
            SVSDALILGQ ANGLITVIRSESTKASLVNVALSKQIQHSIPSLGVLITQAK+KEGETLY
Sbjct  661  SVSDALILGQYANGLITVIRSESTKASLVNVALSKQIQHSIPSLGVLITQAKAKEGETLY  720

Query  726  VQKYAY  731
            VQKYAY
Sbjct  721  VQKYAY  726
```

Fig. 51: pBLAST of VIBHAR_05204

capsular exopolysaccharide family domain protein [Vibrio parahaemolyticus 50]

Sequence ID: gb|ETT16422.1| Length: 719 Number of Matches: 1

Range 1: 1 to 703 GenPept Graphics ▼ Next Match ▲ Previous Match

Score	Expect	Method	Identities	Positives	Gaps
1265 bits(3273)	0.0	Compositional matrix adjust.	614/703(87%)	657/703(93%)	0/703(0%)

```
Query  1    MANHTISSSAPTDDEIDLGKLFGILIDAKWFIVGITLLFATIGIAVALLSTPIYKADALI  60
            MAN TI SSA  DDEIDLGKLFGILIDAKWFI+ ITL FAT+GIAVALLSTPIYKADALI
Sbjct  1    MANQTIQSSALADDEIDLGKLFGILIDAKWFIISITLFFATLGIAVALLSTPIYKADALI  60

Query  61   QIEQKSSGGISAMVGDMGDLFAAESSATTEIEIIKSRMILGDTVDKFNLTTIATPEYFPF  120
            QIE+KSSGGISAMVGDMG+LF+AESSATTEIEIIKSRMILGDTVDKFNLTTIATP+Y PF
Sbjct  61   QIEKKSSGGISAMVGDMGELFSAESSATTEIEIIKSRMILGDTVDKFNLTTIATPDYLPF  120

Query  121  VGKGLARINGTQNYISVSSFEIPRTAQGFRHHLVVSDAEKGTFDLMIEDKIVLSGVVGQT  180
            VGKGLARINGTQNYIS+++FE+PRTA+G  H L+ +D EKG F LM+ED++VLSG VGQ
Sbjct  121  VGKGLARINGTQNYISLTTFEVPRTARGLSHQLIATDVEKGQFSLMLEDQMVLSGSVGQL  180

Query  181  IEMNGYHIKVRELVAQNEDSFSIGKISKLDAINRLASQLSISERGAKTGIVSLSIEGEYP  240
            IEMNGY +KV +L AQNED+F+I KISKLDAIN+LASQLSISERG +TGIVSLSIEGEYP
Sbjct  181  IEMNGYRVKVNQLNAQNEDTFTISKISKLDAINKLASQLSISERGNQTGIVSLSIEGEYP  240

Query  241  ERNQQILNDVVQNYFLQNVRRNSAEAEQSLNFLKDHLPEIKDKLNGSEDVLNRFRQENES  300
            + NQ +LNDVVQNYFLQNVRRNSAEAEQSLNFLK HLPEIKDKL  SED LN FRQENES
Sbjct  241  DHNQLVLNDVVQNYFLQNVRRNSAEAEQSLNFLKGHLPEIKDKLTISEDTLNSFRQENES  300

Query  301  IDLNLEAQSTLKVMVALEAQLNELTFKESEISQKFTQDHPAYKSLLDKRQTLLQEKARLN  360
            IDLNLEAQSTLKVMVALEAQLNELTFKESEISQKFTQDHPAYKSLLDKRQTLLQEK RLN
Sbjct  301  IDLNLEAQSTLKVMVALEAQLNELTFKESEISQKFTQDHPAYKSLLDKRQTLLQEKERLN  360

Query  361  RQVQKLPKTQREVLRMTRDVEVNQQIYIQLLNKVQELNIIKAGTVGNVRIIDSAQSYAIP  420
            +QVQKLPKTQREVLRMTRDVEVNQQIYIQLLNKVQELNIIKAGTVGNVRIID+AQSYA+P
Sbjct  361  KQVQKLPKTQREVLRMTRDVEVNQQIYIQLLNKVQELNIIKAGTVGNVRIIDNAQSYAVP  420

Query  421  VKPKKPLIVVLATLLGGMVAVAFVLVKTAFHRGVTSPDEIEQTGISVYASVPKSVQQLEV  480
            +KPKKPLIVVLATLLGGMVAVAFVLVKTAFHRGVTSPD IEQTGISVYASVPKS QQLEV
Sbjct  421  IKPKKPLIVVLATLLGGMVAVAFVLVKTAFHRGVTSPDVIEQTGISVYASVPKSAQQLEV  480

Query  481  ANKLKRKGNKDLLLLAEENPADLSIESLRGLRTSLHFAMMEAKNNVLMISGPAPSIGKTF  540
            ANKLKRK NKDLLLLA  NPADLSIE+LRGLRTSLHFAM+EAKNNVLMISGPAPSIGKTF
Sbjct  481  ANKLKRKNNKDLLLLANANPADLSIEALRGLRTSLHFAMLEAKNNVLMISGPAPSIGKTF  540

Query  541  VSTNFAAVAAKTGQKVLLVDADMRKGYLQQCFGLAADNGLSDFLSGKISQDMVIKPTKVE  600
            VSTNFAAVAAKTGQKVLLVDADMRKGYLQQCFGL A+ GLSD LSGKI +   IKP++VE
Sbjct  541  VSTNFAAVAAKTGQKVLLVDADMRKGYLQQCFGLTAEQGLSDLLSGKIDRATAIKPSQVE  600

Query  601  NLGVITRGQVPPNPSELLMHPRFAEFVKKASQEYDLVIIDTPPVLAVTDPSIVGAIAGTT  660
            NL V+TRGQVPPNPSELLMHPRF EFV++ S+EYDLVIIDTPPVLAVTDPSIVGA+AGTT
Sbjct  601  NLDVVTRGQVPPNPSELLMHPRFVEFVEQVSKEYDLVIIDTPPVLAVTDPSIVGALAGTT  660

Query  661  LMVARFDQTTSKELEVARSRFEQSGVEVKGVILNAIEKKAASS  703
            LMVARFDQTT KE+EVAR RFEQSGVEVKGVILNA+EKKA++S
Sbjct  661  LMVARFDQTTLKEIEVARGRFEQSGVEVKGVILNAVEKKASNS  703
```

Fig. 52: pBLAST of VIBHAR_06667

cell division inhibitor [Vibrio sp. Ex25]

Sequence ID: refYP_003286770.1| Length: 304 Number of Matches: 1

See 4 more title(s)

Range 1: 1 to 304 GenPept Graphics ▼ Next Match ▲ Previous Match

Score	Expect	Method	Identities	Positives	Gaps
564 bits(1454)	0.0	Compositional matrix adjust.	263/304(87%)	286/304(94%)	0/304(0%)

```
Query  12   MKILLTGGTGFIGSELLKMLTTHQVILLTRTPARAKQRLQHADVGNTEYLDSLDSLEDLN  71
            MKILLTGGTGFIGSELLK+L+THQV+LLTR+P +AKQRLQHAD+GN EYLDSL+S  DLN
Sbjct  1    MKILLTGGTGFIGSELLKLLSTHQVMLLTRSPEQAKQRLQHADLGNIEYLDSLESFADLN  60

Query  72   DVDAVINLAGEPIADKRWSQEQKEIICNSRWKVTERIVELIHASTEPPSVFISGSAVGYY  131
             +DA+INLAGEPIADKRW+ EQKE IC SRWK+TE+IVELIHASTEPP+VFISGSAVGYY
Sbjct  61   HIDAIINLAGEPIADKRWTSEQKEKICKSRWKITEQIVELIHASTEPPAVFISGSAVGYY  120

Query  132  GDQQDHPFDECLHVNSEAFAHSVCARWEQIAKRAESEQTRVCLLRTGVVLGPNGGALAKM  191
            GDQQDHPFDECLHVNSE F H VCA+WEQIAKRAESEQTRVCLLRTGVVLG NGGALAKM
Sbjct  121  GDQQDHPFDECLHVNSEDFPHEVCAKWEQIAKRAESEQTRVCLLRTGVVLGLNGGALAKM  180

Query  192  LLPYKLGLGGPLGSGRQYMPWIHILDMVRAIMYLLETPHAHGEFNLCAPHPVSNKIFSGT  251
            LLPYKLG+GGPLG+G QYMPWIHILDMVRAIMYLLETPHAHG FN+CAPHPV+N+IFSGT
Sbjct  181  LLPYKLGVGGPLGNGNQYMPWIHILDMVRAIMYLLETPHAHGAFNMCAPHPVTNRIFSGT  240

Query  252  LAKTLKRPHILFTPKWVMNVAMGESSCLLFDSIRAKPKKLTELGFKFSYSRVEPALKNLL  311
            LAKTLKRPHILFTPKW M + MGESSCLLFDS+RAKPKKLTELGFKFSYSR+EPALK+LL
Sbjct  241  LAKTLKRPHILFTPKWAMELLMGESSCLLFDSMRAKPKKLTELGFKFSYSRIEPALKHLL  300

Query  312  QDRS  315
             DRS
Sbjct  301  HDRS  304
```

Fig. 53: pBLAST of VIBHAR_01320

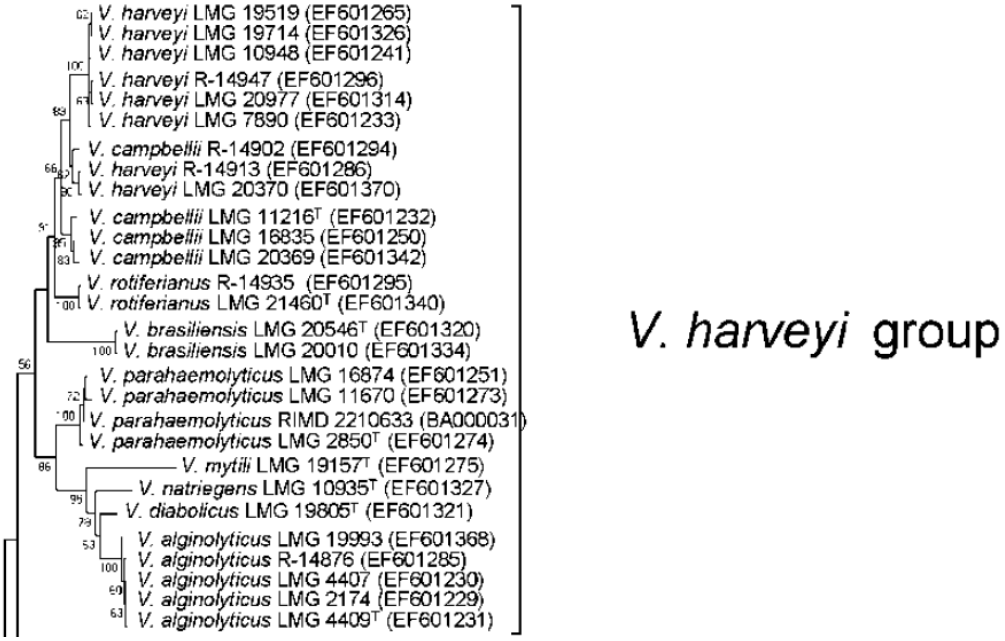

Fig. 54: Phylogenetic tree

Image was modified from Thompson *et al.* (2007) to visualize relation between *V. alginolyticus, V. campbelli, V. harveyi* and *V. parahaemolyticus*

6.2 Mean values of bioluminescence production, biofilm formation as well as glucose production of all strains used as well as the qRT-PCR data

Tab. 14: Bioluminescence data [RLU/OD (600)] of all strains at 5 h of cultivation in AB media used in this thesis

Strain	Mean Value of RLU/OD (600)	Standard deviation	% WT
BB120	2,320,580	578,016	100
Δ*luxO*	2,380,516	209,036	103
EMR2	2,259,396	655,338	97
EMR3	2,095,085	805,694	90
EMR14	1,886,597	194,751	81
EMR17	2,033,776	131,364	88
EMR18	2,209,034	434,529	95
EMR19	1,758,685	355,712	76
EMR20	2,302,163	268,227	99
EMR21	2,197,519	350,735	95
EMR22	2,404,959	185,861	104
EMR23	2,248,808	351,209	97
MR3	412,150	62,247	18
MR15	652	112	0

Tab. 15: Mean value of biofilm volumes [µm³] of all strains used in this thesis

Strain	Mean value of volume [µm³]	Standard deviation	% WT
BB120	34,170,271	1,820,018	100
Δ*luxO*	12,730,870	787,366	37
EMR2	8,621,743	1,374,659	25
EMR3	6,718,098	1,648,717	20
EMR14	12,197,519	2,685,074	36
EMR17	21,027,057	3,499,653	62
EMR18	15,142,780	3,713,487	44
EMR19	9,765,498	401,649	29
EMR20	5,330,152	1,783,600	16
EMR21	12,686,974	2,747,880	37
EMR22	8,369,286	1,552,866	24
EMR23	8,879,307	929,292	26
MR3	1,326,131	317,687	4
MR13	23,805,703	4,117,337	70
MR15	2,403,190	470,264	7
MR18	14,830,138	3,849,701	43

Tab. 16: Mean value of glucose [µg/ml] detected in all strains used in this thesis

Strain	Mean Value of glucose [µg/ml]	Standard deviation	% WT
BB120	3.99	0.27	100
EMR2	1.76	0.33	44
EMR3	1.63	0.11	41
EMR17	4.12	0.30	103
EMR18	3.97	0.27	100
EMR20	1.55	0.10	39
EMR21	3.80	0.37	95
EMR22	1.93	0.26	48
MR15	1.53	0.33	38

Tab. 17: qRT-PCR data of putative exopolsaccharide genes

$OD_{600\,nm}$ at RNA extraction	genexpression in %recA / strain	*VIBHAR_02222*	standard deviation	*VIBHAR_05206*	standard deviation	*VIBHAR_06667*	standard deviation
0,6	BB120	0.63	0.74	2.11	2.54	0.48	0.82
	JMH634	0.23	0.23	0.44	0.12	0.00	0.00
1,3	BB120	1.32	0.13	2.09	0.59	3.67	2.74
	JMH634	0.34	0.28	0.32	0.22	0.00	0.00
2	BB120	2.41	1.94	3.38	2.40	9.15	4.48
	JMH634	0.84	0.21	1.14	0.38	0.00	0.00

Acknowledgements

First, I would like to thank Prof. Dr. Kirsten Jung for giving me the opportunity to work in her lab and to research the bioluminescent bacterium *Vibrio harveyi*. I am very grateful for all of her ideas.

Additionally, I would also like to thank the members of the work groups of Prof. Dr. Kirsten Jung, Prof. Dr. Heinrich Jung and PD Dr. Ralf Heermann for their advice and support, special thanks goes to Dr. Laure Plener, Dr. Jürgen Lassak, Dr. Frank Landgraf, Matthias Reiger and Sophie Bucher. For the technical support I have to thank Sabine Scheu, Ingrid Weitl and Korinna Burdack.

I am thankful for the thesis committee for their interest in my research.

Dr. Kai Thormann, thanks for introducing me to 3D biofilms and the confocal. Also, I would like to thank Prof. Dr. Thomas Ott, Dr. Arthur Schüßler and his team for helping me out with the confocal. Special thank goes to Prof. Dr. Gerhard Wanner and his group for the fixation and scanning of my macrocolonies.

I would like to thank Dr. Robert Moore for his support and his trust in me! Also, Dr. Ludwig Czibere and Dr. Cornelia Hock - thank you so much for your support!

I would like to thank my dear friends Karolin Früh, Ursula Junghans, Susanne Stokes, Sarah Wagner and Ramona Maisch for being honest with me and supporting me throughout my whole thesis! Thanks for keeping me motivated! Also I would like to thank my sister in law Dr. Manuela Rabener for her advice.

I am very grateful to have the love and support of my partner Alexander Mack! Thanks for everything! Thanks for motivating me through all the downs and keeping me focused during the ups!

Special thanks to my mother Christiane Rabener and my siblings Jenny Rabener and Nick Rabener for their tremendous support and encouragement! I would have never made it without you!